

POWER LINE CORRIDOR VEGETATION MANAGEMENT:
CLEARING A PATH TO RELIABLE ELECTRIC SERVICE USING LIDAR

A THESIS PRESENTED TO
THE DEPARTMENT OF HUMANITIES AND SOCIAL SCIENCES
IN CANDIDACY FOR THE DEGREE OF
MASTER OF SCIENCE

By
BRIAN KURINSKY

NORTHWEST MISSOURI STATE UNIVERSITY
MARYVILLE, MISSOURI
OCTOBER, 2013

POWER LINE CORRIDOR VEGETATION MANAGEMENT

Power Line Corridor Vegetation Management:
Clearing a Path to Reliable Electric Service Using LiDAR

Brian Kurinsky

Northwest Missouri State University

THESIS APPROVED

Thesis Advisor, Dr. Ming-Chih Hung Date

Dr. Patricia Drews Date

Dr. Yi-Hwa Wu Date

Dean of Graduate School Date

Power Line Vegetation Management:
Clearing a Path to Reliable Electric Service Using LiDAR

Abstract

Electricity has effectively become the life blood of modern society. To follow the metaphor, it appears just as self-evident that similar preventative and diagnostic efforts that avert a stroke or heart attack in humans need to be applied to preventing power outages and blackouts and their devastating impact on human lives and economic activity. Vegetation such as trees adds beauty and value to the landscape but still proves to be one of the leading causes of power outages and blackouts in the United States. For this reason, management of vegetation along power line corridors is of the utmost importance.

Many utility companies still cling to legacy methods of surveying power line corridors to identify encroaching vegetation to be removed, such as ground field surveys. These methods were constrained by the lack of technology at the time, but the emergence of new technology offers much more effective and efficient methods. One such technology, Light Detection and Ranging (LiDAR), was used to identify vegetation encroachments along several power line corridors located in a residential/commercial section of Callahan, FL, just outside of Jacksonville.

First, a pre-classified LiDAR dataset was used to extract line vector data from LiDAR points that represented conductors. Through a buffering process,

LiDAR vegetation points within a distance of the conductor vectors deemed too close were assigned their own class. This special class of points was exported as an ASCII text file and subsequently converted to a point shapefile. An aggregation process produced vegetation encroachment polygons from clusters of points within a certain distance of one another. A spatial join geoprocessing tool was used to impart vegetation height statistics from the point shapefile to the polygon's attribute table.

The result was a polygon shapefile that represented regions of vegetation within a close enough proximity to the conductor vectors to raise concerns, which also contained height information about the vegetation. The polygons were exported to KML format and displayed in three different applications for analysis. The polygons were symbolized by attributes such as their areas and the amount of vegetation points they were derived from. Utility companies and forestry contractors can use these data to plan vegetation removal without having to visit the field beforehand. Users of the data know exactly where vegetation needs to be removed, how much area it covers, and how high they will have to reach to cut it. The accurate nature of the data provides the means by which to estimate labor and costs correctly.

This research used modern technology to solve an old and potentially disastrous problem. It was an attempt to help push LiDAR technology to the forefront of power line corridor vegetation management and help the industry more effectively manage vegetation.

TABLE OF CONTENTS

ABSTRACT	iii
LIST OF FIGURES	vii
LIST OF TABLES	x
ACKNOWLEDGMENTS	xi
CHAPTER 1: BACKGROUND AND INTRODUCTION.....	1
1.1 Precious Electricity and Its Threats	1
1.2 The Northeast Blackout of 2003.....	7
1.3 Regulatory Framework.....	15
1.4 Research Objective.....	18
CHAPTER 2: LITERATURE REVIEW	20
2.1 Advantages of LiDAR	20
2.2 LiDAR vs. Manual Vegetation Analysis Techniques.....	24
2.3 Satellite and Aerial Imagery Approaches	34
2.4 LiDAR Fusion	38
2.5 Conclusions about Existing Research and Thesis Rationale	41
CHAPTER 3: CONCEPTUAL FRAMEWORK AND METHODOLOGY.....	43
3.1 Study Area	43
3.2 Data Sources	45
3.2.1 LiDAR Data Details	46
3.2.2 Aerial Image Data Details.....	52

3.3 Methodology.....	54
3.3.1 Power Line Pole Definition	56
3.3.2 Conductor Definition.....	59
3.3.3 LiDAR Conductor Point Classification	63
3.3.4 Vegetation Encroachment Analysis.....	71
3.3.5 Vegetation Encroachment Data Processing.....	76
CHAPTER 4: ANALYSIS RESULTS	85
4.1 Displaying the Data	87
4.2 Quantifying the Data and Estimating Cost and Effort	94
CHAPTER 5: CONCLUSIONS	96
5.1 Results vs. Objectives	96
5.2 Limitations and Issues.....	98
5.3 Research Contribution	101
5.4 Further Research	102
REFERENCES	104

LIST OF FIGURES

Figure 1.1 – Basic structure of the electric system	3
Figure 1.2 – Major causes of power outages in the U.S	4
Figure 1.3 – Example of mechanical teardown.....	6
Figure 1.4 – Example of an arc caused by a tree limb.....	7
Figure 2.1 – Example of a fixed wing LiDAR platform collection.....	22
Figure 2.2 – Example of a mobile LiDAR platform mounted atop a van	22
Figure 2.3 – Example of mobile LiDAR data collected near a tollbooth	23
Figure 2.4 – A stationary terrestrial LiDAR system.....	23
Figure 2.5 – Hydro One’s workflow.....	28
Figure 2.6 – A tree missed by AEP’s aerial survey but detected with LiDAR	30
Figure 2.7 – Comparison of “danger tree” grow-in inspection techniques	32
Figure 2.8 – Individual accuracies for the spectral angle mapper.....	40
Figure 2.9 – Individual accuracies for the support vector machine	40
Figure 3.1 – Study area	43
Figure 3.2 – Power lines found in the study area.....	44
Figure 3.3 – Leica Geosystems ALS60 LiDAR system components	46
Figure 3.4 – A Cessna 207 aircraft.....	47
Figure 3.5 – 3D view of the LiDAR source data colored by relative height	47
Figure 3.6 – The source LiDAR data displayed as an 8-bit intensity image.....	48
Figure 3.7 – Source LiDAR data colored by class	50
Figure 3.8 – LiDAR data colored by class	51
Figure 3.9 – Conductors in the high vegetation class (3D view).....	51
Figure 3.10 – A 15 foot long minivan clearly resolved by the camera.....	52
Figure 3.11 – The aerial image orthomosaic over the entire study area.....	53
Figure 3.12 – A sample of the study area orthomosaic	54

Figure 3.13 – Process flow – green indicates a non-ArcMap step.....	55
Figure 3.14 – 2D profile view	57
Figure 3.15 – The initial top and bottom pole points	58
Figure 3.16 – The solved pole vector	59
Figure 3.17 – Points used to solve the conductor vector	61
Figure 3.18 – Solved conductor vector	62
Figure 3.19 – Accepted conductor vector	62
Figure 3.20 – Accepted conductor vectors	63
Figure 3.21 – A selected conductor vector (dashed	64
Figure 3.22 – Conductor point classification settings.....	65
Figure 3.23 – Conductor buffer settings	66
Figure 3.24 – Reclassified conductor points	67
Figure 3.25 – All outer conductors classified as Power Line	68
Figure 3.26 – Profile view of the center wires	69
Figure 3.27 – Center wire classification settings (5 to 14)	69
Figure 3.28 – Manually selected upper/lower center wire points (white)	70
Figure 3.29 – Manually reclassified upper/lower center wire points (yellow)	70
Figure 3.30 – All wire points have been classified to Power Line (3D view)	71
Figure 3.31 – Clear sky buffer	72
Figure 3.32 – Distance between the center and outer wires.....	73
Figure 3.33 – Clear sky buffer of five feet.....	74
Figure 3.34 – Encroachment vegetation classification settings	74
Figure 3.35 – Resulting vegetation encroachment points in 3D view (red).....	75
Figure 3.36 – Resulting vegetation encroachment points in 2D (red).....	76
Figure 3.37 – Text version of vegetation encroachment points	77
Figure 3.38 – The resulting point shapefile created from the 3D ASCII text file .	78
Figure 3.39 – Encroachment points over ground raster.....	79

Figure 3.40 – The point shapefile with the added RASTERVALU attribute	79
Figure 3.41 – The point shapefile with the HAGL attribute populated.....	79
Figure 3.42 – A polygon created from aggregated vegetation encroachment points	80
Figure 3.43 – Settings for the Spatial Join tool	82
Figure 3.44 – Results of the spatial join.....	83
Figure 4.1 – Validated vegetation encroachments within a polygon	85
Figure 4.2 – Validated vegetation encroachments within a polygon	86
Figure 4.3 – Validated vegetation encroachments within a polygon	86
Figure 4.4 – Vegetation encroachment polygons labeled and symbolized by area	88
Figure 4.5 – Vegetation encroachment polygons displayed in GoogleEarth	89
Figure 4.6 – Vegetation encroachment polygons displayed in Street View mode in GoogleEarth	90
Figure 4.7 – Vegetation encroachment polygons displayed in ArcGIS Explorer.	91
Figure 4.8 – Vegetation encroachment polygons symbolized by Join_Count.....	92
Figure 5.1 – Encroaching vegetation in the neighborhood	100
Figure 5.2 – Encroaching vegetation in the neighborhood	101

LIST OF TABLES

Table 1.1 – Number of people affected by the Northeast Blackout of 2003.....	9
Table 2.1 – Comparison of “danger tree” grow-in inspection techniques.....	31
Table 2.2 – LiDAR vs. stereo height estimation for poles	37
Table 2.3 – Overall accuracies – Spectral Angle Mapper and Support Vector Machine	40
Table 3.1 – LiDAR metadata	46
Table 3.2 – LAS 1.4 classes with used classes in green	49
Table 3.3 – The image dataset metadata	52
Table 4.1 – Summary statistics on the vegetation encroachment polygons	94

ACKNOWLEDGMENTS

Special thanks go to Jason Amadori of Data Transfer Solutions in Orlando, FL for being so kind as to provide source data and licenses for Earth Shaper and taking time out of his busy schedule to provide guidance on how to use the software. Jason was extremely patient while I asked for new licenses very frequently because of complications due to short, ironic power outages. It's obvious that Jason is as passionate about the work he does as I am about the work I do, which is part of the reason he was willing to help so much.

Thanks to my wife Sally for her unwavering support and encouragement throughout the research and writing process. When frustration and stress started to get the best of me, she was the reassuring force that kept me going and on track. She has been more than tolerant of the time taken away from activities we could be doing together. I love you baby!!

I would also like to thank Dr. Ming-Chih Hung for chairing my thesis committee, and Drs. Eva Wu and Patty Drews for serving on my committee. All provided valuable guidance starting well before the thesis process, all the way through to the end.

Great thanks go to my family for their encouragement and interest in my progress. I know they're proud of my completing this work.

Thanks to my cat Kramer who made me laugh out loud when I was stressed out by jumping onto my desk in front of the computer monitor.

CHAPTER 1: BACKGROUND AND INTRODUCTION

1.1 Precious Electricity and Its Threats

The North American electricity system is one of the greatest achievements in engineering over the past century. This infrastructure represents more than \$1 trillion (U.S.) in asset value, has over 200,000 miles of transmission lines, 950,000 megawatts of power generation capability, and nearly 3,500 utility organizations serving well over 100 million customers and 283 million people. Modern society has come to depend greatly on reliable electricity as an essential resource for national security; health and welfare; communications; finance; transportation; food and water supply; heating, cooling, and lighting; computers and electronics; commercial enterprise; and certainly entertainment and leisure (U.S.-Canada Power System Outage Task Force, 2004). To put it succinctly, nearly all aspects of modern life are supported by electricity. It is no wonder why delivering electric power reliably is of the utmost importance to utility companies. Not to mention if meters are not running, no profit is being made. Customers have grown to expect that electricity will almost always be available when needed at the flick of a switch. However, when this precious commodity is taken away, even for a short amount of time, one can feel as though life can barely go on. In fact anxiety, frustration, anger, and depression can quickly ensue. The average citizen in modern society probably could not imagine living in a part of the world where electric service is sporadically in operation, if there is any service at all. Interruptions to electric service affect not only the individual consumer, but also economics. Even in such an industrious country as the U.S., it is estimated

that economic losses due to power outages range from \$50 billion to \$100 billion every year (Ituen et al., 2008). This problem requires attention.

Providing reliable electricity is an enormously complex technical challenge even on the most routine days. It involves real-time assessment, control, and coordination of electricity production at thousands of generators, moving electricity across an interconnected network of transmission lines, and finally delivering the electricity to millions of customers via a distribution network (U.S.-Canada Power System Outage Task Force, 2004). Some background on the basic structure of the electric system will form a foundation by which to better understand the remainder of this study (figure 1.1). First, a power plant generates electricity at the range between 10,000 - 25,000 volts. Transmission lines are capable of carrying higher voltage than the plant generates, up to 765,000 volts, so a transformer “steps up” the voltage for traveling long distances. The electricity eventually reaches a substation where it is “stepped down” in voltage to between 4,000 and 13,000 volts. From there the electricity travels along distribution lines atop wooden or concrete poles, or is buried underground. Finally, when the electricity reaches a structure such as a business or home, it is stepped down one more time to the usable 120 or 240 volts (U.S.-Canada Power System Outage Task Force, 2004).

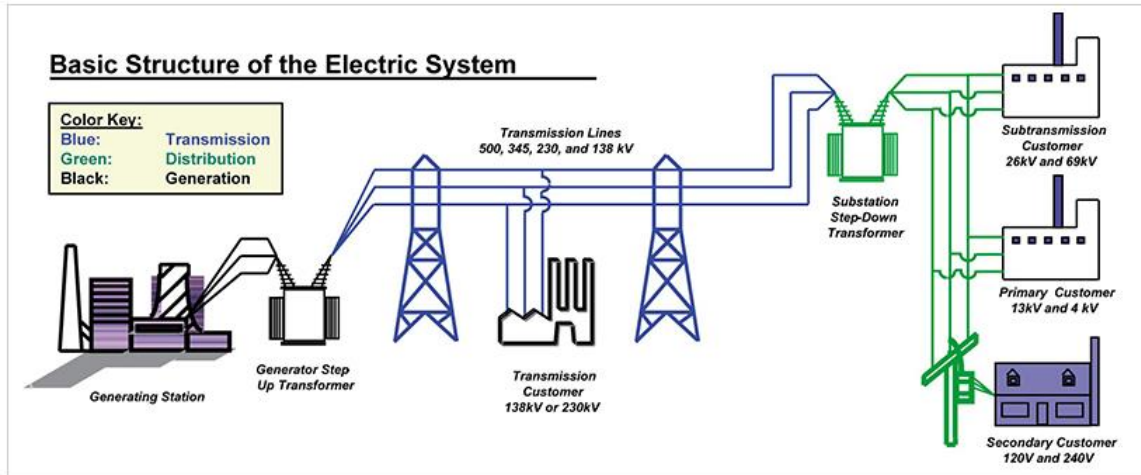


Figure 1.1 – Basic structure of the electric system (U.S. Dept. of Energy, licensed under - <http://creativecommons.org/licenses/by-nc/4.0/legalcode>)

We all have experienced disruptions to electric service at one time or another. Whether it is a mere five minute inconvenience, or, for the more unfortunate, several days or weeks, not having power is never desirable. We all know the feeling when we're deep into important tasks at work or cooling down with air conditioning at home and the power is ripped away. So, what are the types of threats to reliable electricity delivery, and how do they actually cause outages? Figure 1.2 depicts the major causes of power outages in the United States according to the Edison Electric Institute (EEI, 2013). The period of time over which the data were collected is not clear, but they provide a general idea of outage causes in proportion to one another, which is the main point.

The cause with the lowest percentage contribution, maintenance, is when a field worker is performing maintenance on some component of the power grid and power has been shut off for employee safety. This is the only type of power outage that is planned.

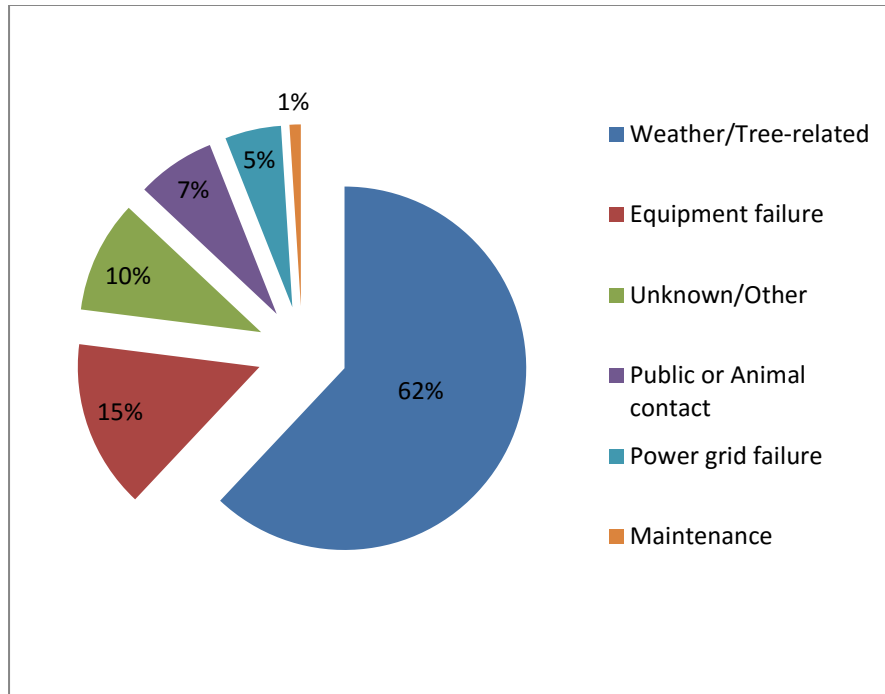


Figure 1.2 – Major causes of power outages in the U.S. (Data according to the Edison Electric Institute)

Power grid failure, with a five percent contribution to causing outages, is when a systematic, widespread failure of the grid occurs due to several different possible factors. Many times the grid is taxed beyond the load it was designed for because of high demand for electricity, and the system simply gives up due to a failure of several components. Utility companies continually face the challenge of satisfying growing energy demands in North America, and it is not always possible to build new power lines due to difficulty acquiring land and environmental approvals (Koop, 2002). Public or animal contact, with a seven percent contribution, can mean that a human or animal has caused some event which, in turn, negatively affects some part of the power grid, causing an outage. Vehicle collisions with support pylon structures are common, and many times damage equipment enough to cause an outage. Contractors or home owners

can contribute to power outages when they damage lines during construction or excavation. Some outages can even be caused by vandalism. Animals capable of climbing support pylon structures or climbing trees in close proximity to those structures can cause outages by coming into contact with electrified conductors or other components. Equipment failure, at a 15% rate of contribution to power outages in the U.S., is a fairly common cause of power outages, especially considering the aging infrastructure in our country. Transformer failures, broken insulators, and bad underground cables are some of the contributing factors of power outages with regard to the equipment failure category (Knoxville Utilities Board, 2013).

Finally, the overall contribution of weather/tree-related events to power outages in the U.S is very important to note, simply because of the sheer dominance of this type of threat. Even though Edison Electric Institute has lumped weather and trees into the same category, it is important to note that it is much more likely for weather to cause a tree to interfere with a power line than a tree simply interfering on its own. A 1984 study by the Electric Power Research Institute showed a high correlation between tree contact faults and adverse weather (Texas Engineering Experiment Station (TEES), 2011). So, how do trees actually cause power failures? TEES (2011) summarized tree-caused outages into two categories: (1) Mechanical tear-down of electric lines and/or apparatus and (2) Electrical short circuits or arcs causing overcurrent faults, which result in the operation of system protection devices to clear the fault, thereby causing an outage. Mechanical tear-down refers to any action that

breaks mechanical supporting insulators, rips conductors from poles, or breaks and drops conductors (TEES, 2011). This would be any object, usually a tree, which falls into a conductor and tears it down (figure 1.3). Arcs and short circuits occur when a tree bridges the gap between two or more conductors or causes two or more conductors to come into contact with one another (figure 1.4). An example would be a branch falling over two parallel energized phase conductors built on horizontal cross arms. Frequently, a combination of both tear-down and short circuit events occur. In fact, either type of event can occur first, leading to the second. For example, lines torn down by trees (mechanical tear-down) can cause conductors to arc when they hit the ground, creating an electrical short circuit. Conversely, an electrical short circuit can burn conductors in two, and cause them to fall to the ground (TEES, 2011). TEES has determined that for electric distribution feeder lines, mechanical tear-down represents the primary cause of vegetation related outages.



Figure 1.3 – Example of mechanical teardown (Photo by the Knoxville Utilities Board)



*Figure 1.4 – Example of an arc caused by a tree limb
(Photo by the Knoxville Utilities Board)*

Not only does vegetation cause disruptions to electric service on a scale from part of a neighborhood to an entire region, but vegetation related power outages also present safety concerns. Brush/forest fires are often a consequence of tree-conductor contact if the contact is sustained long enough and the safety shutdown mechanisms on the line fail. Electrocution is also probable if an electrified conductor gets too close to or falls onto the ground where people are. Sometimes it is assumed that because a power line and associated components look damaged after falling to the ground they are not electrified, when this is not the case, and electrocution is quite possible.

1.2 The Northeast Blackout of 2003

One glaring example of a large scale loss of power, in fact quite possibly the most important one, is the Northeast Blackout of 2003. On August 14, 2003, a few minutes after 4:00 p.m. Eastern Daylight Time, large portions of the

Midwest and Northeast United States and Ontario, Canada experienced an electric power blackout. States affected included Ohio, Michigan, Pennsylvania, New York, Vermont, Massachusetts, Connecticut, and New Jersey. In some parts of the U.S. power was not restored for four days. Parts of Ontario experienced rolling blackouts for more than a week before restoration of full power. It was estimated the total cost of this blackout in the U.S. ranged from \$4 billion to \$10 billion. The Canadian gross domestic product was down 0.7% in August, there was a net loss of 18.9 million work hours, and manufacturing shipments in Ontario were down \$2.3 billion (U.S.-Canada Power System Outage Task Force, 2004).

The Northeast Blackout of 2003 affected an estimated 10 million people in Ontario and 45 million people in eight U.S. states. In New York City and surrounding areas alone, 14.3 million people were affected (U.S.-Canada Power System Outage Task Force, 2004), (table 1.1).

Table 1.1 – Number of people affected by the Northeast Blackout of 2003

City	Number of People Affected
New York City and surrounding areas	14,300,000
Toronto and surrounding areas	8,300,000
Newark and surrounding areas	6,980,000
Detroit and surrounding areas	5,400,000
Cleveland and surrounding areas	2,900,000
Ottawa	780,000 of 1,120,000
Buffalo and surrounding areas	1,100,000
Rochester	1,050,000
Baltimore and surrounding areas	710,000
London, Ontario and surrounding areas	475,000
Toledo	310,000
Windsor, Ontario	208,000
Estimated Total	55,000,000

Referring back to section 1.1 which mentions the many aspects of human existence reliable electricity supports, and taking into account the geographic area and number of large urban population centers affected by this monumental blackout, one could only begin to imagine how everything suddenly came to a screeching halt, and what the effects were. Power generation, water supply, transportation, communication, industry, and more were affected.

Power generation: Voltage fluctuations on the grid caused power plants to go into “safe mode” automatically to prevent damage in the case of an overload. This meant that much normally available power was offline. Plants were eventually brought back online, which brought some electrical power to areas immediately surrounding the plants by the morning of August 15, 2003. Homes and businesses in the affected areas were requested to limit power usage until the grid was back to full power (U.S.-Canada Power System Outage Task Force, 2004).

Water supply: Loss of water pressure in some areas due to the lack of electricity which powers pumps caused potential contamination of the water supply. Four million customers of the Detroit water system were under a boil water advisory until four days after the initial power outage. Macomb County, Michigan ordered all 2,300 of its restaurants closed until they were sanitized after the advisory had been lifted. Twenty people living on the St. Clair River claim to have been sickened after bathing in the river during the blackout. The accidental release of 310 pounds of vinyl chloride from a Sarnia, Ontario chemical plant was not revealed until five days later. Cleveland, Ohio lost water pressure as well, and issued a boil water advisory. Cleveland and New York had sewage spills into waterways, requiring beach closures. Newark, New Jersey and northern cities had major sewage spills into the Passaic and Hackensack rivers, which flow directly into the Atlantic Ocean. Kingston, Ontario lost power to sewage pumps, causing raw waste to be dumped into the Cataraqui River at the base of the Rideau Canal (U.S.-Canada Power System Outage Task Force, 2004).

Transportation: Amtrak's Northeast Corridor railroad service was stopped north of Philadelphia, and all trains running into and out of New York City were shut down. This initially included the Long Island Rail Road and the Metro-North Railroad, but both were able to get running again strictly on diesel power by the morning of August 15th. Canada's Via Rail, which serves Toronto and Montreal, suffered service delays, but most routes were still running, and normal service was resumed on most routes by the next morning. Airports affected by the blackout ceased to have passenger screenings and were subsequently shut down. Even after power was restored, flights were still cancelled due to the fact that there was difficulty accessing electronic ticket information. Many gas stations were unable to pump fuel due to lack of electricity. In some cities traffic problems were compounded by motorists who drove until their cars ran out of gas on the highway. Gas stations operating in sections of Burlington, Ontario which had power were reported to have been charging prices up to 99.9 cents/liter (\$3.776/gallon) when the rate prior to the blackout was lower than 70 cents/liter. Customers still lined up for hours to pay prices most would consider price gouging. Station operators claimed they had a limited supply of gasoline and did not know when their tanks would be refilled, prompting the drastic price increases. Many oil refineries on the East Coast of the United States shut down as a result of the blackout and were slow to resume gasoline production. As a result, gasoline prices were expected to rise approximately 10 cents/gallon (U.S.-Canada Power System Outage Task Force, 2004).

Communication: As one might guess, cellular communication systems were disrupted. This was mainly due to the loss of backup power at the cellular sites as generators ran out of fuel. Wired telephone lines continued to work, although some systems were overwhelmed by the volume of traffic. Most New York and many Ontario radio stations were momentarily knocked off the air but were able to return with backup power. Cable television systems were disabled, and areas that had power restored could not receive information until power was restored to the cable provider. Internet users were also disconnected from their news source for the duration of the blackout, with the exception of dial-up access from laptop computers while their batteries had enough power (U.S.-Canada Power System Outage Task Force, 2004).

Industry: Large numbers of factories were closed in the affected areas of the blackout, and others outside affected areas were forced to close or slow work because of supply problems and the need to conserve energy while the grid was being stabilized. At one point a seven hour wait developed for trucks crossing the Ambassador Bridge between Detroit and Windsor due to the lack of electronic border check systems (U.S.-Canada Power System Outage Task Force, 2004).

Following the blackout, the U.S.-Canada Power System Outage Task Force was formed, which handled the investigation and report concerning what happened on August 14, 2003. The North American Electric Reliability Corporation (NERC) is a not-for-profit entity with the mission to ensure reliability of the bulk power system in North America. NERC develops and enforces

reliability standards, annually assesses seasonal and long term reliability, monitors the bulk power system, and educates, trains, and certifies industry personnel (NERC, 2013). The outage task force's report refers to standards set forth by NERC which were violated and were thought to have contributed to the blackout. It was determined that the blackout originated in Ohio, and four major groups of causes of the blackout were identified by the task force. These are:

Group 1: "FirstEnergy and East Central Area Reliability (ECAR) failed to assess and understand the inadequacies of FE's system, particularly with respect to voltage instability and the vulnerability of the Cleveland-Akron area, and FE did not operate its system with appropriate voltage criteria." FirstEnergy (FE) is the utility company responsible for Ohio's electricity, among other areas, and ECAR is the company's reliability council.

Group 2: "Inadequate situational awareness at FirstEnergy. FE did not recognize or understand the deteriorating condition of its system."

Group 3: "FE failed to manage adequately tree growth in its transmission rights-of-way." Right-of-way is the corridor along which power lines run, and is owned by the power company.

Group 4: "Failure of the interconnected grid's reliability organizations to provide effective real-time diagnostic support" (U.S.-Canada Power System Outage Task Force, 2004).

Group 3 mentions inadequate management of tree growth along power line corridors as a contributing factor to the blackout. This should be no surprise if taking into account the information in section 1.1 concerning the contributing factors to power outages. At 62% weather/trees are the biggest influence to power outages by a large margin, and once again, have contributed not only to

another power outage, but possibly the largest and most influential blackout in the history of North America.

The source of the blackout originated with three failed high voltage power lines which affected many lines connected to them. The failures occurred on August 14, 2003 from 3:05 p.m. to 3:41 p.m. Eastern Daylight Time. Three 345 kV (345,000 volts) power lines failed with power flows at or below each line's emergency rating. Each line tripped as a result of contact between conductors and trees that had encroached into the required clearance height between the line and the tree. The first line failed and the power load was transferred to the remaining lines, which subsequently failed as a result (U.S.-Canada Power System Outage Task Force, 2004).

Transmission lines are designed with the expectation that they will sag lower when they become hotter. The transmission line gets hotter with heavier line loading and under higher ambient temperatures, so towers and conductors are designed to be tall enough and conductors pulled tightly enough to accommodate expected sagging and still meet safety requirements. On a summer day, such as the one on which the blackout occurred, conductor temperatures can rise from 60 degrees Celsius on mornings with average wind to one hundred degrees Celsius with hot air temperatures and low wind conditions. A short circuit occurred on the Harding-Chamberlin 345 kV line due to contact between the line and a tree. This line failed with power flow at only 44% of its normal and emergency line rating. Incremental line current and temperature increases, escalated by the loss of the Harding-Chamberlin line, caused more

sag on the Hanna-Juniper line, which also contacted a tree and failed. The Star-South Canton transmission line contacted a tree three times between 2:27 p.m. and 3:41 p.m. before finally locking out (U.S.-Canada Power System Outage Task Force, 2004).

Each of these three lines failed not because of excessive sag due to overloading or high conductor temperature, but because they came into contact with untrimmed, overgrown trees. While sag of the lines may have contributed to these line failures, these incidents occurred because the trees grew too tall and encroached into the space below the line which is intended to be clear of any objects. In other words, this was not a case of too much sag into short trees, but rather too much tree present. The investigation team involved in the blackout found field evidence of tree contact for all three lines, including human observation of the Hanna-Juniper line failure (U.S.-Canada Power System Outage Task Force, 2004).

1.3 Regulatory Framework

Even though the North American Electric Reliability Corporation had standards in place during the Northeast Blackout of 2003 which pertained to vegetation clearance distances, several vegetation-induced faults occurred. The particular power lines and vegetation in question, astoundingly, were inspected in the spring of 2003, just two or three months prior to the blackout, and passed inspection (Ituen et al., 2008). Since the lines passed inspection, there was

obviously something wrong with the inspection process. Prior to the blackout of 2003, utility companies in North America were not bound by North America-wide regulations when it came to supplying electricity to customers. Instead, standards issued by NERC were mostly followed voluntarily. There was no power of enforcement granted to this regulatory body, so NERC could not force utility companies to comply with its standards. As a result, vegetation management programs have always been a convenient place for budget cutting (Jobes et al., 2008). This, however, would change.

With the passage of the Energy Policy Act of 2005, an “Electric Reliability Organization” was created to develop and enforce compliance with mandatory reliability standards. NERC applied for and was granted the designation in 2006. So, NERC standards became mandatory for North American utility companies. A NERC official asserted that the 2003 blackout also drove the development of new regulations, such as FAC-003 (Richardson, 2011). This regulation is concerned specifically with vegetation management along power transmission rights-of-way. This is aimed at reducing outages caused by vegetation, such as the large-scale cascading failure of summer, 2003. The specific purposes of FAC-003 are to 1.) Prevent outages from vegetation on transmission line rights-of-way, 2.) Minimize outages from vegetation adjacent to rights-of-way, and 3.) Maintain clearances between transmission lines and vegetation on and along transmission rights-of-way. So, FAC-003 requires all utility companies operating power transmission lines at 200 kV or higher to have a transmission vegetation management program, or TVMP, in place. This includes a schedule of inspections where utility

companies are required to identify and document clearances between vegetation and overhead lines. In addition, utility companies are required to report any sustained outages caused by vegetation which are to be broken out into three categories: 1.) Grow-ins – Outages caused by vegetation growing into lines from inside the right-of-way, outside the right way, or both, 2.) Fall-ins – Outages caused by vegetation falling into lines from inside the right-of-way, 3.) Fall-ins – Outages caused by vegetation falling into lines from outside the right-of-way (Richardson, 2011).

Since compliance with these NERC regulations has now become mandatory, associated with violations of them are monetary penalties, which can be up to \$1,000,000 per day, depending on the criticality of the situation (Wolf, 2010b). Data as of August 10, 2009 report that NERC had issued 72 violation notices, with 15 resulting in monetary penalties amounting to \$1,008,000 (Richardson, 2011).

For utility companies, correct, efficient vegetation management reduces cost and aids in continuous electricity supply by preventing damage to power lines through removal of tall trees and other vegetation. Ineffective procedures can result in the loss of reliability in electricity transmission, produce serious hazards, and expose utility companies to significant financial penalties. The key to fending off threats and complying with NERC without fines is to proactively manage power transmission line corridor vegetation in a smart way (Li et al., 2010).

Because of the more stringent, and most importantly, mandatory standards imposed by NERC, every utility company has since been forced to increase the level at which it measures and monitors vegetative threats (Jobes et al., 2008). Vegetation monitoring with regard to FAC-003 requires a physical inspection of power transmission lines on an annual basis (Ituen et al., 2008). There are roughly 450,000 miles of transmission lines in the U.S. alone, so each utility company must have a method of efficiently, accurately, and cost effectively inspecting their rights-of-way vegetation. As one might expect, the introduction of NERC FAC-003 has stirred up much debate concerning how utility companies can successfully comply with the standard and develop an effective transmission vegetation management program (Richardson, 2011). LiDAR technology is the solution examined in this study.

1.4 Research Objective

The predominant objective of this research is to employ LiDAR technology in an effective way by using it to accurately identify vegetation within a hazardous proximity to power distribution lines in the study area.

Achievement of this objective will allow a GIS-centric method for power line corridor vegetation management, where the output hazardous vegetation data are interoperable with a variety of software applications on stationary and mobile hardware. This empowers decision makers in utility and forestry companies to save money and time because they will know exactly where

vegetation needs to be removed, and can quantify the time and money needed to remove it.

This objective will be met with analysis performed on distribution power lines rather than transmission lines. As covered in section 1.1, distribution lines carry lower voltage electricity from transformers to various places such as businesses, factories, and residential neighborhoods. They can be thought of as many branches stemming from a tree trunk. Transmission lines carry high voltage electricity long distances from a power plant to the transformer that reduces the voltage for further use. They can be considered tree trunks.

It has been argued that most vegetation management programs may be effectively implemented for their transmission infrastructure, but they are typically behind in managing vegetation encroaching on their distribution infrastructure (Amadori, 2012). This creates the opportunity to analyze a portion of distribution line infrastructure in the study area.

CHAPTER 2: LITERATURE REVIEW

The need for and practice of vegetation management for utilities is not new. In fact, vegetation management for overhead lines was going on around 40 years before the transmission of electrical power. This may seem surprising, however, the telegraph line was operational in the early 1840s, and the first electric transmission line was constructed in 1882 (Wolf, 2010a). If vegetation contacted a telegraph line, it shorted out, and someone was sent out on patrol to find and repair the problem. Even back then it made sense to keep vegetation away from utility lines. Since that time, and especially since power transmission became more widespread, there has been a constant battle against encroaching vegetation. This chapter discusses various approaches to power line corridor vegetation management in detail.

2.1 Advantages of LiDAR

An advanced technology perfect for rescuing outdated, ineffective, and inefficient power line corridor vegetation management methodologies is LiDAR, which stands for Light Detection and Ranging. This technology uses an active remote sensor that works similarly to Radio Detection and Ranging (RADAR), but instead of radio waves uses laser pulses. The range to an object from the sensor can be calculated based on the time it takes a laser pulse to return to the sensor once emitted. The repetition rate, or the rate at which the laser is pulsing, affects how many data points are collected. LiDAR sensors today are capable of

emitting pulses at a rate of 200 KHz or 200,000 pulses per second. While the laser is pulsing, the scanner is oscillating at a certain frequency known as the scan frequency (Young, 2011). The result of a LiDAR collection is referred to as a point cloud, and is a three-dimensional rendering of object surfaces in the form of a random sampling of points in 3D space. The higher the number of points collected, the better the definition of scanned surfaces will be. The density of points or amount of 3D space between points within a point cloud depends on the repetition and scanning rates of the sensor.

LiDAR collection systems use a powerful laser that includes a transceiver and receiver, a GPS receiver, an inertial measurement unit (IMU), and a scanner. The laser typically produces a wavelength of light between 532 and 1550 nanometers, but varies depending on platform and application. The transceiver emits pulses and return pulses are picked up by the receiver. The GPS receiver reports the location of the sensor platform in the form of latitude, longitude, and elevation. The inertial measurement unit measures the attitude of the sensor attached to its platform. Attitude is known as the roll, pitch, and heading of the platform. Roll is rotation about the y axis, pitch is rotation about the x axis, and heading is rotation about the z axis, also known as yaw. The platform can be a helicopter, fixed wing aircraft (figure 2.1), motor vehicle (figures 2.2 and 2.3), or even a stationary terrestrial setup (figure 2.4). Typically, a terrestrial scanner does not have an IMU. A mirror attached to the scanner spreads the pulses across the surface the system is mapping (Young, 2011).

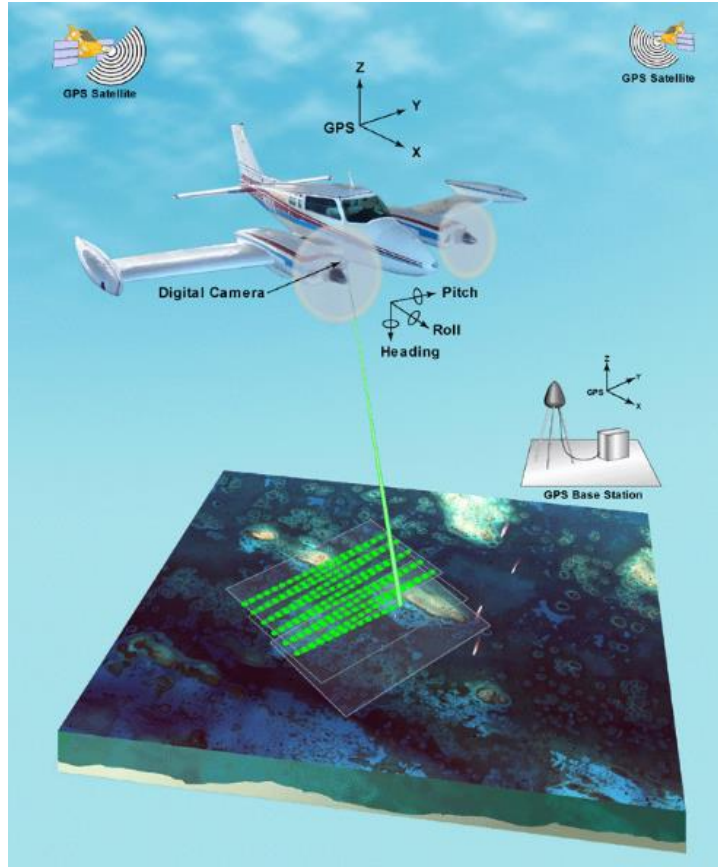


Figure 2.1 – Example of a fixed wing LiDAR platform collection
 (<http://coastal.er.usgs.gov/hurricanes/ivan/lidar/lidar.html>)



Figure 2.2 – Example of a mobile LiDAR sensor mounted atop a van (Photo by Earth Eye, LLC)

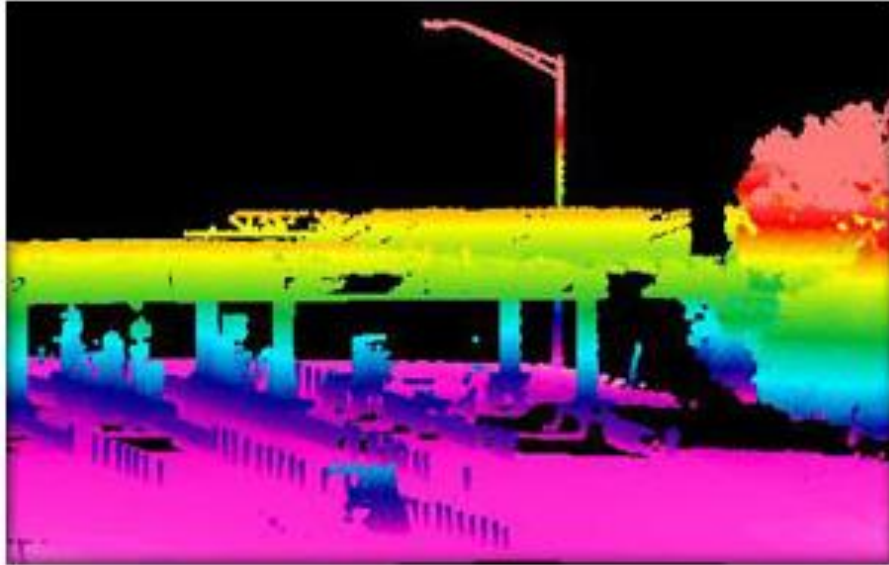


Figure 2.3 – Example of mobile LiDAR data collected near a tollbooth (Image by Earth Eye, LLC)



Figure 2.4 – A stationary terrestrial LiDAR system (British Geological Survey. Non-commercial use license - https://www.bgs.ac.uk/about/copyright/non-commercial_use.html)

LiDAR can essentially “see through” vegetation to the same extent humans can, for instance, when no foliage is present. If the point sample spacing is not dense enough or if the vegetation is very thick, it is less likely that the LiDAR system will be able to emit pulses through the vegetation (Young, 2011). The penetrative capability to show ground and sub-canopy has attracted much attention, as the limitation of approaches that rely on a clear line of sight, such as aerial photography and visual terrestrial patrols, has been removed (Wolf, 2010b).

Otto Lynch, vice president of Power Line Systems, remembered attending a power transmission conference in the early days of LiDAR. A presenter complained about transmission conductors spoiling the beautiful contour mapping he was trying to get done. Excitedly, several of the engineers asked, “You can see the conductor?” Soon utility companies were working with surveying companies to develop a LiDAR system that emphasized power transmission and distribution needs (Wolf, 2010b).

2.2 LiDAR vs. Manual Vegetation Analysis Techniques

When compared to manual methods of vegetation analysis LiDAR offers advantages in the form of speed, coverage, reduced labor, accuracy, objectivity, and ability to be audited. The following are examples:

- *LiDAR is faster* – It is time consuming to take a single point measurement with a ground-based rangefinder. Modern sensors can emit 200,000

pulses per second, which are essentially individual measurements. Also, LiDAR data collection usually takes several hours for a corridor project that is hundreds of miles long, whereas a ground crew can only survey about five to ten spans of line per day (Ussyshkin et al., 2011).

Additionally, foot patrols take a lot of time, and helicopters are expensive to operate and are taxing on the operator and pilot.

- *LiDAR provides more coverage* – Coverage is indiscriminant and records survey points for the entire right-of-way, capturing vegetation that may not appear to be a potential hazard upon visual inspection. LiDAR does not suffer from the requirement of a true line of sight to take measurements, as partial openings in vegetation will allow the laser pulses to penetrate the tree canopy.
- *LiDAR requires less labor* – Conventional ground-based techniques can be viewed as labor intensive due to the manual inspection for each line. In contrast, LiDAR is labor extensive. Only one ground-based technician is required for every 20 kilometer radius of survey coverage, with the aircraft and sensor operated by a pilot and LiDAR operator.
- *LiDAR is more accurate* – It is possible to reach $<\pm 0.33$ feet absolute accuracy with adequate ground control and even greater relative accuracy. In comparison, a high quality commercially available handheld laser rangefinder will typically be accurate in relative terms from ± 1 foot to 3.3 feet.

- *LiDAR is objective, not subjective* – Conventional survey methods are inherently subjective, as they rely on an initial visual interpretation best estimate of the distance between two objects, which may lead to overzealous removal of vegetation determined to be a problem. At the same time, infringement locations will be missed due to the coarse spatial coverage of this manual technique.
- *LiDAR provides an audit trail* – LiDAR survey provides actionable deliverables to direct line maintenance personnel to the specific hazards within and adjacent to the right-of-way and creates an audit trail. The data can be marked up once a violation has been addressed by an arborist, particularly if the data are delivered in a format compatible with handheld devices (Ussyshkin et al., 2011).

Compared to LiDAR, visual and photographic or video patrols suffer the limitations of relying on the subjective interpretations of a conductor position and whether vegetation is truly infringing. While they will provide a more rapid means of inspection than ground-based point measurements, and aerial photographs will provide a record of the patrol, they will suffer from the inability to take accurate measurements of the conductors and vegetation points (Ussyshkin et al., 2011).

Today's LiDAR sensors can typically record up to four or more returns (reflections) per laser pulse. The four returns can record the canopy, sub-canopy, and ground surface, ensuring the vertical profile of everything is captured. This is most definitely a stand-out capability of this technology,

especially with regard to seeing layered vegetation. Just as valuable is the fact that, with sufficient point density, conductor lines can also be seen as a result of laser pulse returns.

Also, Ituen et al. (2008) suggested that unlike 2D imagery, the elevation component of airborne LiDAR provides the ability to represent vertical structure details with very high accuracy, which is an advantage for applications focusing on analysis of elevated features such as 3D vegetation mapping.

Historically, manual inspection methods have been used by a majority of utility companies to manage rights-of-way (ROW) vegetation (Young, 2011). These mostly include foot and/or vehicle patrols and aerial patrols by helicopter while using various tools and techniques for measuring distances between vegetation and power lines (Mills et al., 2010). Like many utility companies, American Electric Power (AEP), based in Columbus, Ohio, has used an aerial patrol technique involving both human visual inspection and video to prioritize vegetation work. Jobes et al. (2008) argued these can be great processes, but they can be subject to human error. The amount of estimation certainly contributes to the error. Another utility company, Hydro One, based in Ontario, Canada, has also historically used ground patrol surveys and helicopter surveys to manage transmission line right-of-way. Below is an example of the company's workflow for managing vegetation (figure 2.5).

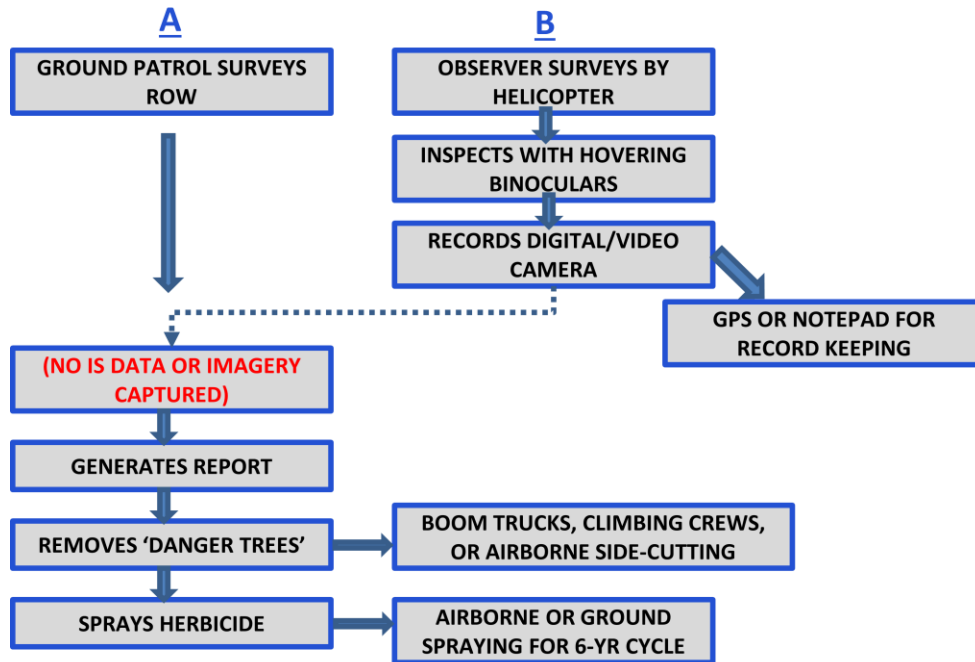


Figure 2.5 – Hydro One’s workflow

When Hydro One used helicopter patrols for inspection, only a notepad or GPS coordinates were used to record the locations of potentially dangerous vegetation. As for the distance between the vegetation and power lines, measurements taken by a field crew were done using laser measuring devices, optical measuring devices, or telescoping poles. The box including the text “(NO GIS DATA OR IMAGERY CAPTURED)” (figure 2.5) is particularly puzzling. No GIS of any kind was used, regardless of inspection method, which has been typical for many utility companies. The workflows these two companies used to identify dangerous vegetation and manage it required two patrols to ensure the job had been done satisfactorily. The first pass was to identify the vegetation, and the second pass was to ensure that vegetation had been removed by the arborists and/or forestry contractors (Ituen et al., 2008).

Again, referring back to the Northeast Blackout of 2003, the vegetation that caused the blackout was inspected just months prior using the same methods just discussed. This fact should, at a minimum, evoke thoughts about the lack of effectiveness of these vegetation management methods, but ultimately spawn a debate about what can be done to better manage vegetation along power line rights-of-way. A faster, more effective, more accurate way to identify dangerous vegetation along power line corridors is needed, and should hinge upon more advanced technology. After all, vegetation management is one of every electric utility company's largest operating costs, and the industry is spending an estimated \$2 billion to \$3 billion every year on this activity (Wolf, 2010a).

There were only two instances of meaningful studies found in the literature where utility organizations actually took the time to evaluate LiDAR against their normal methods of vegetation management. American Electric Power (AEP) and Bonneville Power Administration (BPA) performed the documented studies. In the case of AEP, in an attempt to better its processes, LiDAR was flown over 2,500 miles of transmission lines to identify any immediate or potential vegetative threats that may have been missed by the company's helicopter surveillance team, which typically flew along all transmission lines at least annually (Jobes et al., 2008). The annual helicopter inspections would allow visual identification of dangerous trees or aggressive underbrush. The comparison of these two techniques revealed 247 additional critical events where vegetation or tree growth represented a serious threat to power lines, more than AEP's existing

methods had found. Figure 2.6 shows an example of a hazardous tree missed by prior aerial survey, with GPS coordinates confirmed by handheld tools used by the ground crew (Jobes et al., 2008).

Prior to the employment of LiDAR technology, it was never possible for AEP to be 100% sure that all vegetation had been removed or that it had been removed well enough to eliminate the immediate threat. For the first time ever, LiDAR allowed the AEP team to measure the performance of a vegetation management vendor and ensure that threats were mitigated swiftly (Jobes et al., 2008).

In the case of BPA, a federal nonprofit agency based in the Pacific Northwest and part of the Department of Energy, five power line corridor vegetation inspection techniques were compared in order to critically evaluate vegetation management programs in place in the utility industry (Narolski, 2010).



Figure 2.6 – A hazardous tree missed by AEP’s aerial survey but detected with LiDAR (Photo by AEP)

The following techniques were compared:

- Transmission line maintenance (TLM) working patrol field inspection
- Helicopter aerial survey with TLM observers
- Helicopter aerial survey with natural resource specialist (NRS) observers
- Contract field ground inspection conducted by a private firm
- LiDAR remote sensing

BPA wanted to determine which techniques were most accurate in identifying hazardous vegetation. Table 2.1 shows a comparison of “danger tree” grow-in inspection methods. Figure 2.7 shows the accuracy of determining high brush clearance conflicts by method used.

Table 2.1 – Comparison of “danger tree” grow-in inspection techniques

Danger Tree Grow-In Inspection Method Comparison		
Method	Shared points	Unique points for first method
Aerial TLM vs. Ground contractor	17	61
Aerial TLM vs. Ground TLM	123	81
Aerial TLM vs. aerial NRS	191	14
Ground contractor vs. Aerial TLM	17	603
Ground contractor vs. Ground TLM	63	372
Ground contractor vs. Aerial NRS	28	602
Ground TLM vs. Aerial TLM	123	321
Ground TLM vs. Ground contractor	63	117
Ground TLM vs. Aerial NRS	93	273
Aerial NRS vs. Aerial TLM	191	48
Aerial NRS vs. Ground contractor	28	114
Aerial NRS vs. Ground TLM	93	138

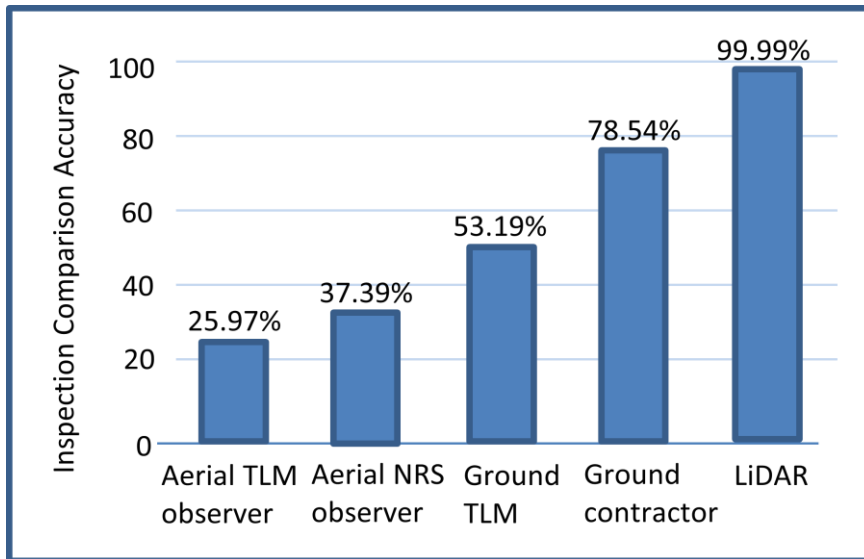


Figure 2.7 – Comparison of “danger tree” grow-in inspection techniques

As determined by BPA, LiDAR outperformed all other field inspection techniques by locating the most clearance violations. This was true even after accounting for an approximate 12% rate of false positives found in verifying LiDAR reports in the field. These false positives were objects other than vegetation such as transmission line hardware, light poles, abandoned wood poles, and birds (Narolski, 2010). LiDAR stood out in this study because of the number of false negatives found in more subjective, human-based inspection methods. While the LiDAR approach located false clearance issues, other methods missed real clearance issues.

An interesting error occurred when 2,800 reports of vegetation were incorrectly identified as “danger tree grow-in” by TLM crews. Clearance distances were actually greater than the specification for this category. Because of this, unnecessary time and resources were diverted from working on critical

problems in order to sort through data to differentiate the mistaken reports. Even worse, they were responded to in the field. These diversions were costly, unnecessary, and increased the risk of missing more critical work (Narolski, 2010).

In the “high brush” category LiDAR outperformed the other inspection techniques, according to BPA. The private firm’s ground inspection and TLM working patrols found the next highest number of field data points. Helicopter surveys performed relatively poorly in identifying any high brush. In terms of detecting vegetation-to-conductor clearance issues, it was determined that only a slight gain in accuracy occurred when using natural resource specialist observers versus transmission line maintenance observers during helicopter aerial inspections. However, other program benefits were arguably important enough for BPA to consider instituting a vegetation-only helicopter aerial inspection with natural resource specialist observers as a new work practice into the company’s vegetation management program. Narolski (2010) suggested that natural resource specialist observers gain a better understanding of the character of the ROW they manage by participating in an annual helicopter tour of their lines. He argued that the aerial perspective they gain imprints spatial relationships in their minds and enhances their memory of the corridors, ROW, and circuits entrusted to them in ways that cannot be obtained from the ground-only perspective.

The study by BPA, as reported by Narolski (2010), was more extensive in that it compared more manual inspection methods to LiDAR, whereas the AEP study, as reported by Jobes et al. (2008), only compared helicopter observations

to LiDAR. In fact, the study by BPA actually went to the trouble to compare results between two different kinds of human observers in helicopter surveys. Further, the BPA study also compared two different kinds of human ground field survey observers. It seems as though the BPA study is somewhat more credible because of the comprehensive comparisons made and the quantification of the results. However, one could argue that if ground surveys are not used, they don't need to be evaluated against other methods.

2.3 Satellite and Aerial Imagery Approaches

Kobayashi et al. (2008) proposed the use of commercially available multispectral stereo satellite image pairs and specially designed software to identify trees endangering power transmission lines. First, the images and transmission tower data were loaded along with the "danger zone" so that the pixel coordinates of each could be calculated. Each pixel within the danger zone was scanned, and the normalized difference vegetation index (NDVI) was calculated in order to determine healthy vegetation, which could endanger power lines. Vegetation was considered healthy when its NDVI was greater than 0.22 – 0.4. Coordinates of healthy vegetation pixels were then recorded. The height of each pixel was determined by stereo matching and subsequent digital surface model generation. This provided the means by which to measure the distance of the vegetation from the conductor. The software displayed highlighted pixel clusters representing hazardous trees based on their proximity to the power

lines. Kobayashi et al. (2008) maintained that utilization of satellite images offered improvements over airplane-based approaches due to wide area coverage, frequent overhead passes, the ability to view areas with restricted physical access, and potential lower cost from processing a large area at one time in an automated workflow. While these are valid reasons why one might turn to satellite imagery for power line corridor vegetation management, the authors did not discuss the relatively coarse spatial resolution of the imagery used. Since the range in resolution for multispectral images used was between four and five meters, and the range for panchromatic images was between 0.4 and 0.61, finding conductor cables would be a challenge, which is why separate data for this were brought into the software. Further, the authors did not discuss how the data showing hazardous trees could be exploited to physically find them on the ground, but the assumption probably could be made that a list of coordinates would be referenced while using a GPS receiver.

Mills et al. (2010) also proposed using imagery to detect trees, measure relative position of them in relation to power lines, and estimate tree height. Tree detection was accomplished using a pulse-coupled neural network and morphologic reconstruction applied to multispectral imagery. Testing revealed that a detection rate of 96% in relation to manual tree delineation was achieved, which sounds promising. However, aerial frame camera images were used, which are capable of significantly higher resolution than the imagery used in the study by Kobayashi et al. (2008). Relative positioning was accomplished simply by directly georeferencing the poles and trees in the images. Direct

georeferencing takes a point in the image plane and maps it to an inertial reference frame using the position of the onboard GPS antenna and the orientation of the aircraft registered by an inertial measurement unit. The bases of trees were used to derive tree location coordinates; however these were estimated due to the fact that tree crowns obstructed them from view – a fundamental problem with satellite and aerial images with regard to this type of analysis. Once the absolute locations of poles and trees were determined, simple trigonometric identities were applied to compute cross track and along track measurements. Problems with this approach were that tree crown size was not taken into consideration, and conductor cables were not even mentioned, which detracts from the validity of the study. Tree height estimation was accomplished through stereo matching, but the average image overlap of less than 50% was an issue. This amount of overlap cannot guarantee two views of each object, which are required to measure heights in stereo. Mills et al. (2010) actually compared LiDAR to stereo matching for power pole height estimation, and results show LiDAR was superior (table 2.2).

It was noted that with the wide use of object-based approaches in remote sensing, individual tree crown delineation becomes a key research focus to improve the accuracy of plant information extraction. Local maxima/minima, template matching, region growing, and multi-scale edge detection algorithms were discussed in this study (Mills et al., 2010).

Table 2.2 - LiDAR vs. stereo height estimation for poles

	LiDAR System	Stereo Matching
Detection Rate	95.4%	95.0%
Sample Size	44	40
Average Error	0.3 m	1.1 m
Standard Deviation	0.4 m	1.5 m
Worst Case	1.5 m	4.7 m

Where trees had constant spacing and crown sizes, the local maxima/minima approaches worked extremely well; however, this configuration of trees appears mostly in orchards or man-made forests and not power line corridors. The template matching approach also proved to do well in areas where mostly trees existed. Since the assumption of most tree crown delineation algorithms is that the center of a crown is brighter than the edge of a crown in an image, Li et al. (2008) thought region growing methods have great potential.

Multi-scale edge detection techniques could not keep the same shape of the tree crowns in the input image due to a Gaussian smoothing filter, so this may limit their application. Surprisingly, Li et al. (2008) maintained that individual tree crown delineation has great potential to make power line corridor vegetation management more effective, but there was no mention of how to utilize the tree crown data, nor was there any mention of power poles, lines, or anything other than tree crowns in the analysis. This literature would be more helpful if it indicated a complete workflow that included how to apply the tree crown data to power line corridors, rather than examining only one piece of the solution.

2.4 LiDAR Fusion

LiDAR sensors and digital cameras have been used separately to map power line corridor scenes in the past. Ituen et al. (2008) suggested that merging their data would provide an even wider range of corridor scene information. They proposed the use of LiDAR along with multiple viewing angle direct georeferenced digital cameras to develop a change detection method of vegetation management, which was a new approach. The images and LiDAR data can be overlain with data collected from a previous survey, which would allow easy detection of the change that has occurred in the vegetation over time. Vegetation growth rates could be projected better as a result, which helps prioritize work. This is an attractive approach because these tools can provide high resolution imagery of the power line scene. Thus, it will depict the corridor vegetation as well as small objects such as insulators with high quality, three-dimensional information. Combining these data types, however, presents unique challenges, particularly with correctly fusing data from two independent sources. It would take testing to determine the maximum flight speed that would be within the tolerance level for accuracy of the two sensors. Having discussed the advantages of LiDAR already, it seems as though this fusion technique would be a great candidate for effective, accurate analysis.

There have been other attempts to fuse LiDAR data with complementary data types. Frank et al. (2010) proposed vegetation management of utility corridors using high resolution hyperspectral imagery in combination with LiDAR data and digital aerial imagery. They discussed a classification approach using

support vector machines (SVM) and a spectral angle mapper (SAM) applied to the datasets to test their ability for discrimination of various vegetation species. An SVM is an algorithm that performs classification by finding the hyperplane that maximizes the margin between classes. The vectors that define the hyperplane are called support vectors and are based on input training samples. An SAM is a spectral classification that uses an n -D angle to match pixels to reference spectra, by calculating the angle between them and treating them as vectors. The vectors are in a space where the number of dimensions equals the number of bands (Kruse et al., 1993). The addition of hyperspectral imagery added the capability to provide a more comprehensive approach to vegetation management. Being able to map individual vegetation species provided the opportunity to calculate individual growth models for every species, identify dead and unhealthy trees, fast growing invasive species, and invasive species in general. Frank et al. (2010) also measured conductor clearances in relation to vegetation. This was done by transforming LiDAR data points that represented conductors into vector data, then running algorithms that measured the distance between vegetation LiDAR points and the vector data. With this solution, not only was dangerous vegetation identified, but the species of vegetation were shown. This is what was meant by hyperspectral imagery providing a more comprehensive approach to vegetation management. As far as species classification, the overall accuracy of the support vector machine was over 10% better for every dataset than the spectral angle mapper. Merged hyperspectral imagery and LiDAR performed best in both classification methods with 80% for

spectral angle mapper and over 92% for the support vector machine, whereas LiDAR performed poorest. Table 2.3, figure 2.8, and figure 2.9 show overall and individual species user accuracies for each data type.

Table 2.3 – Overall accuracies – Spectral Angle Mapper and Support Vector Machine

SAM	Overall Accuracy	Kappa Coefficient
LiDAR	36.47%	0.2873
Hyperspectral	71.09%	0.6615
Hyperspectral + LiDAR	79.58%	0.7609

SVM	Overall Accuracy	Kappa Coefficient
LiDAR	54.24%	0.4859
Hyperspectral	83.26%	0.8039
Hyperspectral + LiDAR	91.75%	0.903

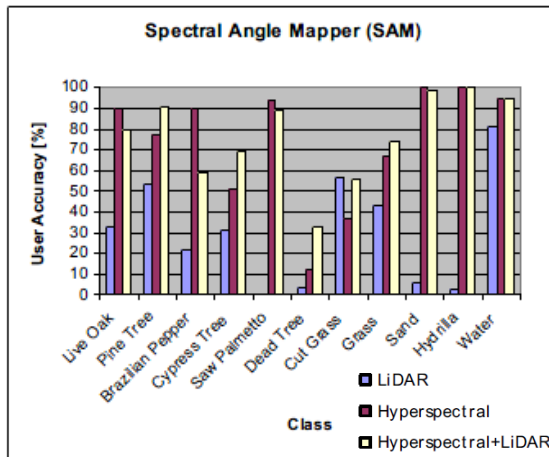


Figure 2.8 – Individual accuracies for the spectral angle mapper

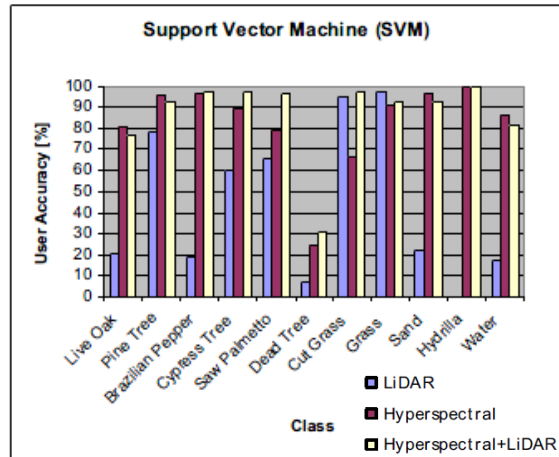


Figure 2.9 – Individual accuracies for the support vector machine

2.5 Conclusions about Existing Research and Thesis Rationale

This chapter discussed the various approaches to accomplishing power line corridor vegetation management. Some could be argued old and inefficient, such as field patrol, and some could be argued quite experimental and fairly unfeasible at present. This study seeks something in between. The evolution of power line corridor vegetation management is influenced by advances in technology as are many aspects of human activities. The two heaviest technological influences to this practice have been argued to be the personal computer and LiDAR (Guggenmoos, 2012). The computer introduced spreadsheets, relational databases, email, and data processing, while LiDAR brought a new way to precisely, accurately, quickly, and thoroughly map features in three dimensional space. In depth discussion of LiDAR provided the basis on which to investigate its application to vegetation management. The cumulative attributes of LiDAR, it was shown, make it a prime candidate for this type of analysis.

Reinforcing this was the discussion that compared LiDAR to various other vegetation management techniques, where the advantages of LiDAR could be quantified though accuracy and the amount of dangerous vegetation found or missed. Without great surprise, methods of power line corridor vegetation management which relied on manual human actions for observation and documentation of findings, whether from above in a helicopter or on the ground, proved to be the least effective methods of inspection. This is not to say they

cannot get the job done, but in today's world they pale in comparison to other methods which hinge upon technological advances.

In general, the literature does not include a great deal of scholarly articles on methodology that uses LiDAR data to detect dangerous vegetation along power line corridors and exploit this information in an effort to accomplish this study's objective. There is plenty of evidence showing that LiDAR data *have* been used for this purpose, but no specific workflows have been discovered through literature searches. Further research and experimentation can help fill this gap.

CHAPTER 3: CONCEPTUAL FRAMEWORK AND METHODOLOGY

This chapter focuses on the specific methodology used to detect and map vegetation deemed hazardous to the safe operation of power lines.

3.1 Study Area

The study area covers approximately seven linear miles of 69 kilovolt distribution power line corridors in a residential/commercial section of Callahan, Florida, just outside of Jacksonville (figure 3.1).

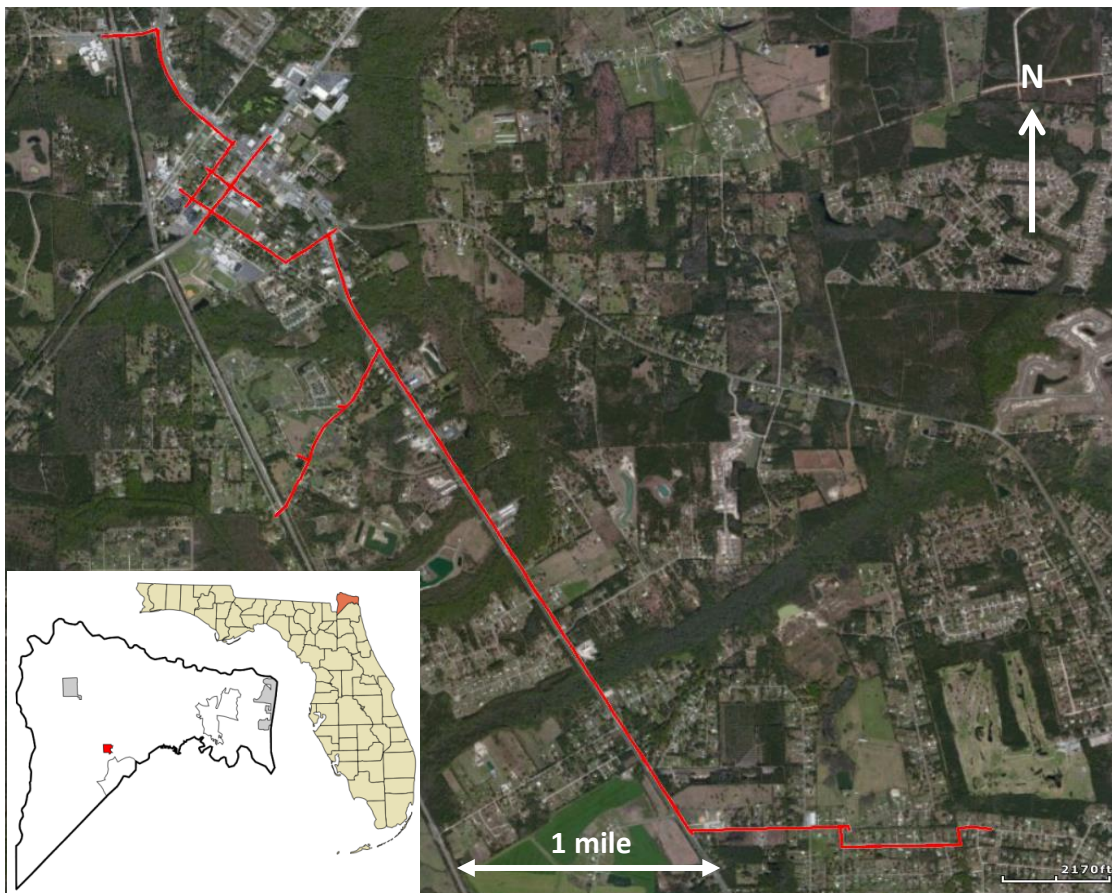


Figure 3.1 – Study area (Inset from Wikipedia, image from ESRI. Creative Commons license for inset - http://en.wikipedia.org/wiki/Wikipedia:Text_of_Creative_Commons_Attribution-ShareAlike_3.0_Unported_License)

These distribution lines are characteristic of those many of us might see while driving around town, perhaps to and from work or the grocery store (figure 3.2). Distribution lines, sometimes referred to as ‘feeder lines’ in the utility industry, distribute electricity from substations to residential neighborhoods and businesses. Figure 3.2 was created by randomly choosing a location along the study area power line corridor and going into “street view” in Google Earth. It is immediately apparent there is vegetation growing in close proximity to the power lines, which makes this area a good one for the type of analysis that will be conducted in this study.



Figure 3.2 –Power lines found in the study area (GoogleEarth Pro).

It is important to note a significant characteristic of the study area and Florida as a whole, which influences power distribution line vulnerability. The entire state of Florida has historically been subject to powerful storms and hurricanes over many years, and many residents can attest to the fact that severe weather has impacted their access to electric power at one time or another. Callahan, like all cities in Florida, is influenced by weather patterns developed both in the Atlantic Ocean and Gulf of Mexico, which can pose major threats. These threats are usually not directly from wind toppling power line support poles, but mostly because of wind moving vegetation into power lines. For this reason, examining any part of Florida's power transmission or distribution line corridors for vegetation encroachments is especially worth the time.

3.2 Data Sources

There are two main data sources that were used to perform the analysis in this chapter. These include LiDAR data and a digital, true color RGB, aerial image orthomosaic. Both datasets were collected and provided by Earth Eye, LLC, of Orlando, FL. The software used to perform the analysis in this study is called Earth Shaper and is an application proprietary to Earth Eye, LLC. Details about the source data are provided in the following sections.

3.2.1 LiDAR Data Details

Metadata about the LiDAR data used in this analysis is in table 3.1.

Figures 3.3 and 3.4 show the sensor system components and aircraft type used in the LiDAR and aerial image data collection.

Table 3.1 – LiDAR metadata

Data Format	LAS (.las)
Sensor	Leica Geosystems ALS60
Platform	Cessna 207 Single Engine Aircraft
Sensor Mode	Linear
Coordinate System	NAD 1983 State Plane Florida East – FIPS 0901 – Feet (2236)
Collection Date	5/30/2012
Point Density	35 points/meter ²
Vertical/Horizontal Accuracy	< 15 centimeters



Figure 3.3 – Leica Geosystems ALS60 LiDAR system components (Photo by Leica Geosystems. Terms of Use - http://www.leica-geosystems.com/en/Web-Site-Legal_1540.htm#6)

A sample of the LiDAR data used for this study is shown in figure 3.5. The point cloud is colored by relative height, and it is apparent that power line conductors, most support poles, trees, and buildings are clearly visible. This is due to the relatively high point density of the data at an average of 35 points per meter². This level of point density is ideal in order for conductor wires to appear in the point cloud, along with several levels of tree canopy.



Figure 3.4 – A Cessna 207 aircraft (Wikipedia, license - http://en.wikipedia.org/wiki/Wikipedia:Text_of_Creative_Commons_Attribution-ShareAlike_3.0_Unported_License)

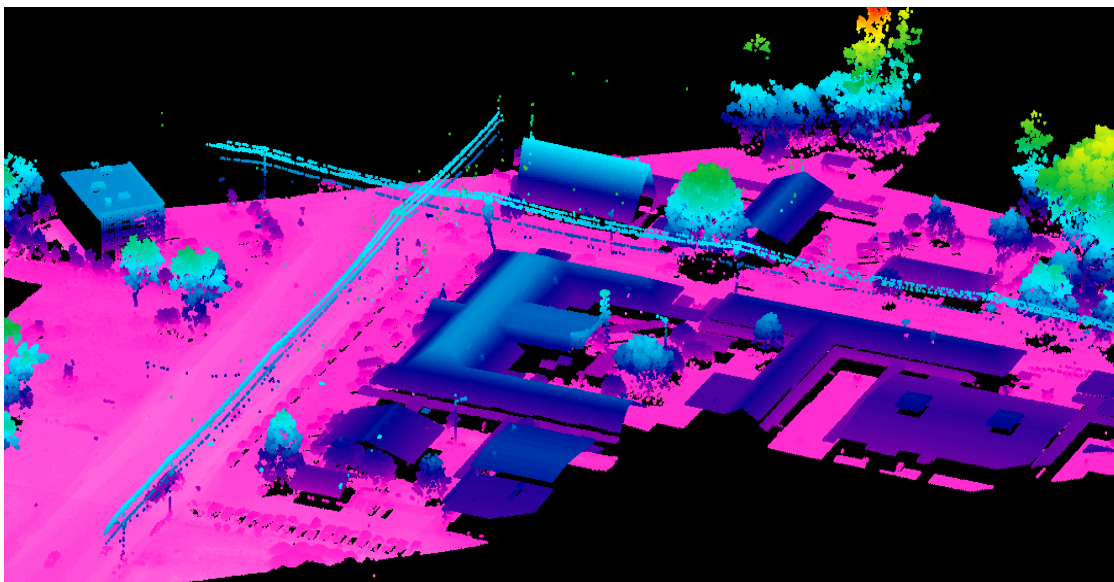


Figure 3.5 – 3D view of the LiDAR source data, colored by relative height

Figure 3.6 shows the results of the LiDAR collection over the entire study area. The data are displayed in greyscale according to intensity, which means that if a laser pulse is strongly reflected from a feature it will display more toward the white end of the scale, and less reflectance from a feature will display more toward the black end of the scale. The data are displayed this way only to allow the vector data representing the conductors to stand out, and this study will not be concerned with intensity values. The vector data were created using a process that will be explained later.

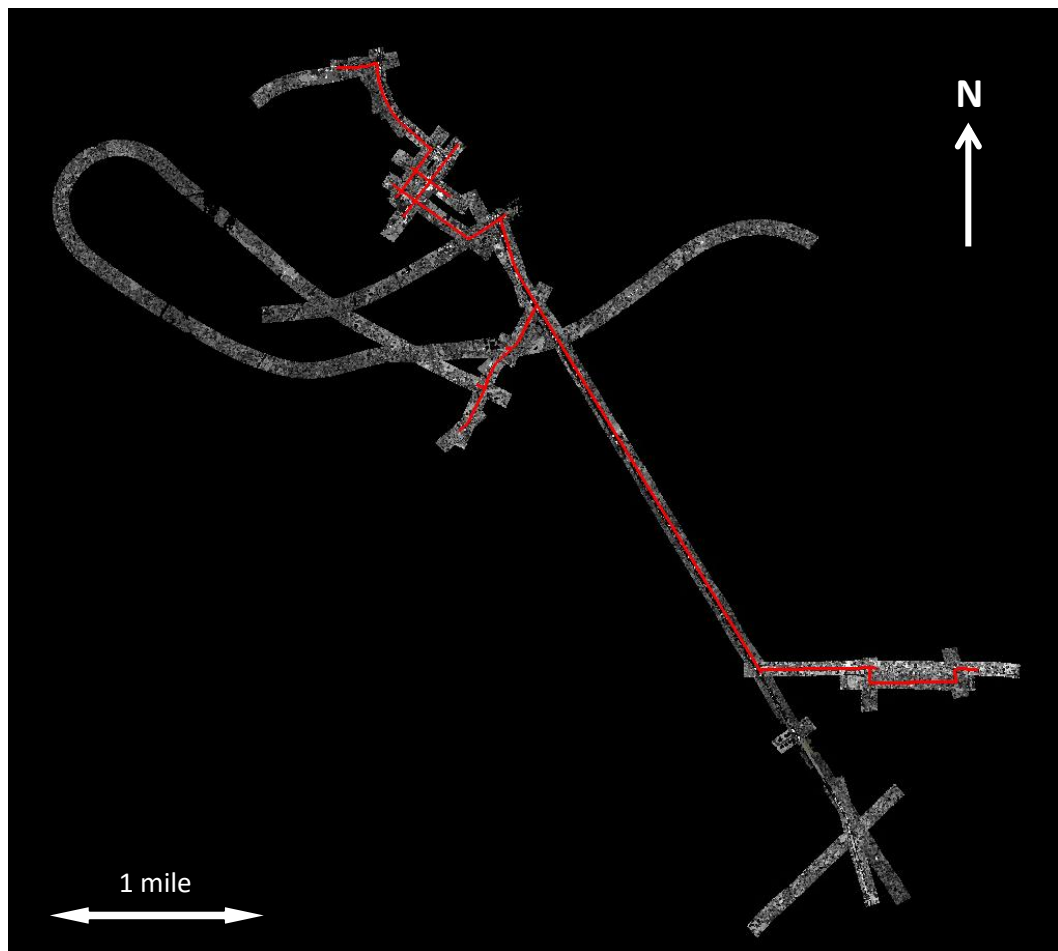


Figure 3.6 – The source LiDAR data displayed as an 8-bit intensity image

The raw point cloud was preprocessed by the data vendor after collection with proprietary filtering (classification) algorithms and formatted to LAS. LAS is “a public file format for the interchange of 3-dimensional point cloud data between data users,” as defined by the American Society for Photogrammetry and Remote Sensing (ASPRS), the organization that initiated the format. LAS is not an acronym, but simply part of the word laser. The LAS format was created as an alternative to the generic ASCII file interchange, which was argued by ASPRS to be slow to be read and interpreted, too large in file size many times, and that all information specific to the LiDAR data was lost (ASPRS, 2013). Part of the LAS format is a classification scheme. There are 256 possible classes in the scheme, where classes 64 – 256 are user definable. Table 3.2 shows all possible classes, with those used in this study highlighted in green.

Table 3.2 – LAS 1.4 classes with used classes in green

Class Value	Description
0	Created, never classified
1	Unclassified
2	Ground
3	Low Vegetation
4	Medium Vegetation
5	High Vegetation
6	Building
7	Low Point
8	High Point
9	Water
10	Rail
11	Road Surface
12	Bridge Deck
13	Wire – Guard (Renamed to “ROI” for this study)
14	Wire - Conductor
15	Transmission Tower
16	Insulator
17	Reserved
18-43	Reserved
64-255	User definable

Proof that LiDAR data are being used to analyze power lines is the fact that the LAS 1.4 format includes classes for wire guard (13), conductor (14), tower (15), and insulator (16). Also, evidence of the gradual adoption of LiDAR over time to analyze power lines is shown by the fact that definitions for classes 13 – 16 did not exist until LAS format version 1.4 was finalized in 2011, eight years after version 1.0 was introduced.

For the preprocessing, a ground filter was run on the LiDAR data to assign the ground points to class 2. In this case, the LiDAR data vendor left out the building class (6) to speed up processing time and reduce labor, as the data were collected at no charge to the customer. The buildings represented in the LiDAR data were classified as one of the vegetation classes as a result. Figures 3.7 and 3.8 show a sample of the source data classified as obtained.

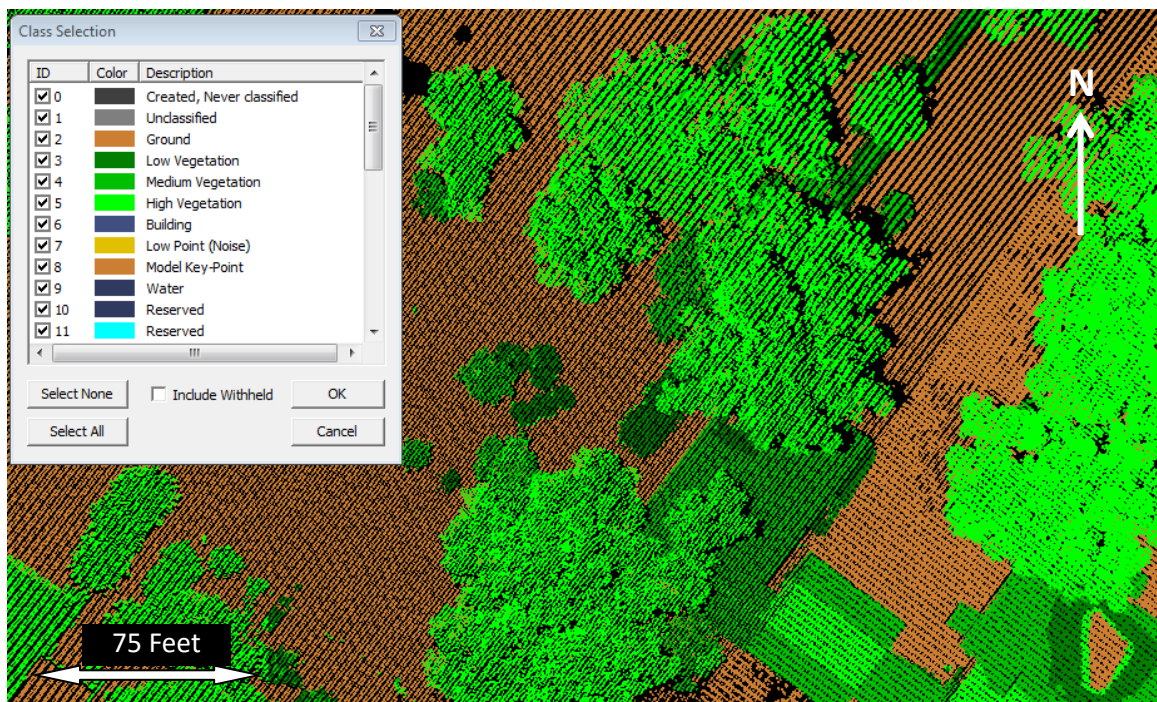


Figure 3.7 – Source LiDAR data colored by class

The absence of the building class and the fact that buildings have been lumped into three vegetation classes are not necessarily a problem. For this analysis, the most critical detail regarding classification of the data is that points representing conductors are in a different class than vegetation or any other classes. However, they too have been put in the vegetation classes (figure 3.9). The process of conductor classification is a necessary step, and will be explained later.

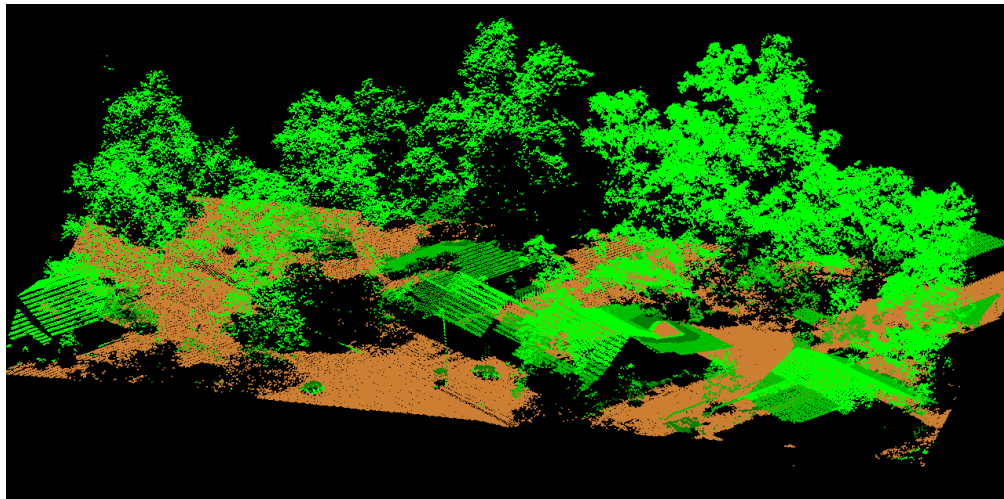


Figure 3.8 – Source LiDAR data colored by class (3D view)

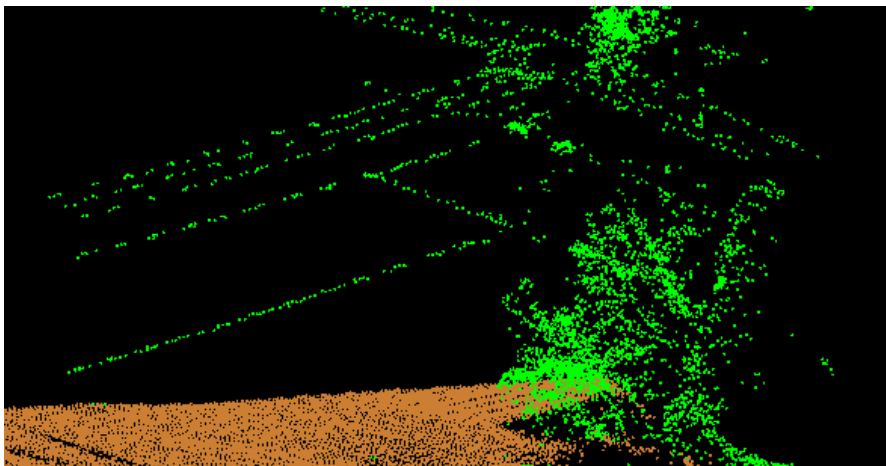


Figure 3.9 – Conductors in the high vegetation class (3D view)

3.2.2 Aerial Image Data Details

An integrated aerial camera was used to collect the image data, so collection of both datasets occurred at the same time using one sensor unit. This means it was not necessary for the data provider to register one dataset to the other due to measures taken to calibrate the two sensors simultaneously. This is a key advantage of the configuration of the hardware used to collect the data, which reduces processing time needed before data exploitation and reduces cost. The camera captured true color RGB image frames of the study area that were processed into a seamless orthomosaic by the data vendor. Table 3.3 shows the image metadata. Figure 3.10 shows an example of the output image resolution at close range; figure 3.11 shows the image dataset collection over the entire study area, and figure 3.12 is a closer view of a section of the mosaic dataset. The conductors are visible due to the high spatial resolution.

Table 3.3 – The image dataset metadata

Image Format	Enhanced Compressed Wavelet (ECW), (.ecw)
Sensor	Leica RCD-105 Medium Format Digital Aerial Camera
Spectral Sensitivity	True color RGB
Spatial Resolution	0.25 feet/pixel
Collection Date	5/30/2012
Coordinate System	NAD 1983 State Plane Florida East - FIPS 0901 - Feet (2236)



Figure 3.10 – A 15 foot long minivan clearly resolved by the camera

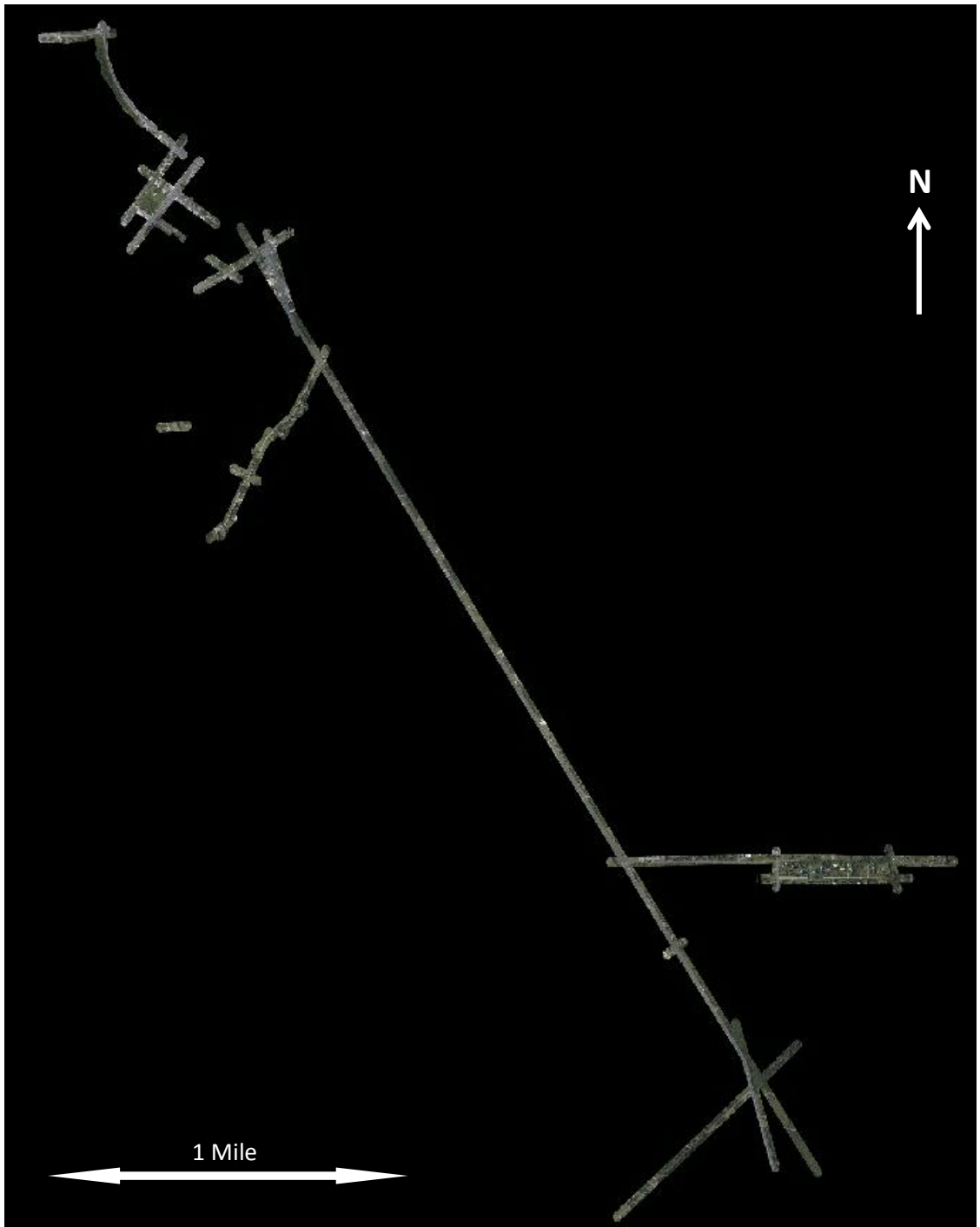


Figure 3.11 – The aerial image orthomosaic over the entire study area



Figure 3.12 – A sample of the study area orthomosaic

3.3 Methodology

This section explains the procedures (figure 3.13) used to exploit the source LiDAR data in order to provide a GIS-centric way to map dangerous vegetation along the study area power line corridors. The process starts with a LiDAR point cloud and ends with dangerous vegetation polygons and power line conductor vectors in shapefile and KMZ formats. These data are produced in a way that makes meaningful information available through attributes which can be viewed in a variety of software applications.

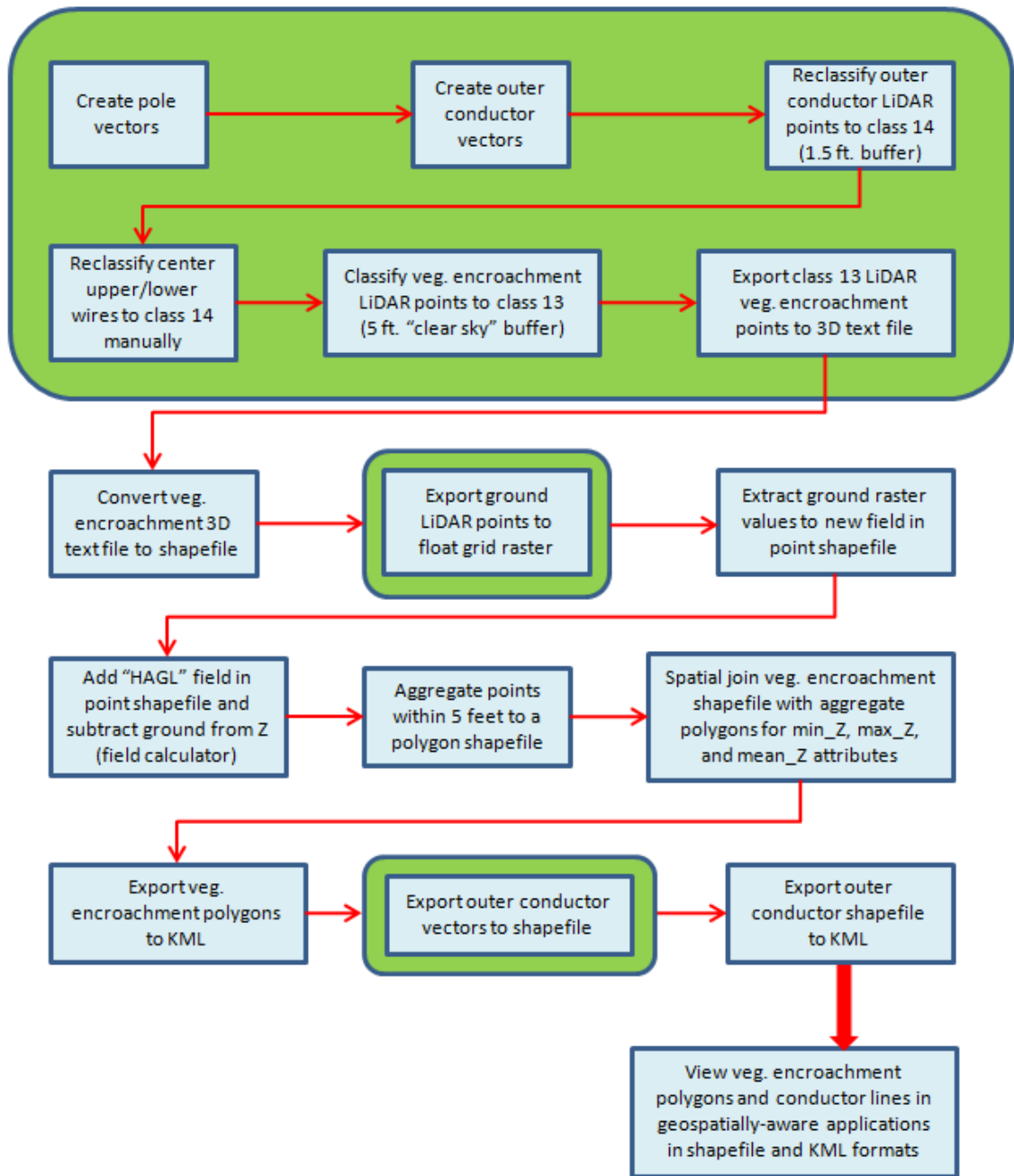


Figure 3.13 – Process flow – green indicates a non-ArcMap step

3.3.1 Power Line Pole Definition

The first step in the process is to define where the poles supporting the conductors are, based on the LiDAR data. After identifying a span (a section of conductor wires between two poles) in the 2D view, the profile was drawn over this area to create a cross section (figure 3.14). Within the cross section the conductors are clearly visible. The poles are not as visible due to their perpendicular orientation to the LiDAR sensor. However, two things help identify the poles despite this. First, since the point density of the LiDAR dataset is high, there are a small number of points that are produced from reflection off the poles, and are vertically oriented to one another. Second, the parabolic nature of the conductors makes it fairly easy to find the poles, since there is a distinct point where two parabolas meet, which is at each pole. The more sag there is in the conductors, the easier it is to find poles because the meeting point of two parabolic shapes is more distinct or “pointy.” With distribution lines the spans are shorter, conductors lighter, and less current runs through them; therefore, there is less sag than seen with transmission lines, making the parabola joint points less pronounced. Nonetheless, sufficient point density was achieved with this dataset, and is a contributing factor to the identification of support pole locations.

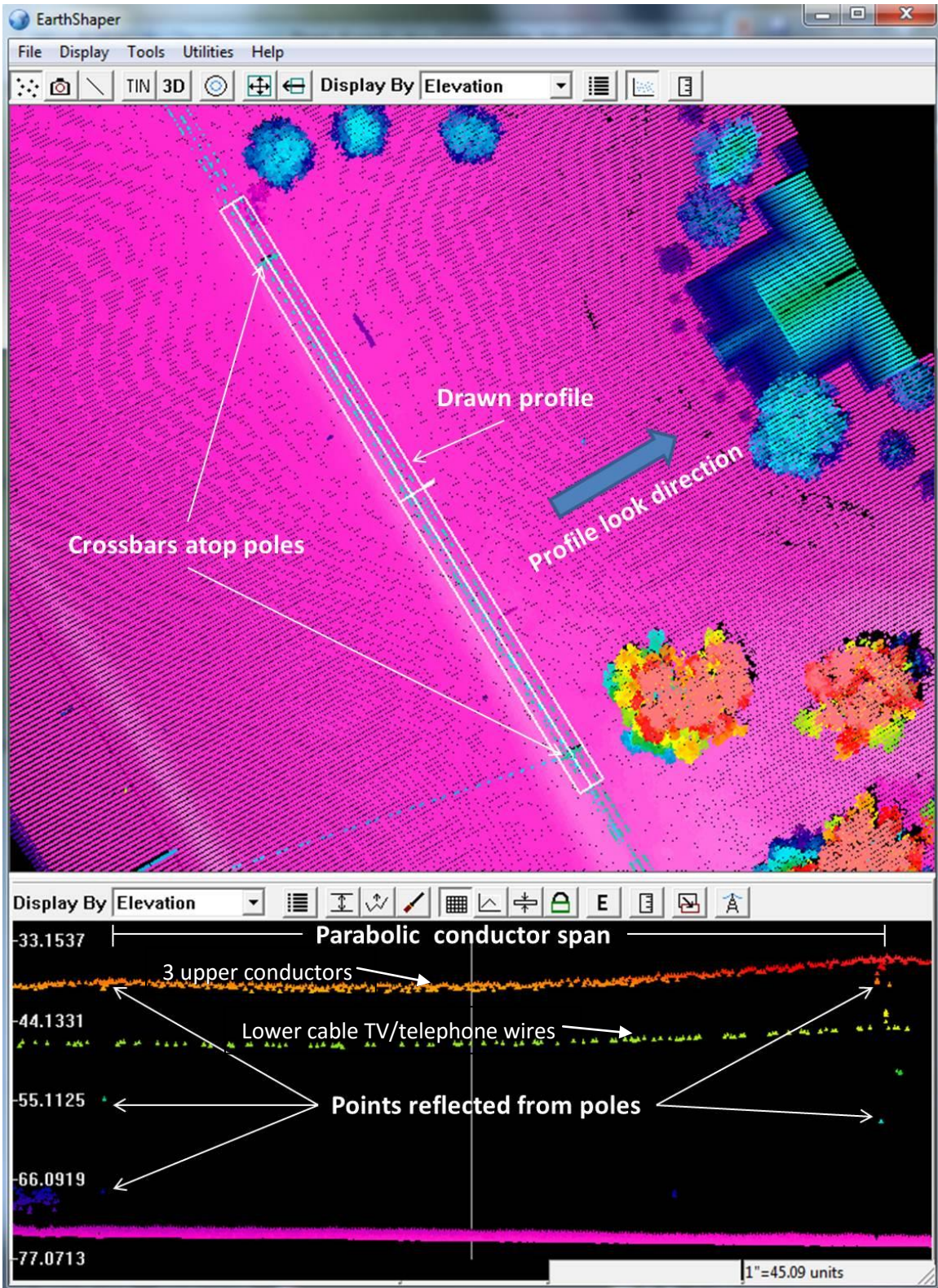


Figure 3.14 – 2D profile view

While in profile mode, the Power Line tool became available and was opened. Next, the view was switched to 3D so the tops of poles could be accurately identified. For each pole, a white point was placed at the top, and the Power Line tool placed a white point directly (vertically) below it, lying on the lowest LiDAR point beneath (figure 3.15). When this looked satisfactory the Add Tower command was invoked, and the pole vector was created (figure 3.16). This process was repeated until all desired support pole vectors were created.

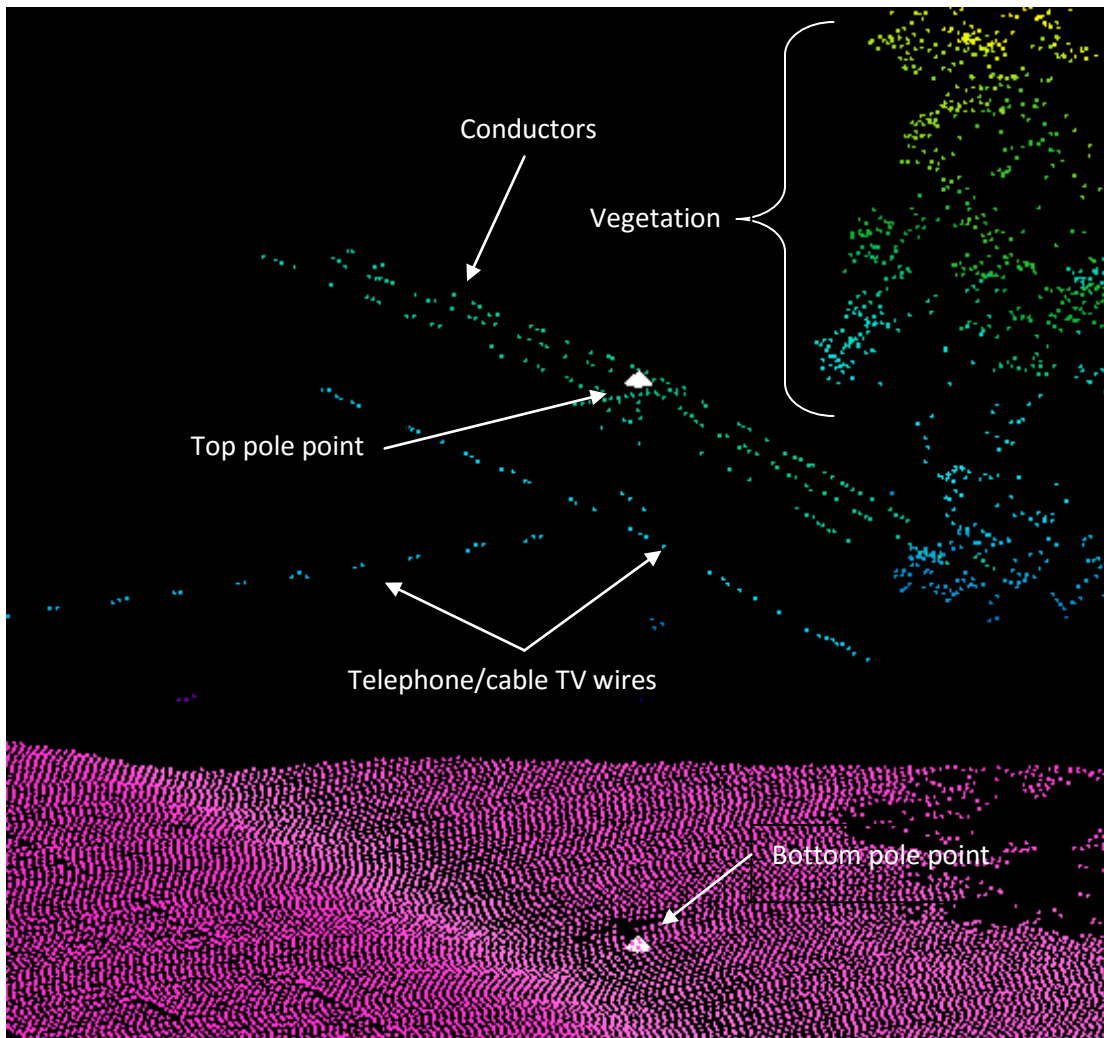


Figure 3.15 – The initial top and bottom pole points

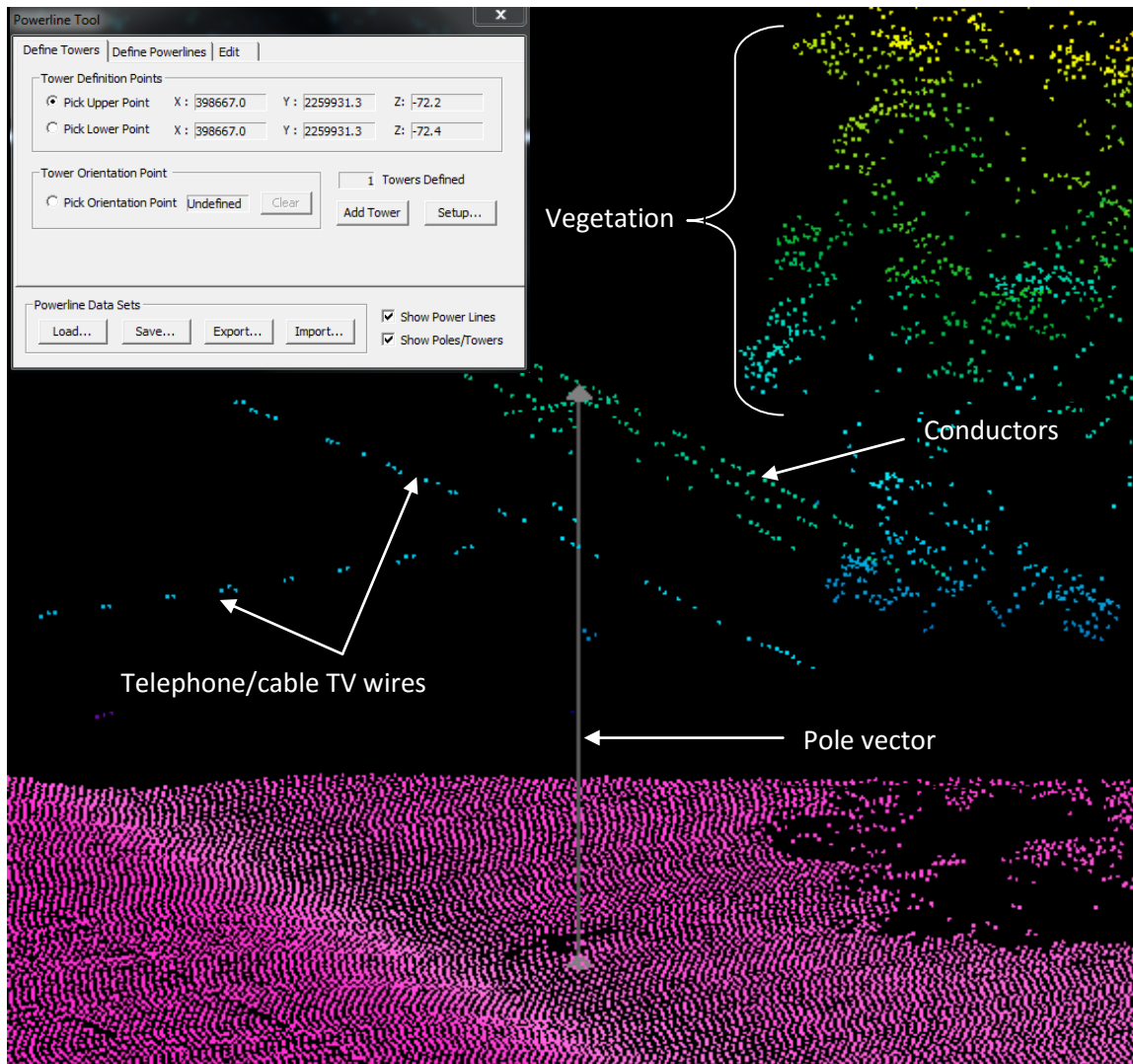


Figure 3.16 – The solved pole vector

3.3.2 Conductor Definition

Definition of the conductors as vector data was done in a similar manner to the poles, as the profile and 3D data view were set up the same way. The conductor LiDAR points were transformed into line vector data using a “best fit” parabolic curve algorithm. Again, the Power Line tool was opened from the

profile view window, and the 3D view was used to reference the position of the profile view box.

Each span between poles was visited using the profile tool. To ensure only one conductor (or phase) was being vectorized at a time, the profile width had to be narrowed so other phases did not appear in the view. With a single phase of a span in the profile view, the Define Power Lines tab of the Power Line tool was opened. To create a vector out of the LiDAR points that represented the conductor, a minimum of four points had to be placed on it in the profile view (figure 3.17). The software will accept more, but four were usually satisfactory. After at least four points were placed on the conductor, a “best fit” algorithm was run to create a vector from the LiDAR points. It was a necessary step to collect the poles first, because the conductor vector solving algorithm will not work without them. Figure 3.18 shows a solved conductor (dashed line) that could be accepted or rejected. Figure 3.19 shows an accepted conductor vector (solid line).

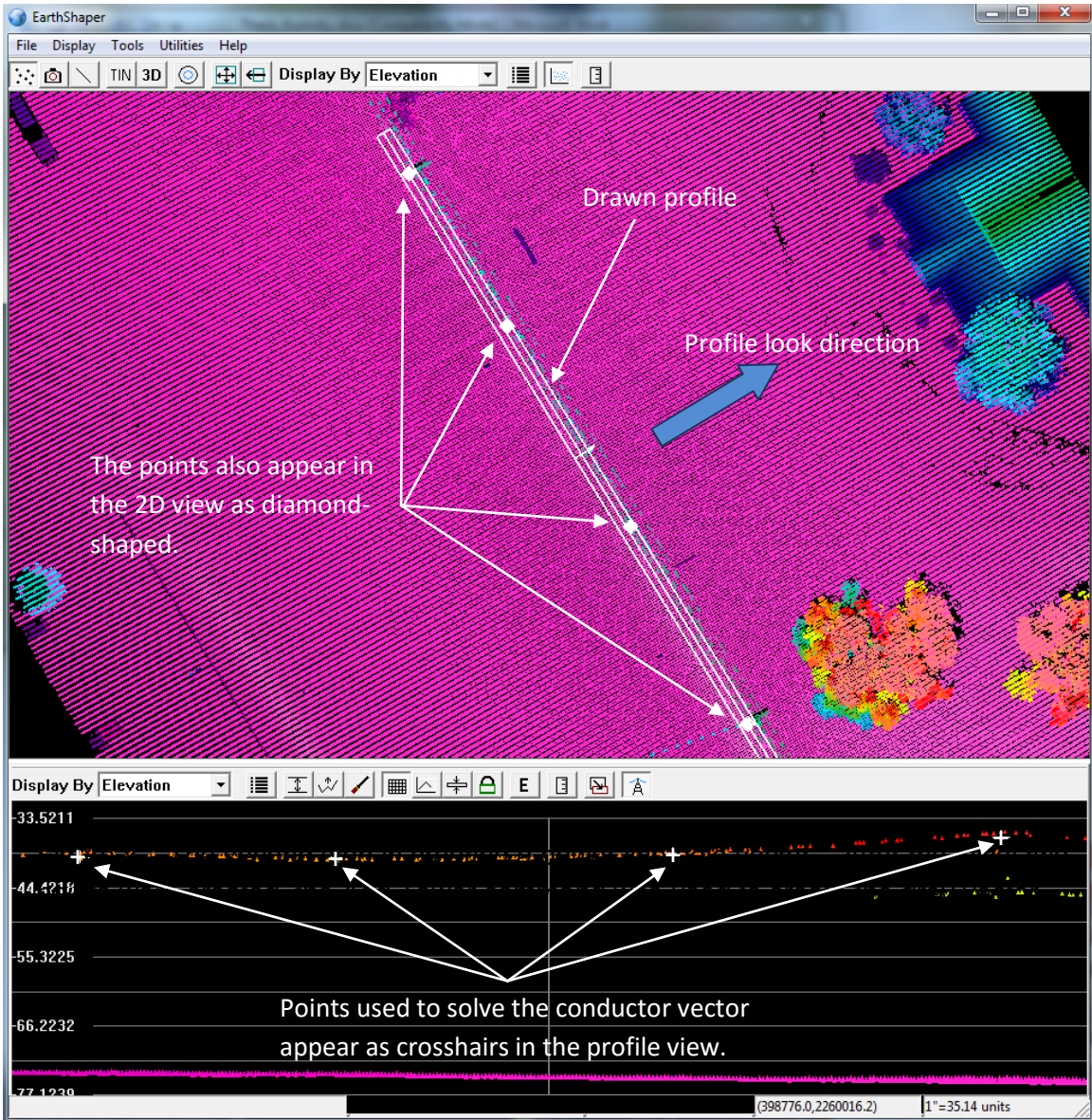


Figure 3.17 – Points used to solve the conductor vector

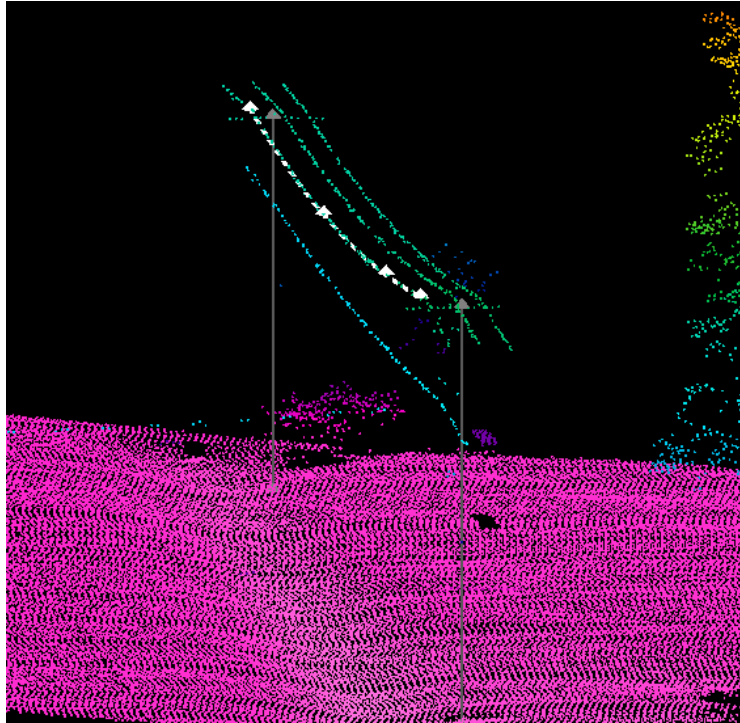


Figure 3.18 – Solved conductor vector

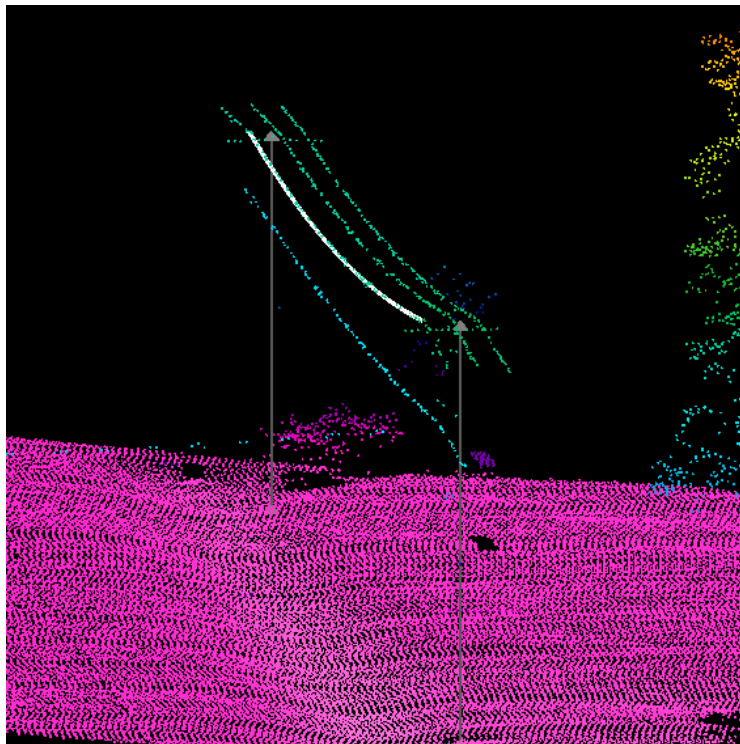


Figure 3.19 – Accepted conductor vector

The process of collecting the conductor vectors was continued with this method until all outer conductor vectors were complete. At this point vector data had been extracted for both the poles and outer conductors.

3.3.3 LiDAR Conductor Point Classification

The next step was to classify the points that represented conductors in the data as something other than the vegetation classes they were originally assigned by the data vendor. To do this, vector data representing the conductors is necessary, which is why these data were extracted first. The basic idea for the reclassification of the LiDAR conductor points is that since the vector data extracted from them were a best fit to the arrangement of the points in 3D space, the vectors do not perfectly intersect every point. In other words, the LiDAR points are in a sense “floating around” the vector data in 3D space, but their proximity is still very close, within a foot (figure 3.20).

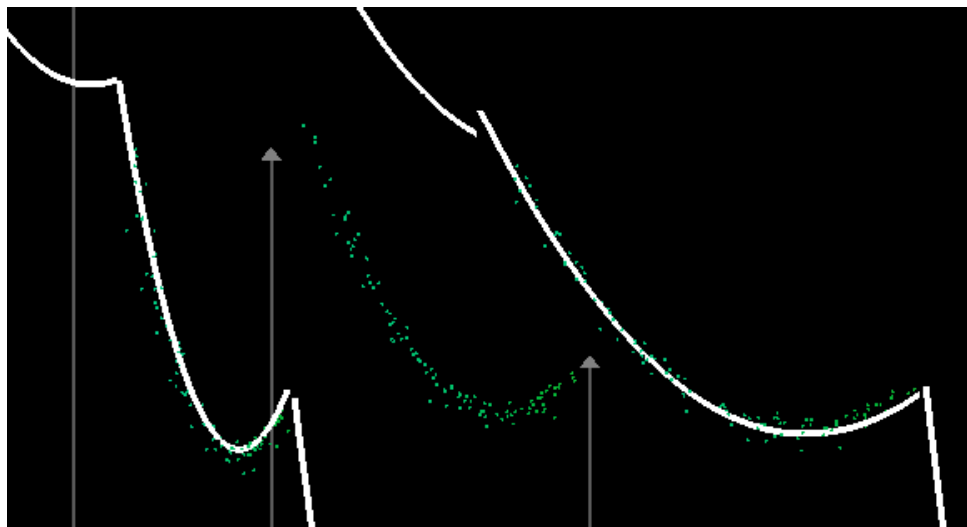


Figure 3.20 – Accepted conductor vectors

The close proximity of the points to the vectors helped with this part of the analysis because of the way it was carried out. The classification of LiDAR points, that is, changing the class of one or a group of points, is a common function in any software that is truly meant to exploit LiDAR data. In the application used for this study, this can be done several different ways. One of them is specifically meant to classify points representing a conductor like shown in figure 3.20 and is based on a buffer around the vector.

A conductor span vector to be used for point classification was selected from the profile view, and it appears as a dashed line in the 3D view (figure 3.21). The box spanning across the lines is the drawn profile.

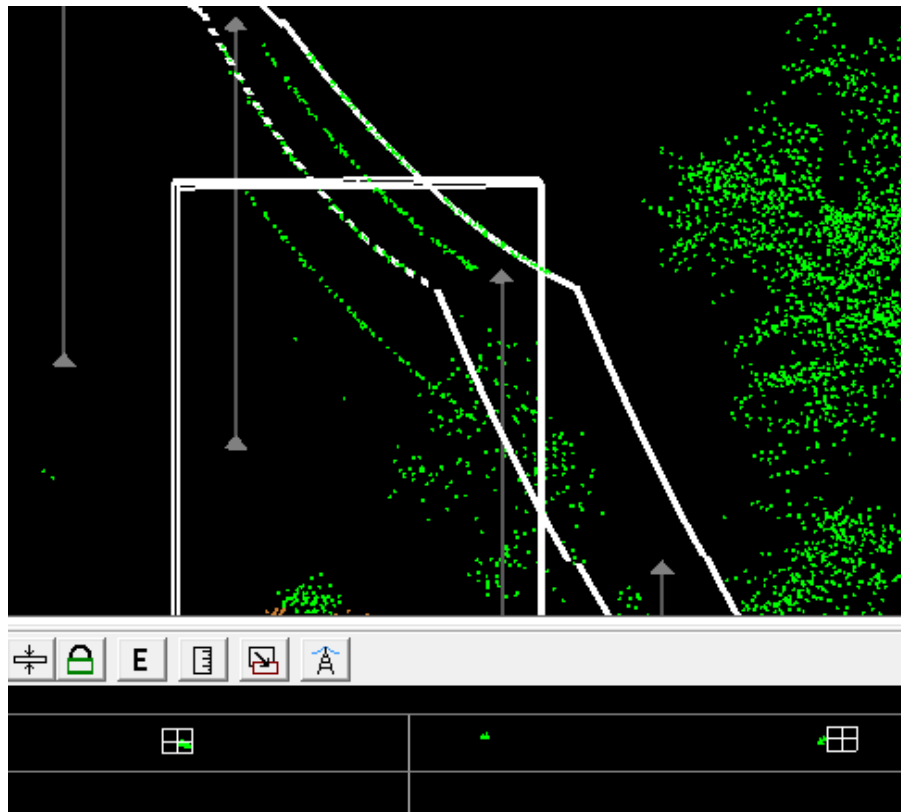


Figure 3.21 – A selected conductor vector (dashed)

Next, the parameters by which the software will reclassify points were set. The software must know what the present class of the points is, and what class they will be changed to. In this case, since the conductor points are in the high vegetation class and they need to be put into the Power Line class, the input class was set to 5 (High Vegetation), and the target class was set to 14 (Power Line), (figure 3.22).

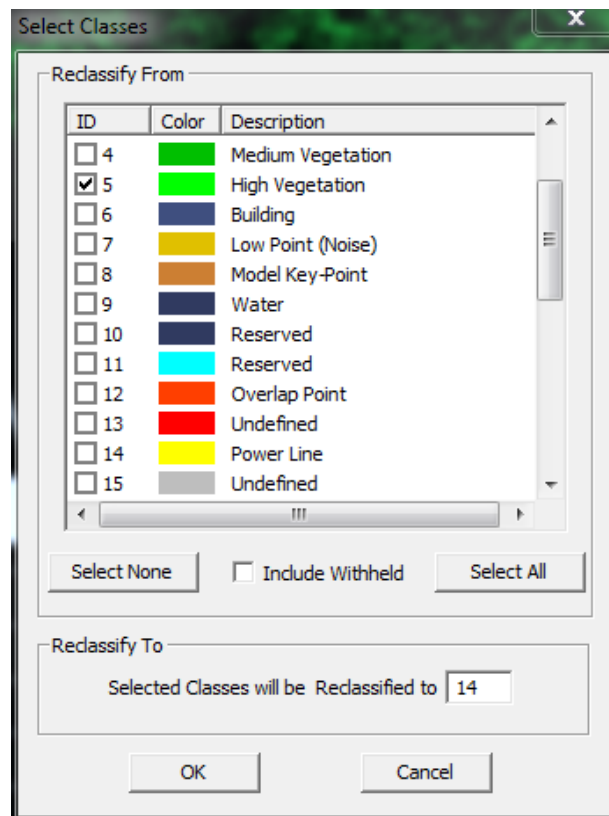


Figure 3.22 – Conductor point classification settings

This process works by reclassifying points within a buffer set around the conductor vector. This is a circular buffer that can be thought of as a “tube” surrounding the vector. The buffer radius was set to 1.5 feet (figure 3.23) which is a distance that should include the conductor points without erroneously including any other points. The points within the buffer were reclassified from High Vegetation to Power Line by invoking the buffer function. Notice the conductor points within the buffer of the selected vector have changed color from bright green to yellow (figure 3.24).

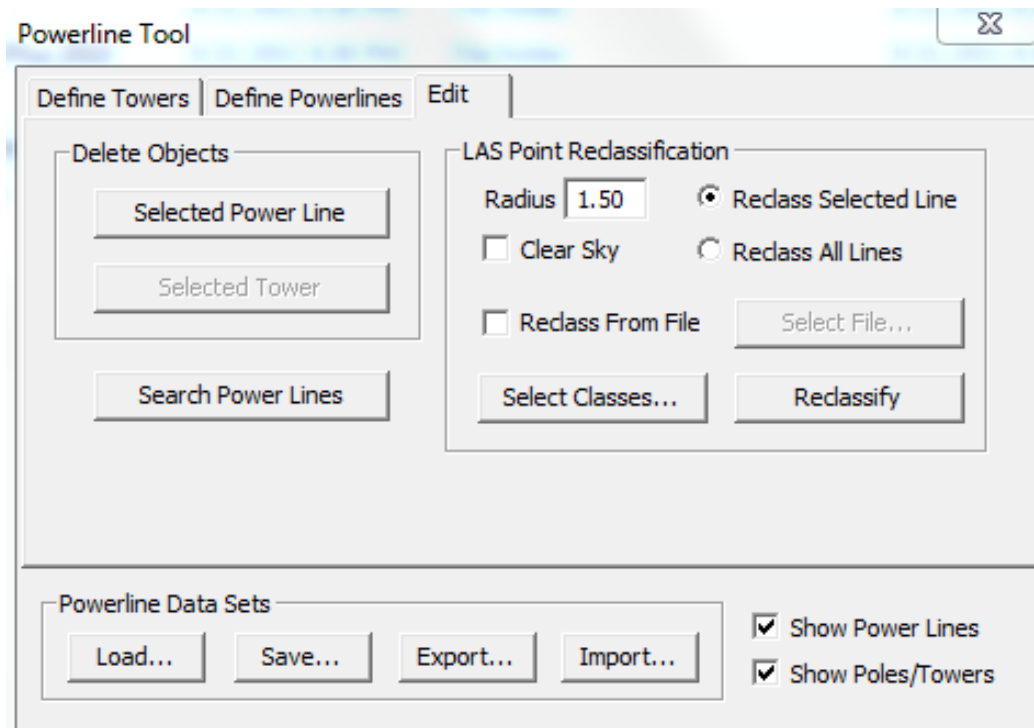


Figure 3.23 – Conductor buffer settings

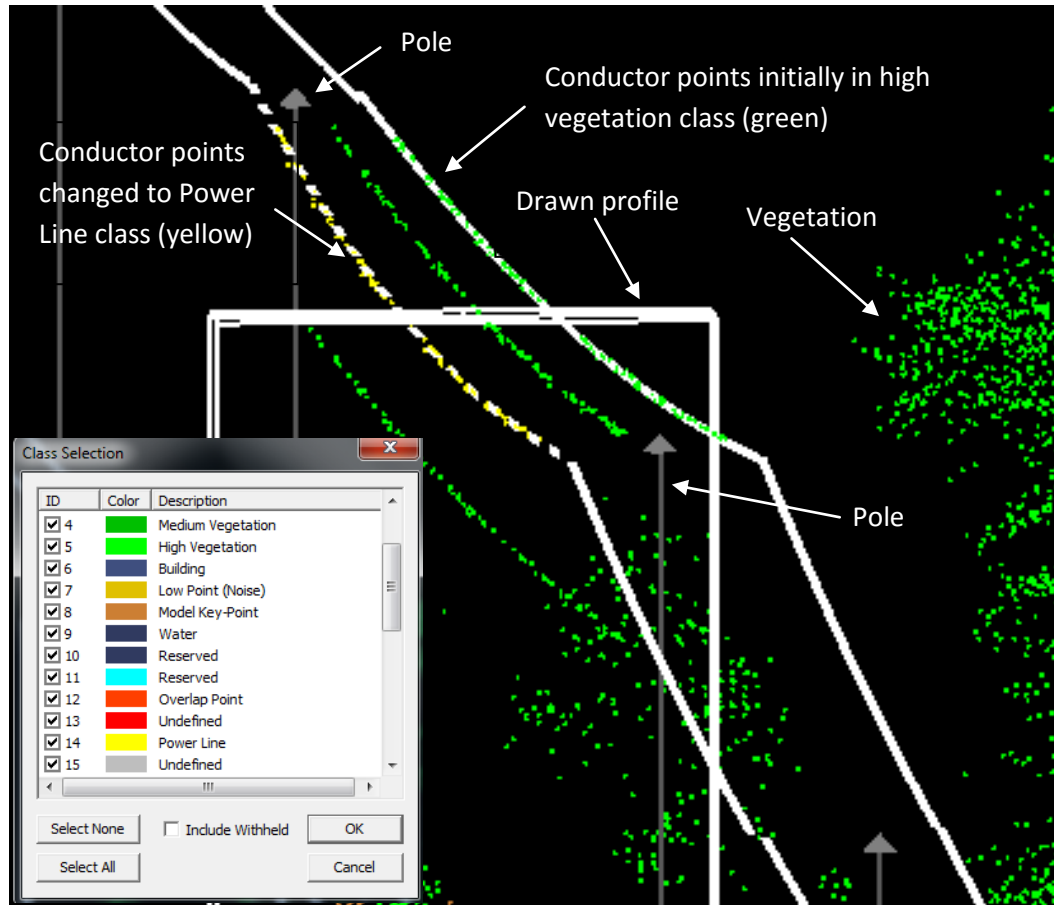


Figure 3.24 – Reclassified conductor points

A single span worth of points was first reclassified so the results could be observed before moving forward with the rest of the classification. This ensured any undesired behavior of the classification was not applied to all conductors. The buffer radius of 1.5 feet was satisfactory, so all points in the dataset within the buffers of the conductor vectors were reclassified from High Vegetation to Power Line (figure 3.25).

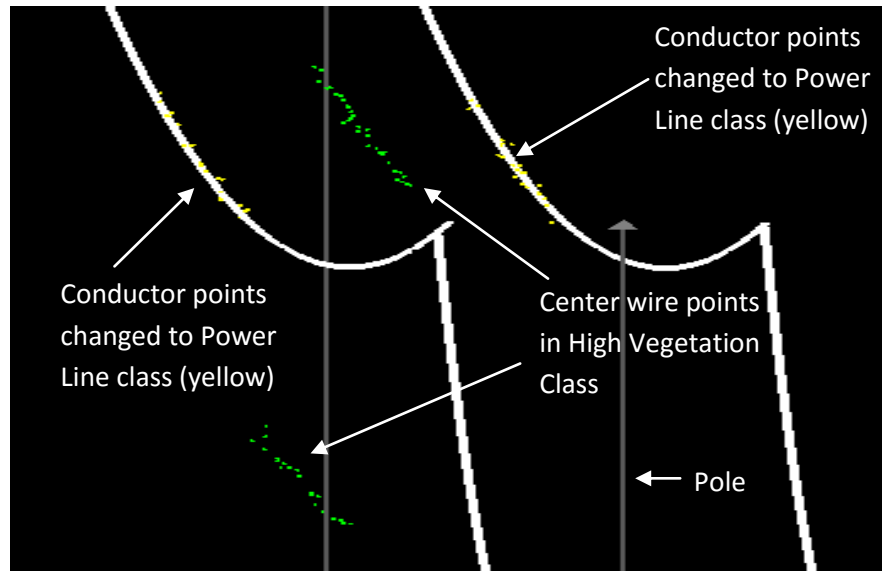


Figure 3.25 – All outer conductors classified as Power Line

Vector data were generated only for the outer conductors because these are the only necessary vector data to perform the steps shown in the next section. This means at this point only the outer conductor points have been reclassified to the Power Line class, class 14. However, the points representing the center wires above and below the outer conductors (a ground and telephone/cable wire respectively) still needed to be classified as Power Line in order to properly prepare for subsequent processing. This was done without vector data, as a manual process.

A profile was drawn over the power lines narrow enough to only show the upper and lower wires in the center, between the outer wires that were already reclassified (figure 3.26). To reclassify these points throughout the dataset a tool called Polyline Edit was used. Like the other classification tools in the application, a “from” class and a “to” class had to be set (figure 3.27).

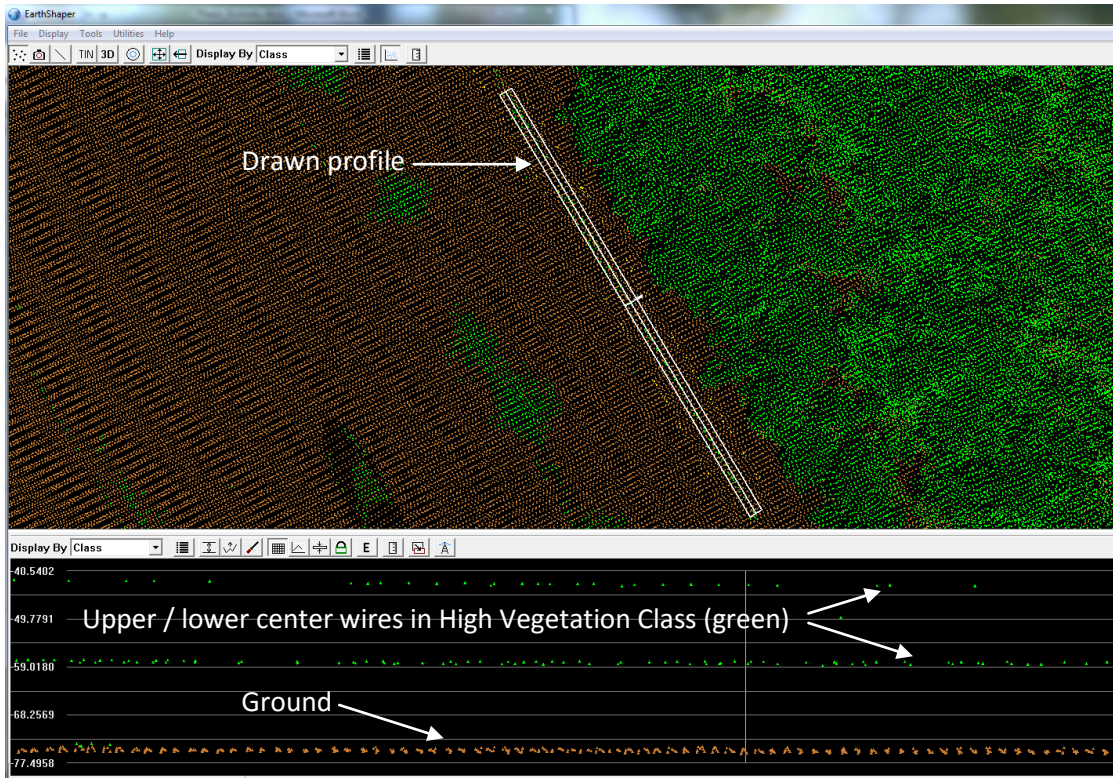


Figure 3.26 – Profile view of the center wires

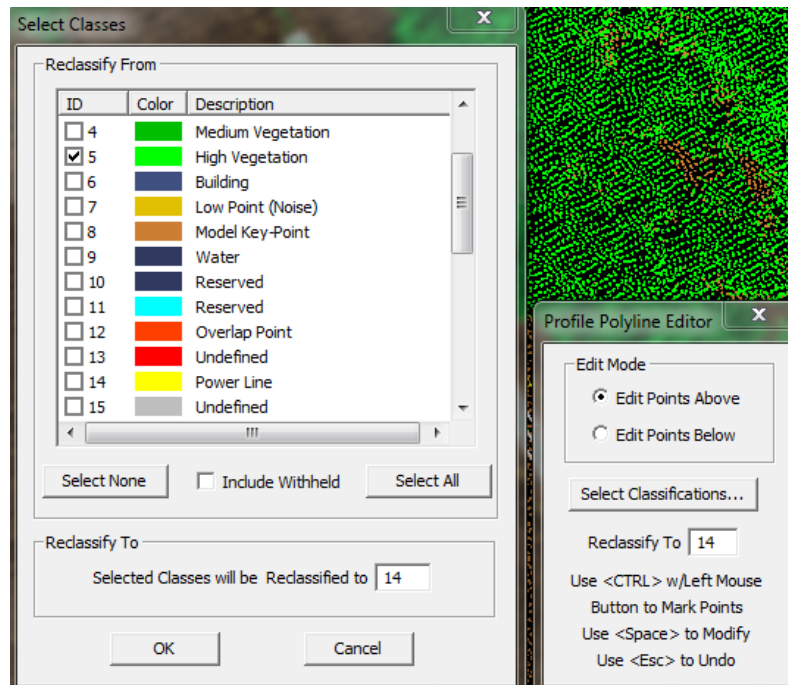


Figure 3.27 – Center wire reclassification settings (5 to 14)

Once the class settings were made, the center wires were ready for reclassification. Notice the setting in figure 3.27 where the Polyline Editor tool Edit Mode says “Edit Points Above.” While in the profile view, a polyline was drawn below the points to be reclassified, points above the line were selected (figure 3.28), and the selected upper and lower center wire points were reclassified from High Vegetation to Power Line (figure 3.29).

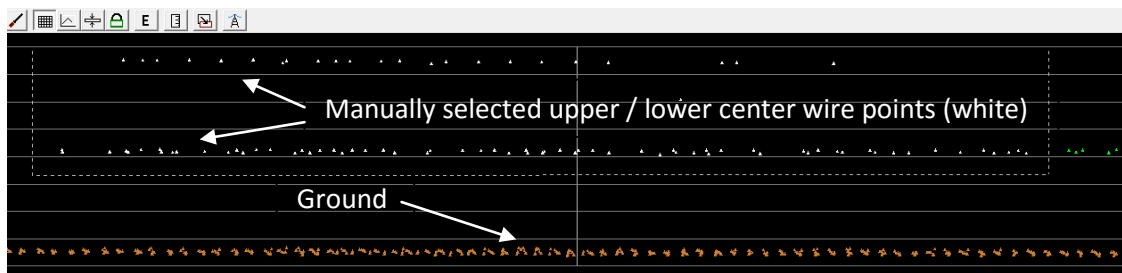


Figure 3.28 – Manually selected upper / lower center wire points (white)



Figure 3.29 – Manually reclassified upper / lower center wire points (yellow)

This process was continued until all center wires were classified as Power Line, class 14. For this part, manual labor was focused on reclassifying the points rather than generating vector data used to reclassify the points, because vector data were not needed for the center wires. At this point all wires were now classified as Power Line (figure 3.30), and further analysis could be performed.

3.3.4 Vegetation Encroachment Analysis

Now that all the necessary preliminary steps have been completed, vegetation encroachment identification can take place. Like the classification of the outer conductor points using a buffer around vector data, vegetation encroachment points were identified in a similar way. The Power Line Tool within the Earth Shaper application was used the same way it was for the conductor points, with some changes to the buffer settings.

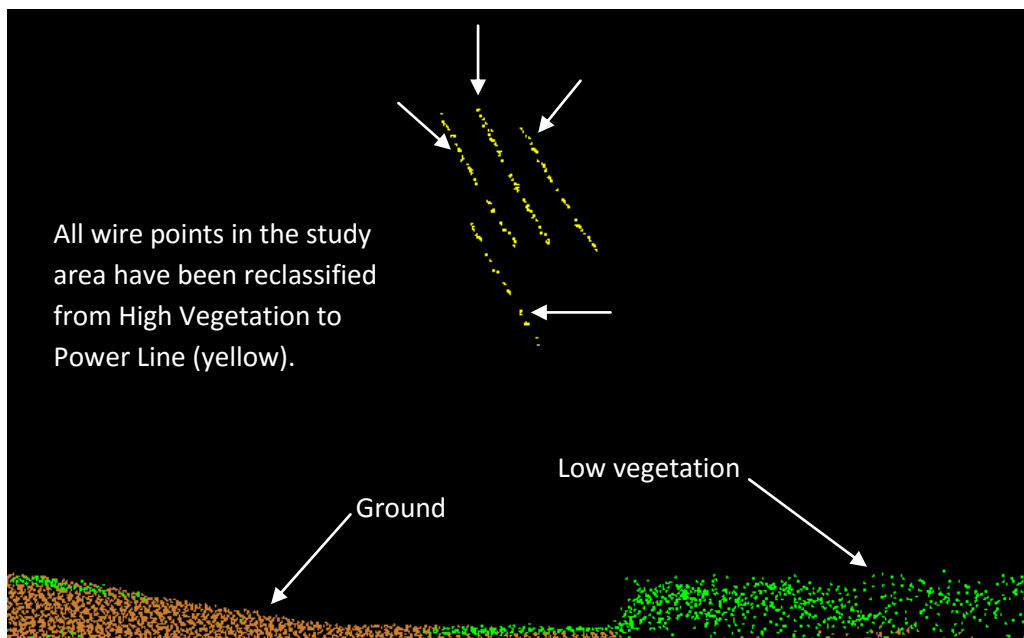


Figure 3.30 – All wire points have been reclassified to Power Line (3D view)

First, the decision was made as to what constitutes a vegetation encroachment, based on input from the data vendor. The definition of an encroachment was established as any vegetation point falling within a five foot buffer surrounding a conductor. This buffer, however, is different from the buffer used to classify the conductors. Instead of a “tube-like” circular buffer around the conductor vectors, a “clear sky” buffer was used (figure 3.31). The difference here is that instead of a closed circle around the vectors, a U-shaped buffer was used. This special type of buffer algorithm is referred to as a clear sky buffer because the top of it in 3D space is open, and the sides infinitely reach upward toward the sky. The effect of a “wall” on either side of each outer conductor vector is created. This makes good sense, because any vegetation hanging over power lines is a threat, in that it could fall causing a short, fire, or mechanical damage. The buffer will include any vegetation reaching into the five foot zone on either side of the outer conductors, regardless of its height.

Referring back to the collection of the conductor vector data, it was discussed that the only necessary vector data collection pertained to the outer conductors. The buffer distance is the reason for this, because a five foot buffer around the center wires would be completely inside the outer conductor buffers, rendering it useless (figure 3.32).

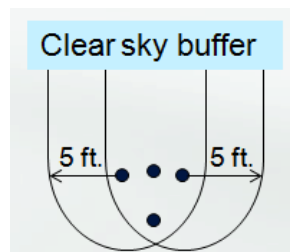


Figure 3.31 – Clear sky buffer

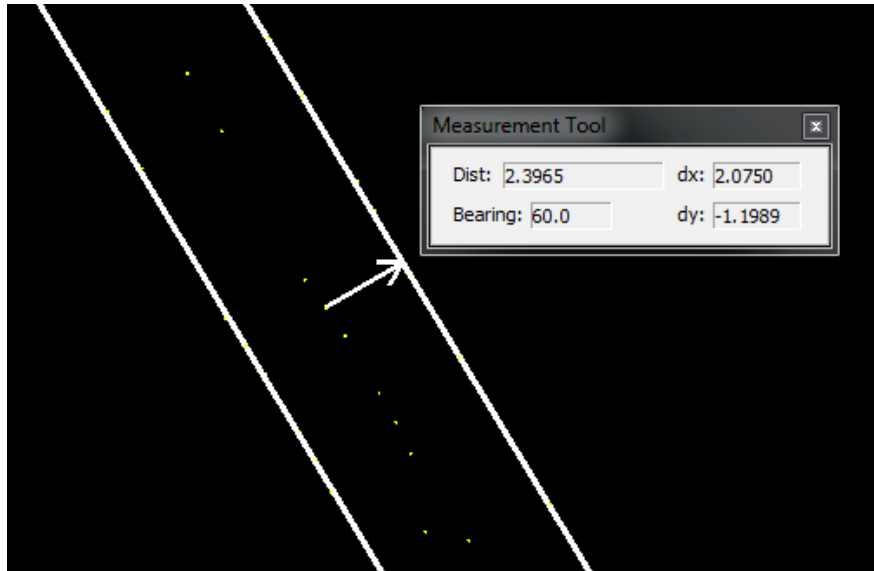


Figure 3.32 – Distance between the center and outer wires

Now that the buffer distance has been established, it's time to make the class settings, just like was done for the reclassification of the conductor points. In this case, any points in any of the vegetation classes that fall inside the buffers of the two conductor vectors need to be changed to their own unique class as a result of the reclassification. A class called ROI, which stands for region of interest, was created simply by renaming class 13 to "ROI" and giving it a red color. In the LAS 1.4 classification schema, class 13 is called Wire-guard, but was renamed and recolored for this study. In this case, any point from classes 3, 4, or 5 falling inside the buffers of the conductors needs to be put into class 13, the ROI class. Class 13 will represent vegetation encroachment points. Figures 3.33 and 3.34 show the settings made prior to running the buffer analysis for encroachment vegetation.

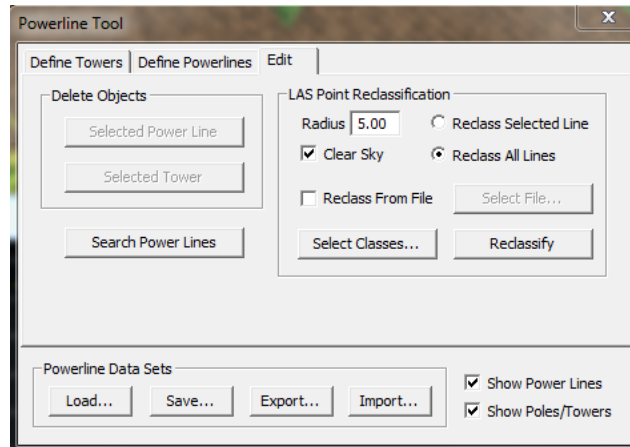


Figure 3.33 – Clear sky buffer of five feet

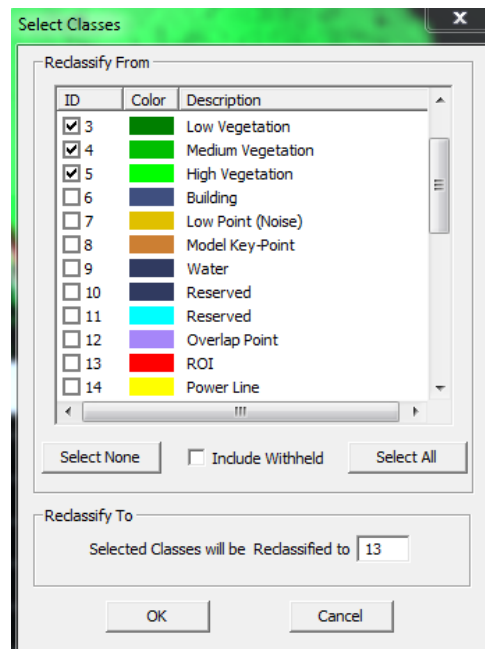


Figure 3.34 – Encroachment vegetation classification settings

Notice the only classes selected as the “Reclassify From” classes are 3, 4, and 5, the vegetation classes. The reason for classifying all conductor and other wires as class 14 was to protect them from being classified as encroachment vegetation. In other words, if they were still classified as vegetation, they would end up as class 13, the region of interest class due to their proximity.

Finally, now that the necessary data preprocessing steps and appropriate settings were made, the buffer analysis for encroachment vegetation could be run. The software then reclassified any points from classes 3, 4, or 5 that fell within the five foot buffers to class 13. The result was a single LiDAR point class with only vegetation encroachment points (figures 3.35 and 3.36).

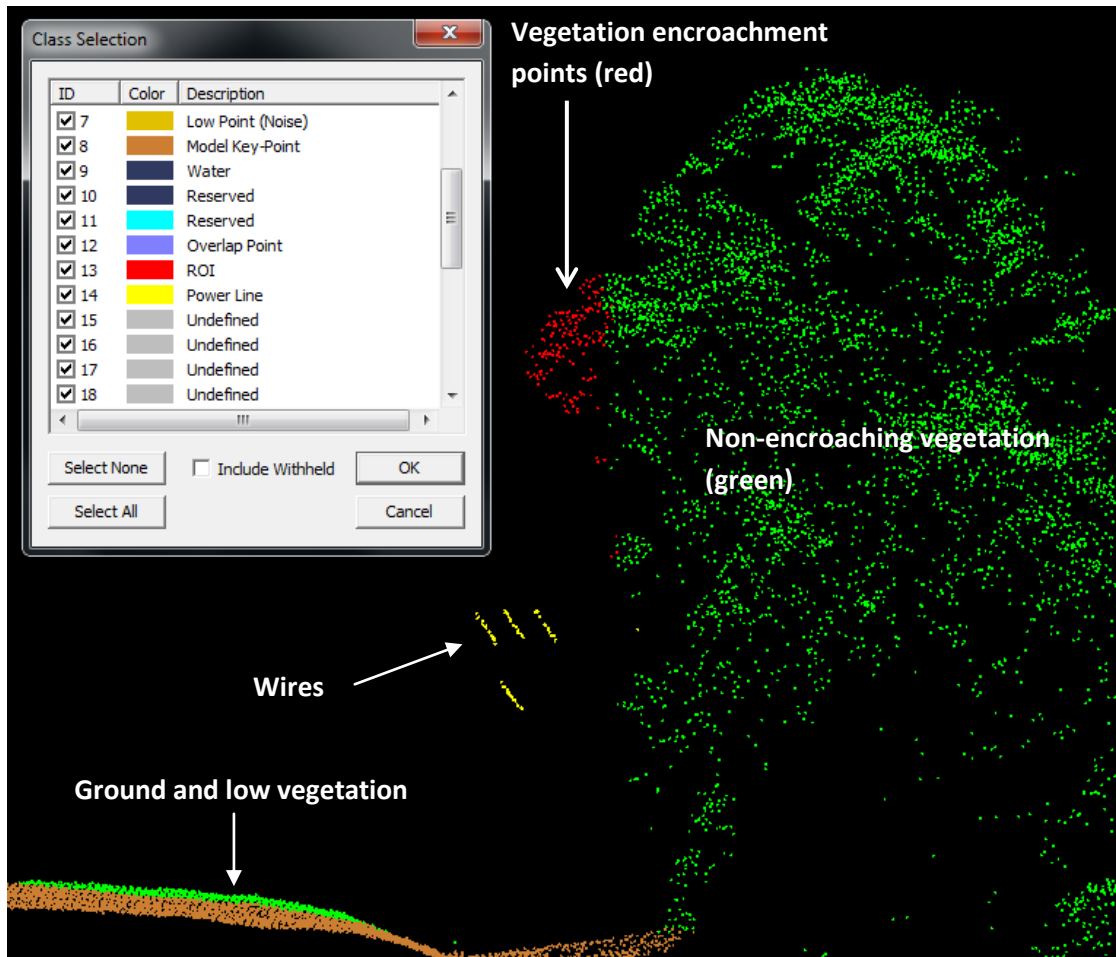


Figure 3.35 – Resulting vegetation encroachment points in 3D view (red)

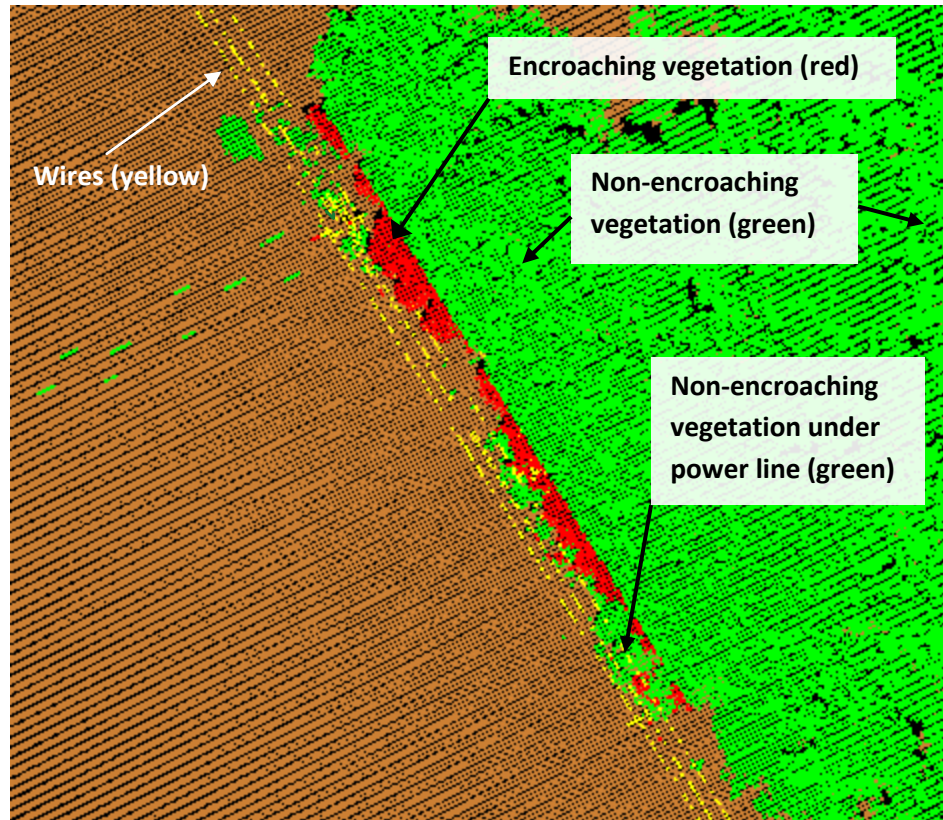
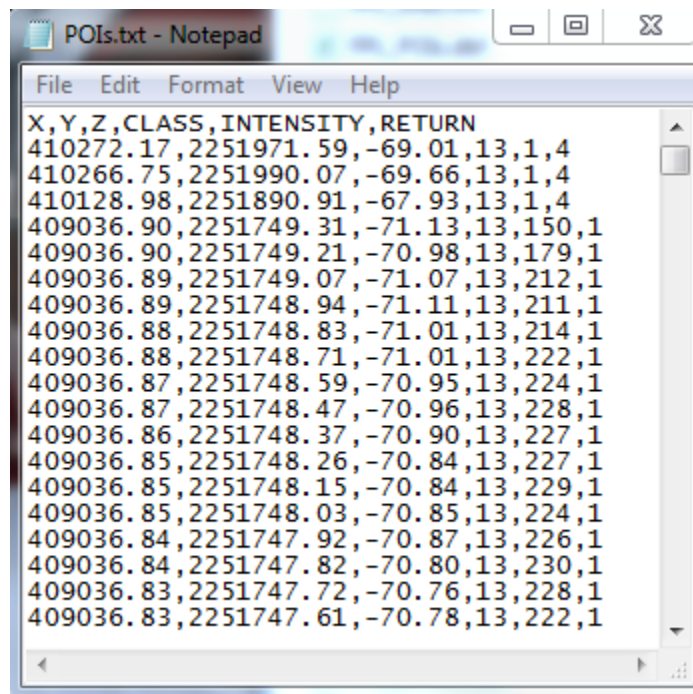


Figure 3.36 – Resulting vegetation encroachment points in 2D (red)

3.3.5 Vegetation Encroachment Data Processing

The next series of steps were used to convert the 3D LiDAR vegetation encroachment data points to 2D polygons using GIS software. The main objective here was to enable the LiDAR vegetation encroachment points to represent regions where dangerous vegetation existed, rather than having 3D clusters of points. For many users, 2D data are easier to display, interpret, and quantify in order to make decisions, especially users with no experience in GIS.

First, the LiDAR vegetation encroachment points were exported as ASCII text. This resulted in a .txt file containing only points from class 13, the class named ROI (figure 3.37). The file contained X, Y, and Z coordinates, point class, the intensity value of each point, and the return number of each point by default. The .txt file was then converted to a point shapefile. The resulting point shapefile contained all attributes indicated in the first line of the .txt file (figure 3.38).



```
POIs.txt - Notepad
File Edit Format View Help
X, Y, Z, CLASS, INTENSITY, RETURN
410272.17, 2251971.59, -69.01, 13, 1, 4
410266.75, 2251990.07, -69.66, 13, 1, 4
410128.98, 2251890.91, -67.93, 13, 1, 4
409036.90, 2251749.31, -71.13, 13, 150, 1
409036.90, 2251749.21, -70.98, 13, 179, 1
409036.89, 2251749.07, -71.07, 13, 212, 1
409036.89, 2251748.94, -71.11, 13, 211, 1
409036.88, 2251748.83, -71.01, 13, 214, 1
409036.88, 2251748.71, -71.01, 13, 222, 1
409036.87, 2251748.59, -70.95, 13, 224, 1
409036.87, 2251748.47, -70.96, 13, 228, 1
409036.86, 2251748.37, -70.90, 13, 227, 1
409036.85, 2251748.26, -70.84, 13, 227, 1
409036.85, 2251748.15, -70.84, 13, 229, 1
409036.85, 2251748.03, -70.85, 13, 224, 1
409036.84, 2251747.92, -70.87, 13, 226, 1
409036.84, 2251747.82, -70.80, 13, 230, 1
409036.83, 2251747.72, -70.76, 13, 228, 1
409036.83, 2251747.61, -70.78, 13, 222, 1
```

Figure 3.37 – Text version of vegetation encroachment points

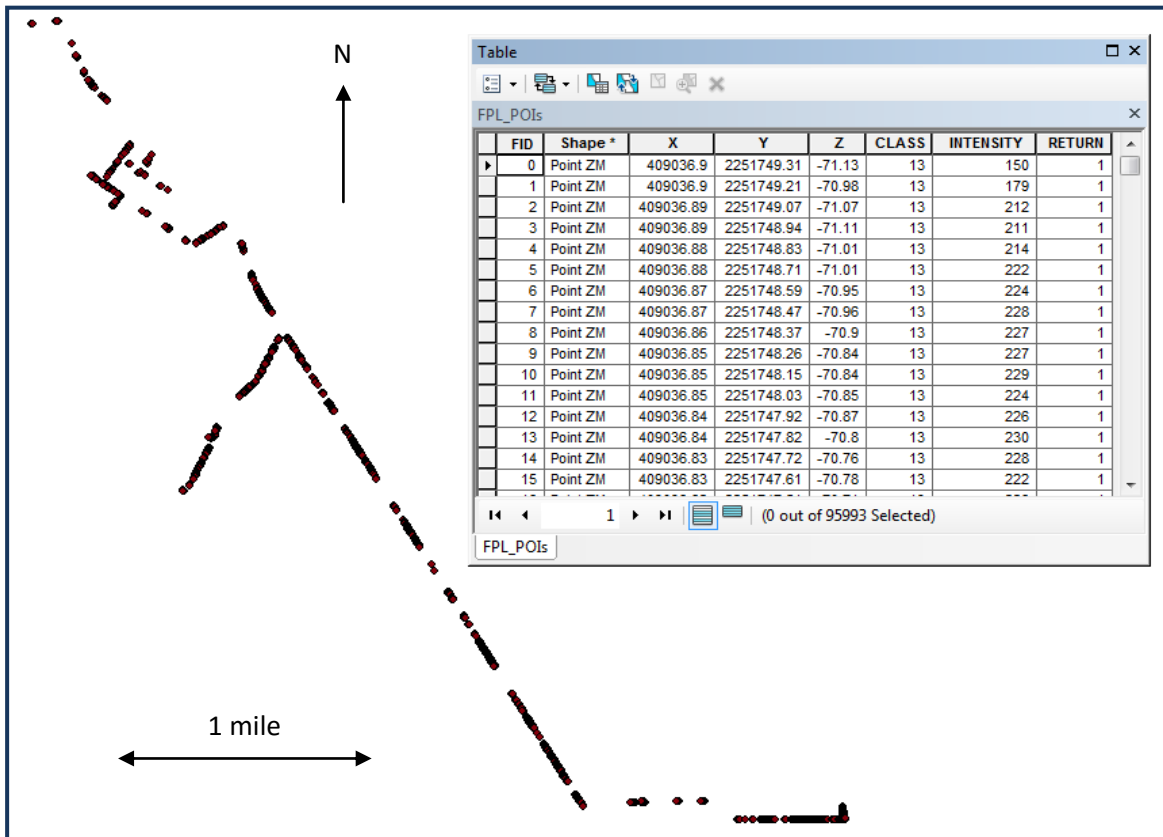


Figure 3.38 – The resulting point shapefile created from the 3D ASCII text file.

The elevation of each point is known from the Z attribute value, but it would be more helpful to know the height above ground level for each point. Since the LiDAR data were filtered to include a ground class, class 2, the elevation of the ground under each point can be subtracted from each point, resulting in a height above ground level value. To do this the ground LiDAR points were exported from Earth Shaper as a float grid raster (figure 3.39). The ground raster and vegetation encroachment point shapefile were then brought into ArcMap, where the Extract Values to Points tool was used to output a new point shapefile that contained the original attributes, plus a new attribute containing the Z value of the ground pixel beneath each point. The new attribute

was called “RASTERVALU” by default (figure 3.40). To obtain the height above ground level of each point, an additional field was added to this shapefile manually to store these values, called “HAGL,” which is short for height above ground level. To calculate each point’s height above ground level a simple expression of $[Z] - [RASTERVALU]$ was used. The heights above ground level were now populated in the HAGL field (figure 3.41).

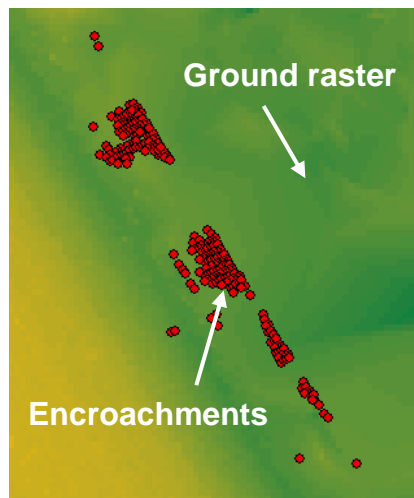


Figure 3.39 – Encroachment points over ground raster

FID	Shape	X	Y	Z	CLASS	INTENSITY	RETURN	Count	RASTERVALU
382	Point ZM	406201.42	2251914.09	-43.82	13	120	1	1	-69.073456
383	Point ZM	406201.41	2251913.6	-43.65	13	33	1	1	-69.073456
384	Point ZM	406201.4	2251913.12	-43.41	13	56	1	1	-68.982285
385	Point ZM	406201.4	2251912.65	-42.95	13	84	1	1	-68.982285
386	Point ZM	406201.4	2251911.71	-41.6	13	70	1	1	-68.975128
387	Point ZM	406200.73	2251914.85	-44.32	13	135	1	1	-69.071144

Figure 3.40 – The point shapefile with the added RASTERVALU attribute

FID	Shape	X	Y	Z	CLASS	INTENSITY	RETURN	Count	RASTERVALU	HAGL
382	Point ZM	406201.42	2251914.09	-43.82	13	120	1	1	-69.073456	25.25345
383	Point ZM	406201.41	2251913.6	-43.65	13	33	1	1	-69.073456	25.42345
384	Point ZM	406201.4	2251913.12	-43.41	13	56	1	1	-68.982285	25.57228
385	Point ZM	406201.4	2251912.65	-42.95	13	84	1	1	-68.982285	26.03228
386	Point ZM	406201.4	2251911.71	-41.6	13	70	1	1	-68.975128	27.37512
387	Point ZM	406200.73	2251914.85	-44.32	13	135	1	1	-69.071144	24.75114

Figure 3.41 – The point shapefile with the HAGL attribute populated

Next, the point shapefile was converted to a polygon shapefile using the Aggregate Points algorithm in ArcToolbox that creates polygon features around clusters of proximate point features. There were three basic inputs to the tool, which were input point features, output polygon feature class, and aggregation distance. In this case an aggregation distance of five feet was used, based on the general observed proximity of the original LiDAR points to one another. The result of this step was a series of polygons created from LiDAR vegetation encroachment points within five feet of one another in the X and Y dimensions (figure 3.42).

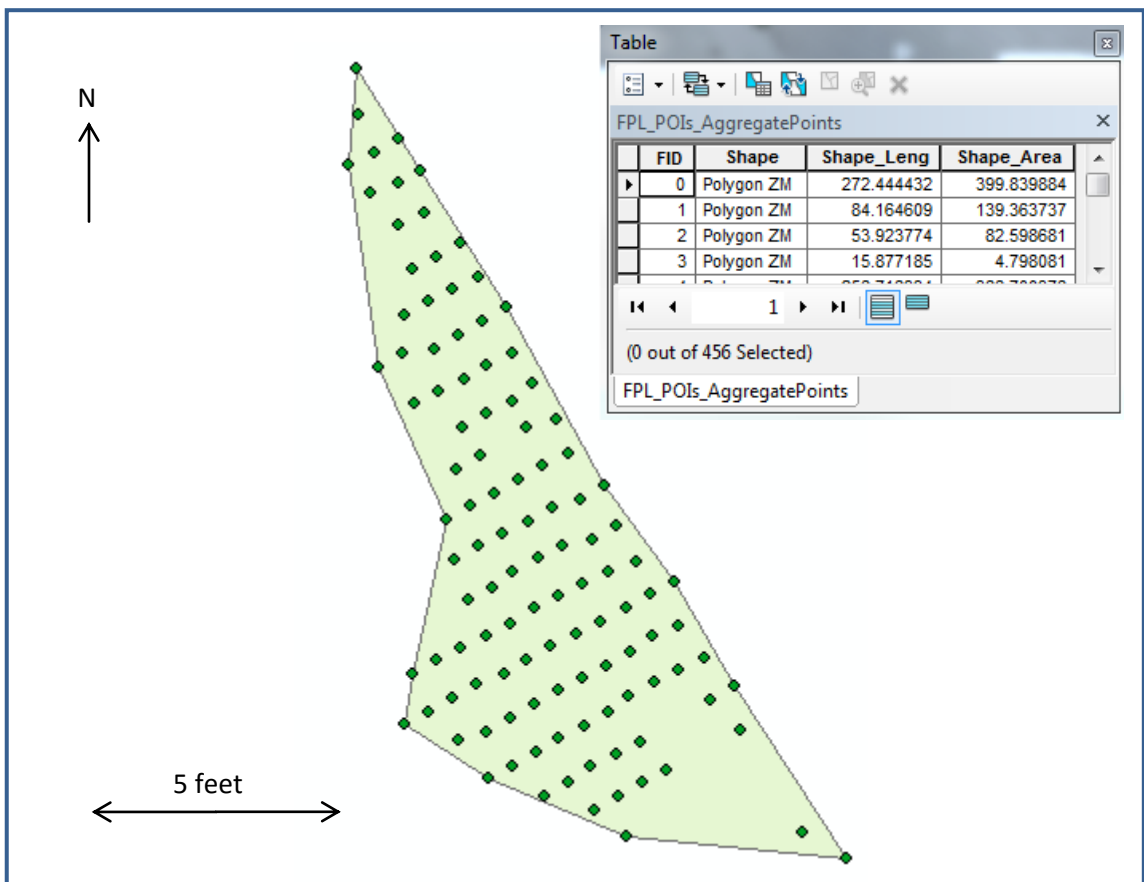


Figure 3.42 – A polygon created from aggregated vegetation encroachment points

Now there is one polygon for every cluster of at least three vegetation encroachment points within five feet of one another. Two of the attributes of the polygon shapefile created during the aggregation process were “Shape_Area,” and “Shape_Length,” which describe each polygon’s area and perimeter in feet, the units of the source dataset.

Having the area and perimeter of each vegetation encroachment polygon as attributes is definitely helpful, but it would also be wise to take advantage of the precise and accurate elevation values associated with the point shapefile derived from the source LiDAR data. Statistics for each vegetation encroachment polygon derived from the vegetation points that were aggregated to create them would be helpful, such as the minimum height above ground level, maximum height above ground level, and mean height above ground level. These statistics, along with the area figures would allow the user of the data to get a handle on how big of a job it would be to deal with vegetation removal.

The next series of steps deal with adding height statistics to the polygon shapefile attribute table based on the vegetation points aggregated to create them. The first steps involve performing a spatial join on the points and polygons, where the polygons are the target features and the points are the join features. The Spatial Join function in ArcToolbox transfers attributes from one feature class to another, based on the spatial relationships between the classes. The attributes of the join features (points) will be transferred to the target features (polygons).

Since the intention is to transfer the “HAGL” attribute from the point shapefile to the polygon shapefile while at the same time generating statistics on it, a few preparatory steps were first done to accommodate how the Spatial Join tool works. Three additional fields were added to the point shapefile called “Min_HAGL,” “Max_HAGL,” and “Mean_HAGL.” These new fields were given identical values to the original HAGL field using the field calculator with the simple expression “= HAGL.” When the target and join features are specified in the Spatial Join tool dialog, all attributes from both feature classes are shown in the Field Map of Join Features section. The only attributes that will be retained in the new output polygon shapefile will be “Shape_Leng,” “Shape_Area,” “Min_HAGL,” “Max_HAGL,” and “Mean_HAGL” (figure 3.43).

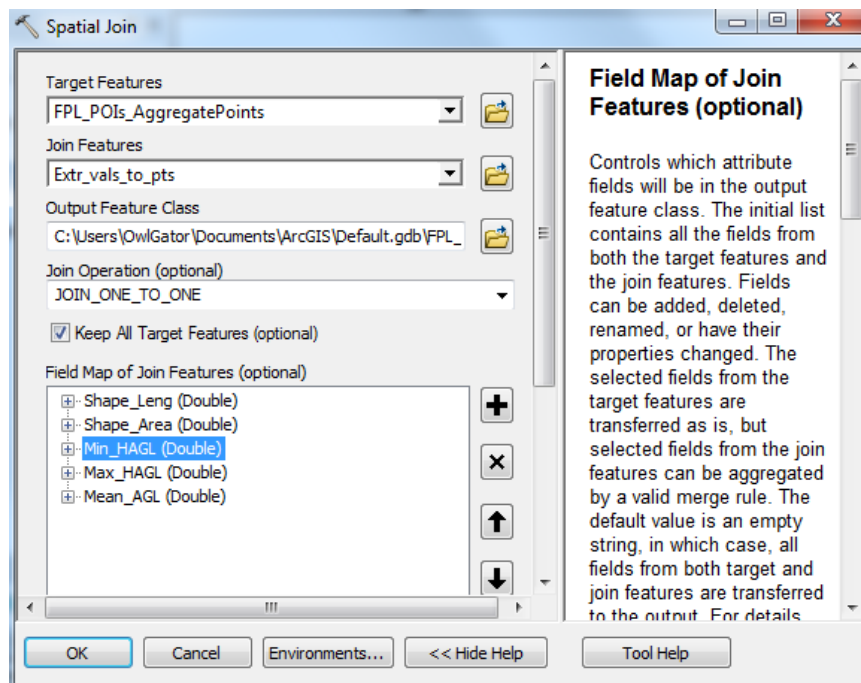


Figure 3.43 – Settings for the Spatial Join tool

Since there are multiple points that intersect each polygon, the HAGL values in the points are aggregated and given one value for each polygon. The aggregation method for this has several choices. For the three HAGL attributes the aggregation methods were set to minimum, maximum, and mean. The Spatial Join was run, and the resulting polygon attribute table is shown in figure 3.44.

The new attribute table includes the new fields containing vegetation height statistics for each vegetation encroachment polygon. The table also includes a new “Join_Count” field which indicates how many join point features intersected each target polygon, and was added as a result of the spatial join by default. In other words, it indicates how many LiDAR vegetation encroachment points make up each polygon.

FID	Shape *	Join_Count	Shape_Leng	Shape_Area	Min_HAGL	Max_HAGL	Mean_HAGL
10	Polygon ZM	139	69.965796	93.64047	20.215	85.227571	47.352336
11	Polygon ZM	14	16.917473	3.82106	29.850004	52.993998	49.774731
12	Polygon ZM	42	16.031744	11.825949	74.763505	82.671002	80.237322
13	Polygon ZM	3	8.625908	0.119427	33.6985	34.555666	34.102723
14	Polygon ZM	4	4.946257	0.076594	34.335996	34.665666	34.491582
15	Polygon ZM	7	13.968133	0.35536	34.101001	34.791001	34.325262
16	Polygon ZM	162	89.520776	162.320252	20.225797	36.861893	24.660082
17	Polygon ZM	496	234.709429	507.746578	24.896753	81.600288	53.741939
18	Polygon ZM	3	2.193873	0.17462	67.476337	68.143588	67.714504
19	Polygon ZM	61	29.389661	33.939419	28.728728	85.168498	71.959815
20	Polygon ZM	1256	131.744203	475.885588	31.323003	95.815505	88.234369

Figure 3.44 – Results of the spatial join

In order to make the resulting data from this chapter usable in a variety of applications, it was processed to include a shapefile and KML version of the vegetation encroachment points, vegetation encroachment polygons, and power line conductor vectors. The points and polygons were already in shapefile format, so they were then converted to KML in ArcToolbox using the Layer to KML function. The conductor vectors were exported from Earth Shaper as a shapefile and then converted to KML the same way. There are now points and polygons in two exploitable formats (.shp and .kml) showing vegetation encroachment information and the conductors they threaten in the same two formats.

CHAPTER 4: ANALYSIS RESULTS

Chapter 3 presented a process that produced accurate and precise 2D vegetation encroachment data from a 3D LiDAR point cloud. These data are actionable for vegetation removal efforts because they include coordinate, dimension, and height information. When used in conjunction with imagery, this is quite a useful source for important decision making. There are a variety of applications, both for purchase and for free, that can display and exploit the two formats of data produced in the previous chapter. To demonstrate the polygons do indeed represent encroaching vegetation figures 4.1, 4.2 and 4.3 are shown.

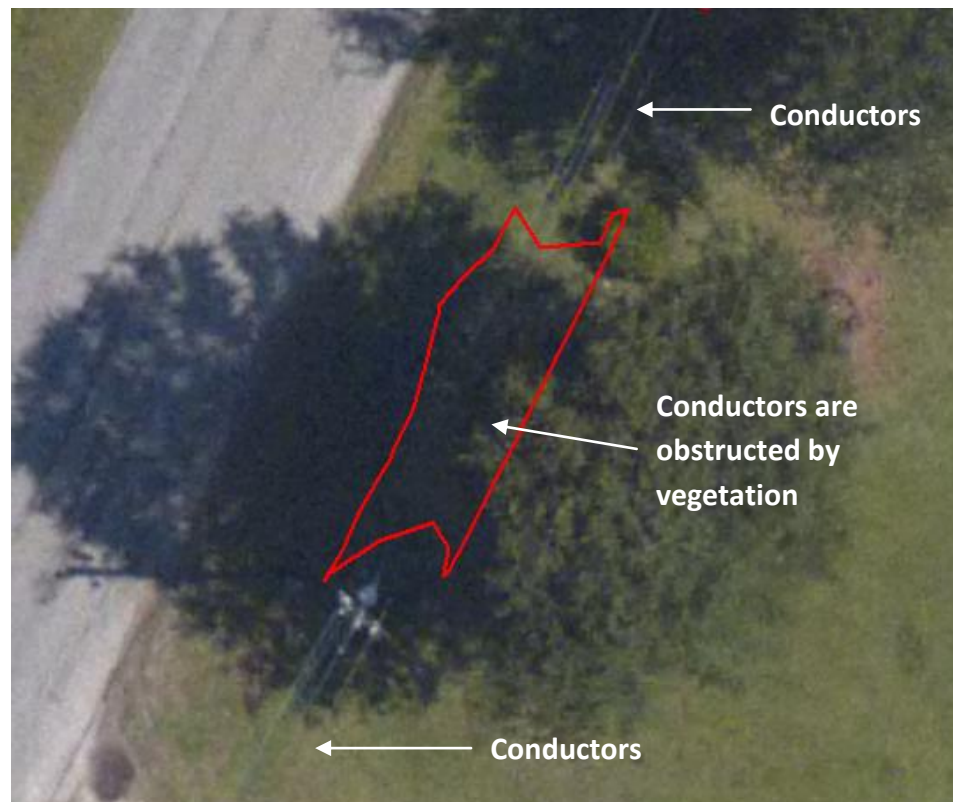


Figure 4.1 – Validated vegetation encroachments within a polygon

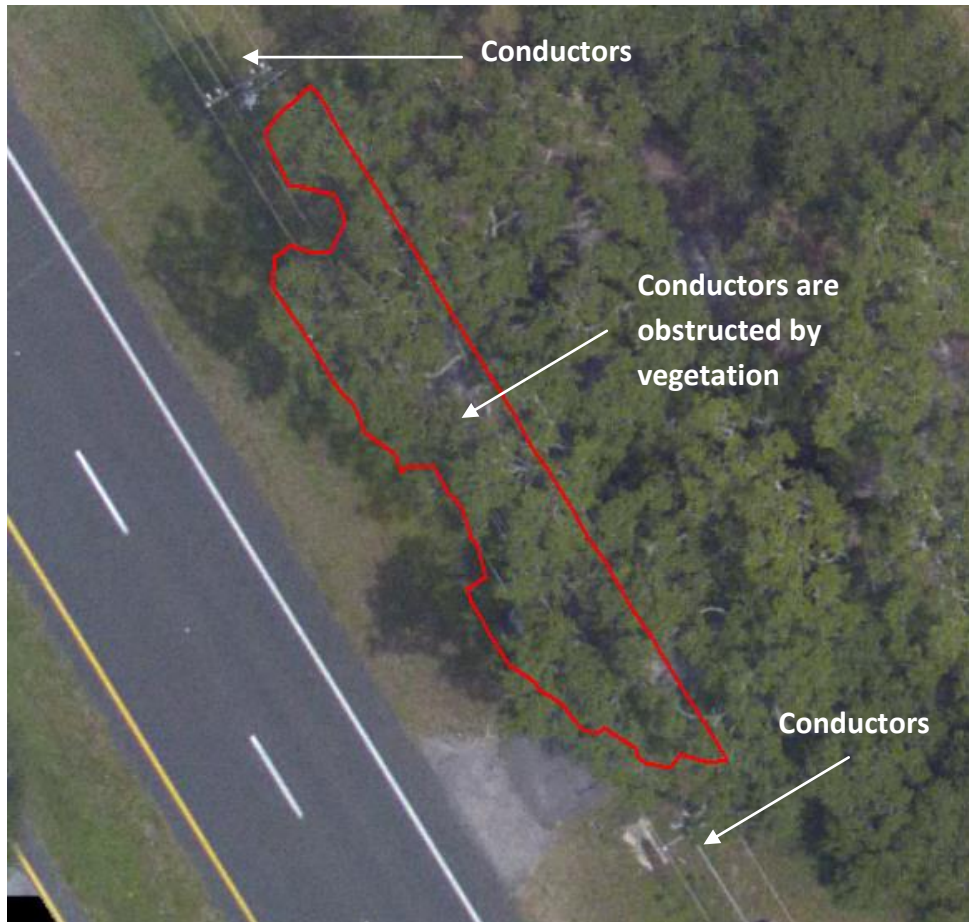


Figure 4.2 – Validated vegetation encroachments within a polygon

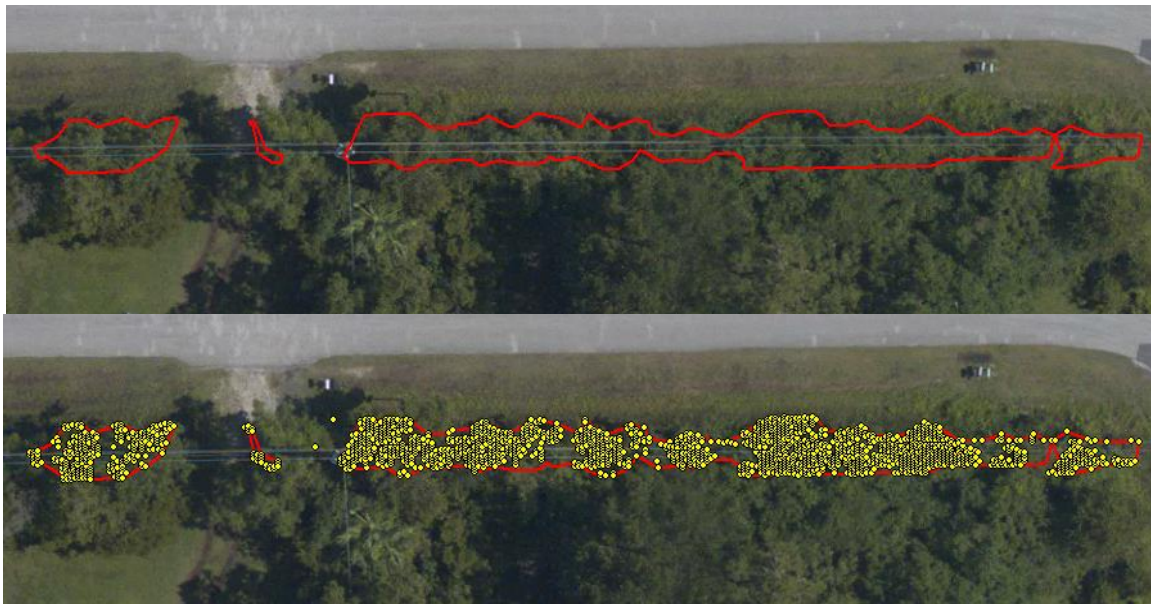


Figure 4.3 – Validated vegetation encroachments within a polygon

Since a visit to the field was not feasible due to the vegetation configuration having changed, the only other way to validate the vegetation encroachment results was to overlay the polygons on an image base showing a point in time before vegetation was trimmed. Logically, the aerial image orthomosaic collected simultaneously with the LiDAR was used to show vegetation corresponding to encroachment polygons derived from the LiDAR. This planimetric view is not the most ideal for representing the three-dimensional nature of vegetation, but at least shows vegetation obstructing the power lines. This suggests the “clear sky” buffer was legitimate in identifying vegetation above and around the power lines.

4.1 Displaying the Data

The first use case for the vegetation and conductor data involves display of the data in ArcMap, an application familiar to a vast majority of persons, businesses, and entities that deal with geospatially-aware data. For this discussion it will be assumed that the data produced so far will be given to a utility company, who will then present them to a forestry contractor, which will produce an estimate of costs. It is a fundamental function of ArcMap to display and symbolize data according to certain attribute values. In this case, one way the data can be displayed for analysis is by the area in square feet of each polygon, with a red to green color ramp (figure 4.4). The vegetation removal work could be prioritized by the size of vegetation encroachment polygons. The interpreter of the data could also prioritize work based on the density of polygons in certain areas. In figure 4.4 the Natural Breaks classification was used with

three classes; red, yellow, and green, according to area. Green indicates the smallest polygons, yellow indicates the medium polygons, and red indicates the largest polygons.

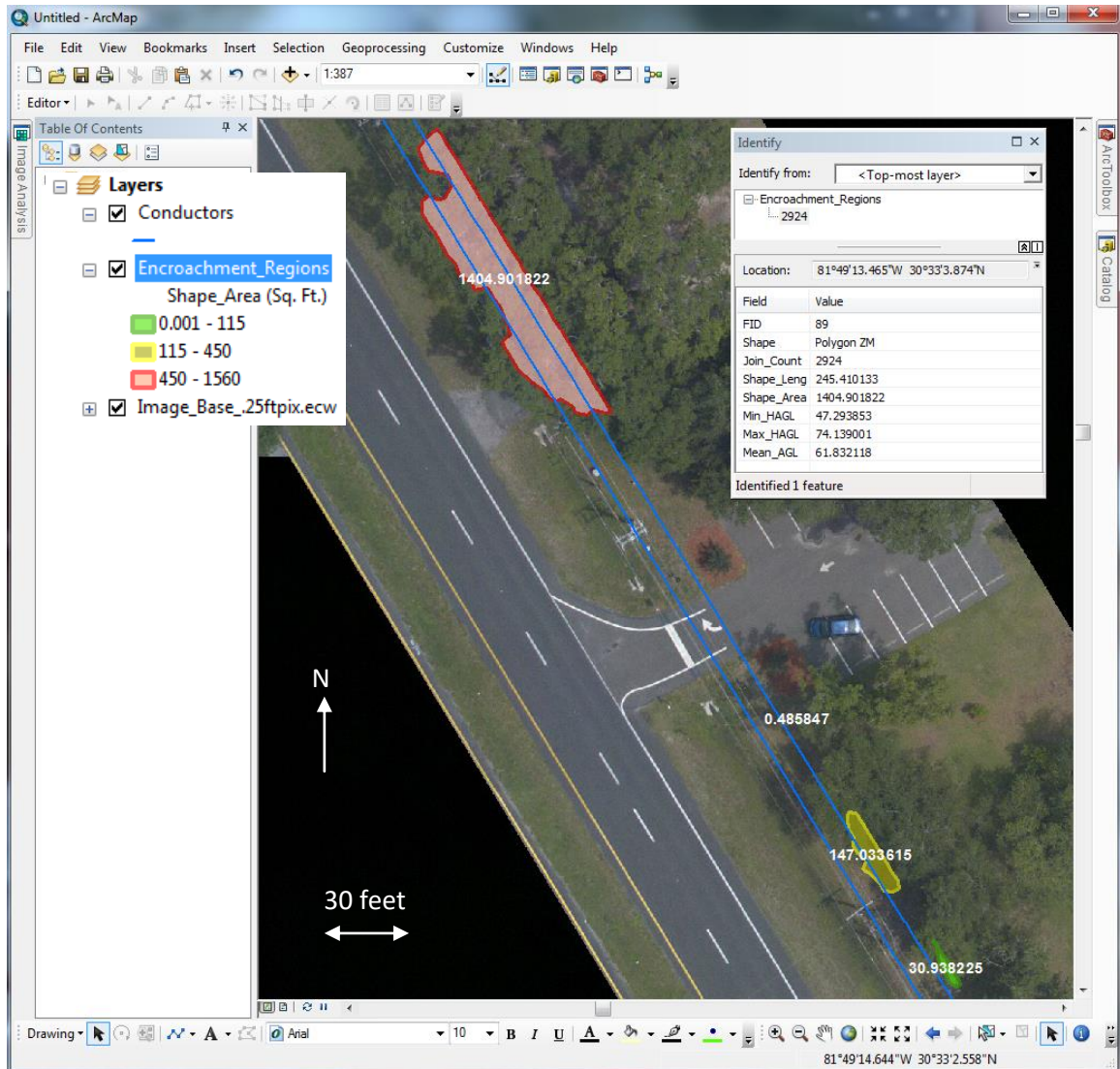


Figure 4.4 – Vegetation encroachment polygons labeled and symbolized by area

For users who don't have access to software such as ArcGIS, the KML version of the vegetation encroachment data can be viewed in GoogleEarth, which has a free version (figures 4.5 and 4.6). GoogleEarth failed to display the "Shape_Area" attribute in the popup window for the vegetation encroachment polygons even though this attribute was present at the time of KML export. This is probably because the free version of GoogleEarth does not include the ability to measure areas, so it is assumed it will not display area measurement attributes for the same reason. Perhaps Google chose one of the right incentives to spend \$399.00 on the Pro version (if purchasing between one and 10 licenses).

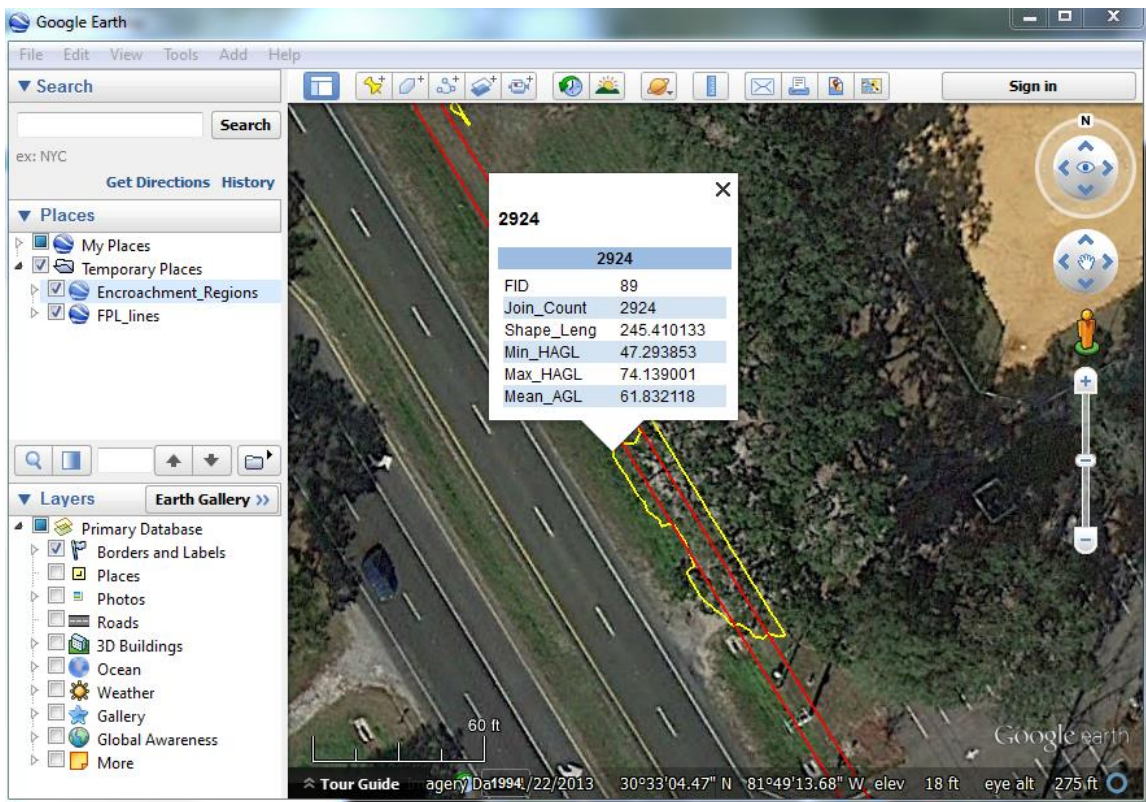


Figure 4.5 – Vegetation encroachment polygons displayed in GoogleEarth

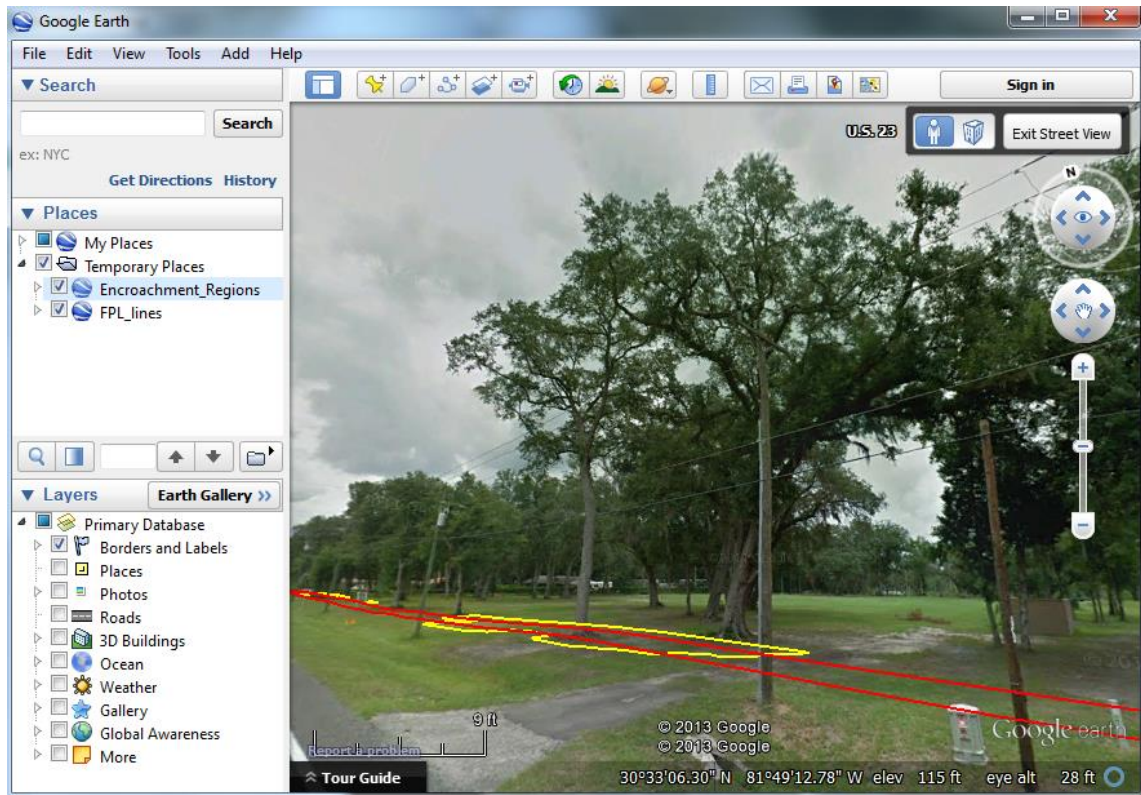


Figure 4.6 – Vegetation encroachment polygons displayed in Street View mode in GoogleEarth.

Another viewing option for this data is to use ArcGIS Explorer, which is also a free application that can be downloaded from the ESRI website. ArcGIS Explorer can read both shapefile and KML formats, among others, and also has the ability to measure areas and display area measurement attributes (figure 4.7). If the user of the data did not have an orthomosaic such as the one produced at the same time as the LiDAR data used in this study, there are free high-resolution multispectral image base services available that can be consumed in ArcGIS Explorer such as the ones served by Bing, ESRI, and Google.

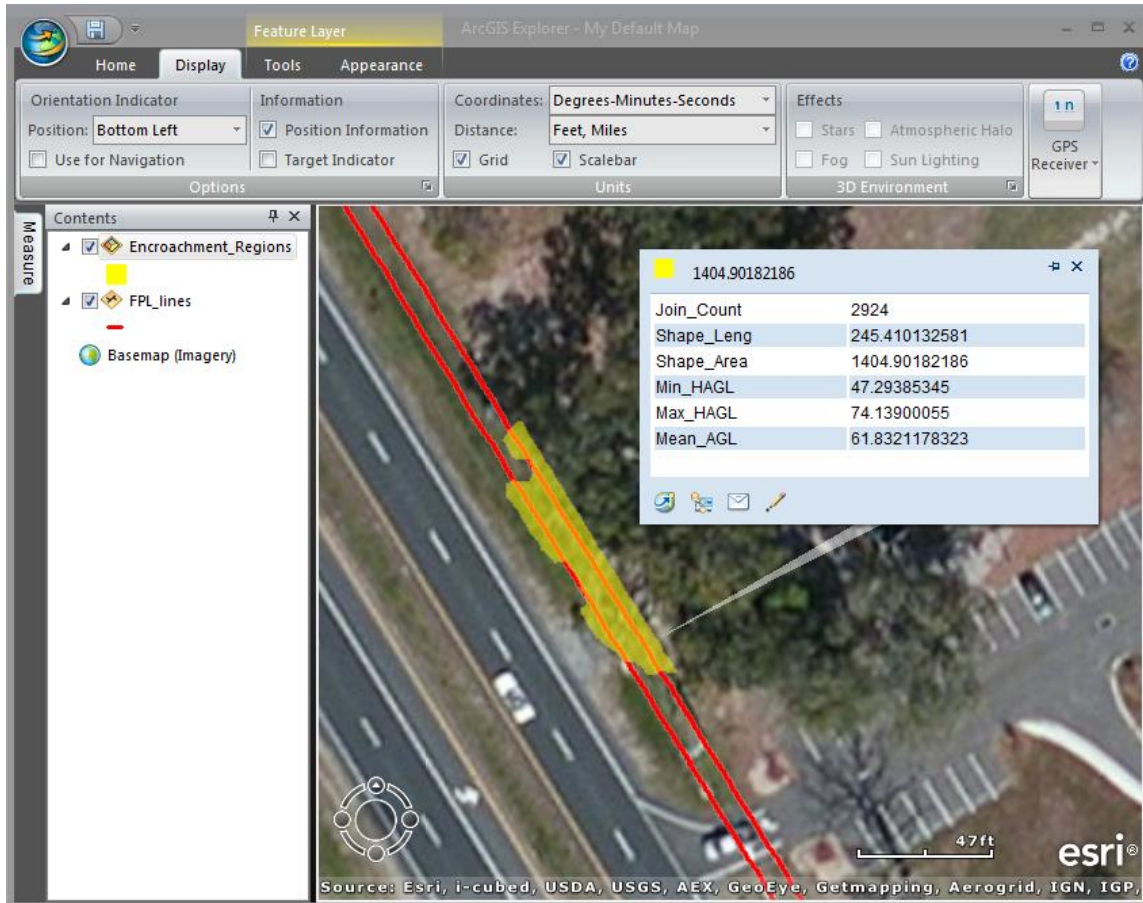


Figure 4.7 - Vegetation encroachment polygons displayed in ArcGIS Explorer

In general, the free applications do not provide much freedom in terms of symbolizing of features according to certain attribute values. For instance, it is not possible in GoogleEarth or ArcGIS Explorer to symbolize vegetation encroachment polygons by their relative area. This is not a critical lack of functionality, but it helps in quickly getting a handle on the magnitude of the vegetation removal job at hand. If the data were full of red polygons, one would know right away that a large task was to be completed.

Another way to symbolize the data would be by the “Join_Count” attribute, which indicates how many LiDAR vegetation points comprised each polygon

(figure 4.8). A five class natural breaks classification was used. This can provide a sense of how dense the vegetation is when considering individual polygons. The only problem with displaying the data according to the “Join_Count” attribute is that some areas of the data have been flown over twice, and in some areas three times.

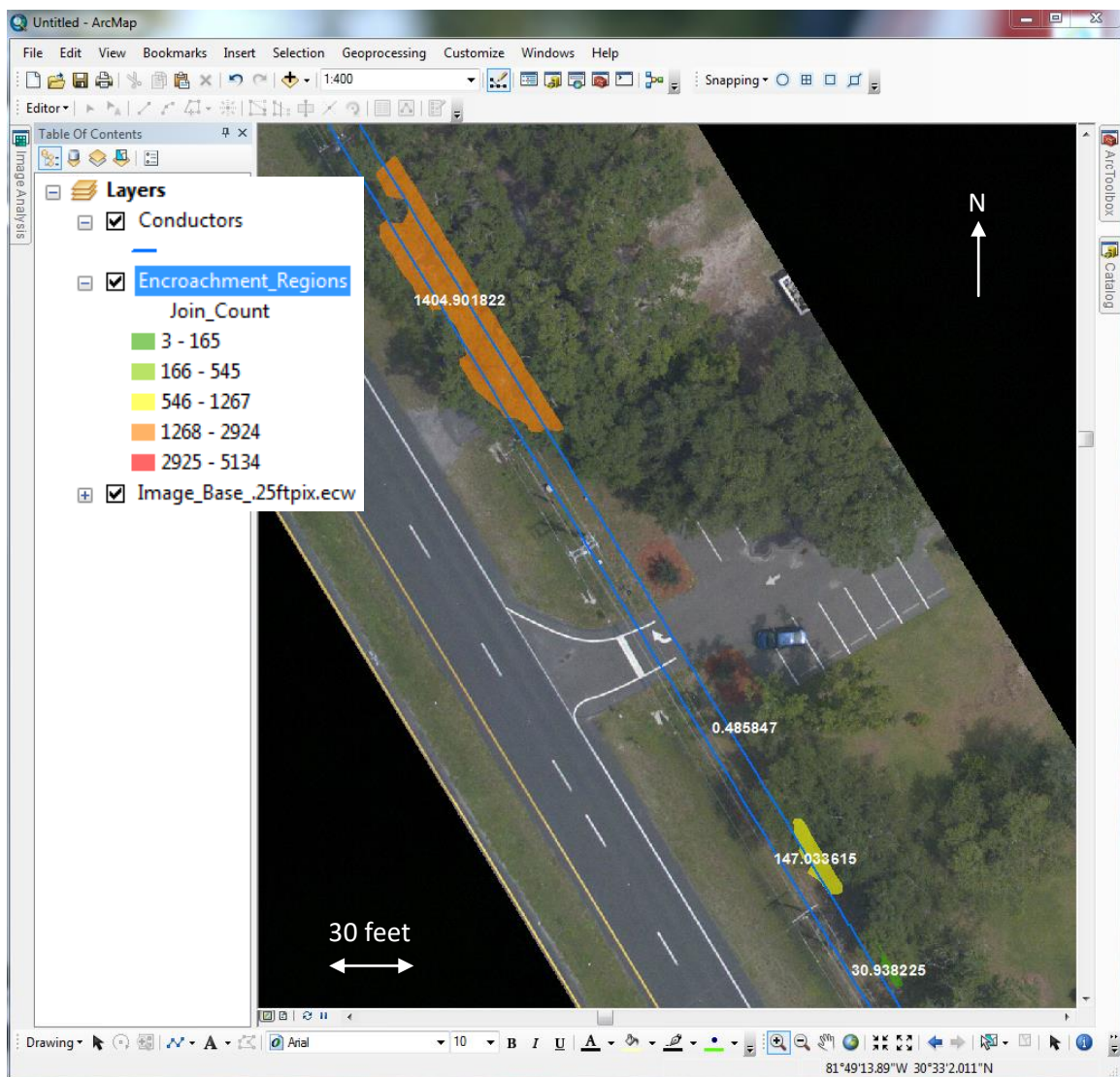


Figure 4.8 – Vegetation encroachment polygons symbolized by Join_Count

This could result in a false sense of the amount or density of vegetation contained in polygons that are comprised of two or more passes worth of LiDAR data. In other words, two polygons of the same size could have significantly different numbers of LiDAR points inside them because one area could have been flown over once, and the other area twice. This is why it would be wiser to rely on polygon size rather than the “Join_Count” attribute when analyzing how much vegetation must be dealt with.

Another possibility for displaying and analyzing the vegetation encroachment data pertains to a driving or walking field survey. The purchaser of vegetation encroachment data like that discussed so far may want to go out into the field to validate actual field conditions against what the LiDAR-derived vegetation encroachment data says. This is possible with the Real Time GPS Tracking feature of GoogleEarth. With a GPS receiver connected to a laptop computer, GoogleEarth can display conductor and vegetation encroachment data in KML format while tracking the position of the GPS receiver in real time. There are several handheld devices that can do this as well, and this could be a very convenient way to not only validate data in the field, but to actually find the vegetation that needs to be removed.

4.2 Quantifying the Data and Estimating Cost and Effort

Now that the vegetation encroachment data have been produced and can be viewed in a variety of applications where it can provide very useful information, quantifying the data as a whole will provide more insight into the amount of work that will be involved in removing the dangerous vegetation. Statistics about the vegetation heights and dimensions within each polygon have been shown, but it is not yet known what the overall “big picture” is with regard to how much total vegetation there is to be removed. A series of statistics about the vegetation encroachment polygons were generated, and can be found in table 4.1.

Table 4.1 – Summary statistics on the vegetation encroachment polygons

Polygon Count	456
Maximum Join Count	5,134
Minimum Join Count	3
Mean Join Count	210
Total Join Count	95,687
Maximum Polygon Length	0.3 ft.
Maximum Polygon Length	333 ft.
Mean Polygon Length	39 ft.
Total Polygon Length	17,761 ft.
Maximum Polygon Area	1,560 sq. ft.
Minimum Polygon Area	0.001 sq. ft.
Mean Polygon Area	75 sq. ft.
Total Polygon Area	34,158 sq. ft.

These statistics are very easy to generate in ArcMap. The total area of all vegetation encroachment polygons was calculated as 34,158 square feet, or 0.784 acres. A forestry contractor could take this number and vegetation height statistics and perhaps multiply them by some factor designed to account for labor, equipment, and other supplies such as herbicides. The major drawback, however, of using two-dimensional data is that it is not easy to get a good idea of the *volume* of vegetation that needs to be removed simply by looking at the data in a GIS or in map form. This is why the effort was made to at least include statistics about the vegetation heights within each polygon provided by the three-dimensional quality of the LiDAR data. The 2D data, however, can be used by a contractor to easily identify areas of vegetation where removal efforts should be focused in the field. If the contractor is able to conduct a field survey using the vegetation encroachment data produced in Chapter 3, more accurate cost estimation could possibly be made by physically seeing the condition and configuration of the vegetation to be removed from the perspective of the ground.

CHAPTER 5: CONCLUSIONS

5.1 Results vs. Objectives

An important component of this study is the realization of accomplishing the research objective as stated in Chapter 1 before the analysis was begun. The following section discusses the relationship between the research objective and the results of the analysis.

To reiterate, the predominant objective of this study is to employ LiDAR technology in an effective way by using it to accurately identify vegetation within a hazardous proximity to power distribution lines in the study area. As shown in the Methodology section, the process started with a LiDAR point cloud and ended with attributed vegetation encroachment polygons based on a minimum clearance distance of five feet from the conductor line vectors. The horizontal and vertical accuracies of the source LiDAR data were reported by the data vendor at <15 cm. This accuracy transfers to the vegetation encroachment polygons because no interpolation was performed. In other words, the envelopes of clusters (aggregations) of points became the polygons. For this reason, the polygons should have a horizontal accuracy very close to the source LiDAR data sample point aggregations they were derived from. The final polygons are two-dimensional, so vertical accuracy is not applicable. However, the vegetation height statistics attribute values are taken directly from the elevation values of the source LiDAR data, so they take on the same vertical accuracy of <15 cm.

In essence, vegetation within the five foot minimum encroachment distance from the conductor vectors was effectively and accurately identified using buffering techniques to classify the LiDAR data. The classified LiDAR data were converted to polygon shapefile and KML, making them interoperable with a wide variety of software applications. For instance, the data were displayed in ArcMap, ArcGIS Explorer, and GoogleEarth to show the end user is not constrained to a particular software application when using the data. Nor does the user necessarily need to spend money on software to turn the data into information, since two of the applications demonstrated are free. In fact, the user doesn't even need to spend money on imagery data because of free services such as Bing Maps, ESRI world imagery, and Google Maps.

The value of the type of vegetation encroachment data produced in this study is twofold. First, GIS-centric analysis of vegetation encroachments empowers decision makers in utility and forestry companies. They can put together a well-informed plan of action and budget to remove undesired vegetation based on knowing exactly where the vegetation is, accurately estimating how much there is, and prioritizing areas to be visited in the field. This can all be done in the office, with no visit to the field necessary. Second, the same data used to devise a vegetation removal plan and budget in the office can be used to locate candidate vegetation to be removed in the field. For instance, mobile phones, handheld devices such as tablets, and laptop computers can be used with the data in the field to locate removal sites through GPS tracking.

The key to the methodology used in this study was the ability to manipulate and process data with regard to spatial relationships (aggregation of points into polygons, spatial join, buffering, etc.), a fundamental capability of any GIS. The power of GIS was exercised in an effort to encourage utility companies to adopt new, technology-driven approaches to their vegetation management. Too often, purely physical methods involving human observation miss precarious situations where vegetation is too close to power lines. The prime example of this, of course, was the fact that vegetation which contacted power lines that caused the largest blackout in North America were inspected by humans in a helicopter only months prior.

5.2 Limitations and Issues

One limitation of the methodology used in this study is the fact that in order to create polygons that can be displayed in available software from a LiDAR point cloud, the points had to be converted to a two-dimensional shapefile. This is the only way ArcGIS could aggregate the points into polygons. The points are essentially “flattened down” into two dimensions in order to provide the basis for 2D polygons. This is why statistics about the original LiDAR points were used to describe the elevation characteristics of the vegetation.

Additionally, the conductor vectors required a fair amount of manual input in order to be generated, and no automatic method to do this is known at the present time. For the center wires along the corridor the effort was put forth to

reclassify the LiDAR points without using conductors, which would have needed to be generated beforehand. Since these vectors were not necessary, the effort to create them would have been wasted. In fact, it was faster not to use the conductor vectors to reclassify the upper and lower center wire points.

There is also the possibility of using pre-existing vectors that represent the conductors to reduce and possibly eliminate the manual labor required to create these data. These data would need to line up correctly with the LiDAR conductor points in order for the reclassification process to work properly, and would need to be three-dimensional in nature.

Also, the Z values of the LiDAR data points were all negative for some undetermined reason, possibly as the result of a preprocessing step done by the vendor that encountered problems. This did not affect the calculation of the height above ground level values and statistics for the vegetation heights, however, because this is simply the difference (a positive number) between ground elevations and vegetation point elevations.

Other than a visit to the study area before any cutting was done to the vegetation, which was not possible, the only other way to validate the final encroachment data results was with the orthomosaic collected with the LiDAR. This is not ideal, as it is two-dimensional. The determination can be made, however, whether vegetation is in close proximity to the power lines within the encroachment polygons. Nonetheless, the consumer of this data would be close to the field and could easily conduct a validation field survey.

Finally, and ironically, there were no fewer than 10 short power interruptions during the process of writing this thesis. This would not normally be a real issue, but every time the power turned off and back on, the media access control (MAC) address for the computer's wireless card used to write this thesis would change. This would not normally be an issue either, but since the Earth Shaper application is node locked to this MAC address, the license no longer worked after each short power outage. A new license had to be requested each time one of these small outages occurred. Below are two pictures of the distribution lines used to carry power to the home in which the writing of this thesis occurred (figures 5.1 and 5.2). One might question the proximity of the vegetation to these distribution lines.



Figure 5.1 – Encroaching vegetation in the neighborhood (Google Earth)



Figure 5.2 – Encroaching vegetation in the neighborhood (Google Earth)

5.3 Research Contribution

There was not a great deal of scholarly literature found pertaining directly to the application of airborne LiDAR data to power line corridor vegetation management at first. This was both a bit unnerving, but at the same time somewhat attractive. Initially, the consideration was made to altogether switch thesis subjects to one that a significant amount of literature pertained to. As the search for literature went on, however, many industry professional magazine articles, trade studies, and a fair amount of journal articles were found. Most indicated that airborne LiDAR *could* be and *was* used for power line corridor vegetation management, but virtually none indicated how exactly this was

accomplished. Perhaps this was so LiDAR vendors didn't reveal proprietary processes that might give an advantage to the competition. This fact opened the perfect opportunity to research a way to construct a workflow that used LiDAR data to better accomplish vegetation management.

An attempt to fill the gap in shared knowledge was made through the research performed and workflow created in this study. Hopefully this kind of research will be carried on further in an effort to find better ways to protect the precious electricity our society so heavily relies on every day. To follow the metaphor, it appears just as self-evident that similar preventative and diagnostic efforts that avert a stroke or heart attack in humans need to be applied to preventing power blackouts and their devastating impact on human lives and economic activity. Advancing technology such as LiDAR moves this effort along, and more research is needed.

5.4 Further Research

Three major avenues for further research were realized during this thesis research. The first has to do with fully exploiting the true 3D nature of LiDAR point clouds for power line corridor vegetation encroachments. In the process flow shown in Chapter 3, 2D polygons were created from a 3D point cloud with statistics about the elevations of points aggregated to create them as attributes. For better visualization and more meaningful statistics, creating 3D volumetric shapes from aggregations of LiDAR points would be ideal. This way a volume

could be calculated per feature rather than just area in two dimensions. Ideally, these volumetric shapes could be viewed with the conductor vectors in 3D capable software. Perhaps some TIN-like mesh that creates a surface out of the outer points of aggregations of LiDAR points could be applied. The aggregations of points would then need to be done in 3D space rather than 2D space.

The second avenue for further research would be to investigate a way to automatically generate conductor vectors from the LiDAR point cloud. The workflow used in this thesis uses a “semi-automatic” method where at least four input seed points are required for each span between poles. For a large project this could prove labor intensive and time consuming. The creation of an algorithm that recognizes the parabolic nature of LiDAR points associated with power lines could be created, and a best fit could be used to generate vectors from these recognized points.

Finally, as unmanned aerial vehicles become more ubiquitous and sensor technology advances, it would be worth researching ways to optimize the collection of aerial LiDAR using this type of platform. This method would inevitably be cheaper than flying a full sized aircraft because it would consume less fuel, could be run on batteries and solar power, and would not require the employment of a licensed pilot.

REFERENCES

- Amadori, J., 2012. Utility infrastructure vegetation management using LiDAR, imagery, and GIS. *LiDAR News*, 2(6) [online] Available at: <<http://www.lidarnews.com/content/view/9231/198/>> [Accessed 22 July 2013].
- American Society for Photogrammetry and Remote Sensing, 2013. *LAS file format exchange activities* [online] Available at: <<http://www.asprs.org/Committee-General/LASer-LAS-File-Format-Exchange-Activities.html>> [Accessed 8 June 2013].
- Edison Electric Institute, 2013. *The history of electricity* [online] Available at: <<http://www.eei.org/Pages/default.aspx>> [Accessed 8 June 2013].
- Frank, M., Pan, Z., Raber, B., and Lenart, C., 2010. Vegetation management of utility corridors using high-resolution hyperspectral imaging and LiDAR. In: *Hyperspectral Image and Signal Processing: Evolution in Remote Sensing (WHISPERS)*. 14-16 June 2010, Reykjavik, Iceland [pdf] Available at: <<http://ieeexplore.ieee.org/stamp/stamp.jsp?tp=&arnumber=5594887>> [Accessed 2 July 2013].
- Guggenmoos, S., 2012. The evolution of utility vegetation management. *Transmission and Distribution World*, January 2012, 1-2 [online]. Available at: <<http://tdworld.com/vegetation-management/evolution-utility-vegetation-management-part-1>> [Accessed 8 June 2013].
- Ituen, I., Sohn, G., and Jenkins, A., 2008. A case study: Workflow analysis of power line systems for risk management. In: *The International Archives of the Photogrammetry, Remote Sensing and Spatial Information Sciences*, Volume XXXVII, Part B3b, Beijing, China, 3-11 July 2008.
- Jobes, T., Moore, L., and Rousselle, A., 2008. Cutting-edge LiDAR exposes clearances. *Transmission and Distribution World*, May 2008, 40-46.
- Knoxville Utilities Board, 2013. *What causes outages?* [online] Available at: <http://www.kub.org/wps/portal/Customers/Home/SafetyAndOutages/PowerOutages/WhatCausesOutages!/ut/p/b1/hZC5DsMgEES_JV-wCxgEJZaDQMqpnN7GoogiRz6aKN8fO0qTljDdSO8VM0BQcxQFcgEVhyvQEF_tPT7bcYjd3Ek1XsvyEAqOWx8MBi3O6l-SaSsnoJ4A_BOLvz5WuxL5qjoZuXR-r9jXTwAJfy0x7c9A0mc5n-X2X4A-SOqB3AeUG7nxY3-DnjrnnAmPwi7etpDuiA!!/dl4/d5/L2dBISvZ0FBIS9nQSEh/> [Accessed 9 June 2013].
- Kobayashi, Y., Moeller, M.S., Karady, G.G., Heydt, G.T., and Olsen, R.G., 2008. *The utilization of satellite images to identify trees endangering transmission lines*. [pdf] Power Systems Engineering Research Center.

Available at:

<https://www.google.com/url?q=http://pserc.wisc.edu/documents/general_information/presentations/pserc_seminars/4psercsemin/karady_pserc_vegetation_mgt_project_teleseminar_mar08.pdf&sa=U&ei=UYBJUrTTJcOw2wW7I4HQDA&ved=0CacQFjAA&client=internal-uds-cse&usq=AFQjCNH8kAtZgj9Kjl4lo6balZdOgAwhqQ> [Accessed 29 August 2013].

- Koop, J.E., 2002. Advanced technology for transmission line modeling. *Transmission and Distribution World*, April 2002, 90-93.
- Kruse, F.A., Lefkoff, A.B., Boardman, J.B., Heidebrecht, K.B., Shapiro, A.T., Barloon, P.J., and Goetz, A.F.H., 1993. The spectral image processing system (SIPS) – interactive visualization and analysis of imaging spectrometer data. *Remote Sensing of the Environment*, 44, 145-163.
- Li, Z., Hayward, R., Zhang, J., and Liu, Y., 2008. Individual tree crown delineation techniques for vegetation management in power line corridors. In: *10th International Conference on Digital Image Computing: Techniques and Applications*. Canberra, Australia, December 1-3, 2008.
- Li, Z., Walker, R., Hayward, R., and Mejias, L., 2010. Advances in vegetation management for power line corridor monitoring using aerial remote sensing techniques. In: *1st International Conference on Applied Robotics for the Power Industry*. Montreal, Canada, October 5-7, 2010. Montreal: Cooperative Research Centres Programme.
- Mills, S., Gerrardo, M., Li, Z., Cai, J., Hayward, R.F., Mejias, L, and Walker, R.A., 2010. Evaluation of aerial remote sensing techniques for vegetation management in power line corridors [pdf]. *IEEE Transactions on Geoscience and Remote Sensing*, 48(9), 3379-3390.
- Narolski, S., 2010. Is that tree too close? *Transmission and Distribution World*, July 2010, 46-51 [online]. Available at: <<http://tdworld.com/%5Bprimary-term%5D/tree-too-close>> [Accessed 10 June 2013].
- North American Electric Reliability Corporation (NERC), 2013. About NERC [online]. Available at: <<http://www.nerc.com/Pages/default.aspx>> [Accessed 12 July, 2013].
- Richardson, P., 2011. Compliance through deployment of LiDAR technology – NERC FAC-003. *Electric Light and Power*, March 2011, 28-30.
- Texas Engineering Experiment Station, 2011. *Best practices in vegetation management for enhancing electric service in texas*. College Station: Texas Engineering Experiment Station.
- U.S.-Canada Power System Outage Task Force, 2004. *Final report on the august 14, 2003 blackout in the united states and canada: causes and*

recommendations. United States and Canada: U.S.-Canada Power System Outage Task Force.

Ussyshkin, R.V., Theriault, L., Sitar, M., and Kou, T., 2011. *Advantages of airborne LiDAR technology in power line asset management* [pdf]. In: Multi-Platform/Multi-Sensor Remote Sensing and Mapping (M2RSM) Workshop. Xiamen, China, 4-5 May 2011 . Available at: <<http://ieeexplore.ieee.org/stamp/stamp.jsp?tp=&arnumber=5697427>> [Accessed 9 June 2013].

Wolf, G., 2010a. Lighting up the grid with intelligent tools. *Transmission and Distribution World*, February 2010, 1-4 [online]. Available at: <<http://tdworld.com/smart-grid/lighting-grid-intelligent-tools>> [Accessed 22 July 2013].

Wolf, G., 2010b. LiDAR: Illuminating hazardous vegetation. *Transmission and Distribution World*, February 2010, 13-18.

Young, J., 2011. *LiDAR for dummies*. [pdf] Hoboken: Wiley. Available at: <<http://www.dlt.com/library/whitepaper/lidar-for-dummies-ebook>> [Accessed 7 July 2013].